

## FINAL REPORT

Soil Moisture Characterization for Biogenic Emissions Modeling in Texas

AQRP Project 14-008

Prepared for:

David Sullivan  
Texas Air Quality Research Program  
The University of Texas at Austin

Prepared by:

Gary McGaughey, Yosuke Kimura,  
Ling Huang, Elena McDonald-Buller (Principal Investigator)  
Center for Energy and Environmental Resources  
The University of Texas at Austin

and

Ying Sun, Rong Fu (Co-Principal Investigator)  
Jackson School of Geosciences  
The University of Texas at Austin

August 2015

QA Requirements: Audits of Data Quality: 10% Required

## ACKNOWLEDGMENT

The preparation of this report is based on work supported by the State of Texas through the Air Quality Research Program administered by The University of Texas at Austin by means of a Grant from the Texas Commission on Environmental Quality.

# Contents

1.0 Introduction.....	8
1.1 Technical Context and Motivation .....	8
1.2 Objective.....	9
1.3 Report overview .....	10
1.4 References.....	11
2.0 Overview of soil moisture databases .....	13
2.1 Ground-based.....	13
2.2 Satellite-based .....	14
2.3 Model-based.....	16
2.4 Soil moisture datasets employed in our study .....	17
2.5 References.....	17
3.0 In-situ soil moisture monitoring.....	22
3.1 Overview of large-scale networks .....	22
3.2 Eastern Texas in-situ data during 2006-2013.....	27
3.3 Summary.....	35
3.4 References.....	35
4.0 Comparison of NLDAS-2 and in-situ soil moisture .....	37
4.1 NLDAS-2 datasets .....	37
4.2 Methodology .....	38
4.3 Results .....	44
4.4 Summary.....	55
4.5 References.....	56
5.0 Comparison of in-situ and NLDAS-2 soil moisture at eastern Texas locations.....	59
5.1 Methodology .....	59
5.2 Results .....	59
5.3 Summary.....	74
5.4 References.....	74
6.0 Intercomparison of NLDAS-2 simulated soil moisture datasets during 2006-2013 .....	75
6.1 Methods .....	75
6.2 Results .....	76

6.3 Summary.....	85
6.4 References.....	85
7.0 MEGAN simulations.....	86
7.1 MEGAN methodology.....	86
7.2 Results .....	90
7.3 Summary.....	111
7.4 References.....	112
8.0 Discussion .....	114
9.0 Recommendations for Future Work.....	119
10.0 Audits of Data Quality .....	121

Figure 1 The analysis of soil moisture will be conducted for regions within the 12-km (blue) grid domain; MEGAN simulations to predict isoprene concentrations will be focused on eastern Texas regions within the 4-km (green) grid domain (Source: <http://www.tceq.texas.gov/airquality/airmod/rider8/modeling/domain>). ..... 9

Figure 2 Thirty-six land cover/land use types in eastern Texas (Source: Popescu et al., 2011) with boundaries of Texas climate divisions (Source: National Oceanic and Atmospheric Administration) and developed metropolitan areas shown in red. .... 10

Figure 3 Locations of soil moisture observation stations in Texas overlain on a soils type map. The boundaries show the ten Texas climate divisions. The intensive TxSON monitoring area is shown by the dark green square. A summary of soil moisture measurements during 2006-2013 collected at the four labeled locations in eastern Texas (and one additional location in southeastern Oklahoma) are presented in the Section 3.2 of this report. .... 25

Figure 4 Daily average soil moisture and rainfall at the Palestine monitoring location during 2011. .... 29

Figure 5 Average seasonal soil moisture contents ( $m^3/m^3$ ) during 2006-2013 for (a) Palestine, (b) Prairie View, (c) Port Aransas, (d) Austin, and (e) Durant (OK). Data completeness criteria were applied so that at least 2 of 3 months had 60% valid data based on hourly observations. (spring==Mar/Apr/May; summer==Jun/Jul/Aug; fall==Sep/Oct/Nov; winter==Dec/Jan/Feb). .... 30

Figure 6 Average seasonal soil moisture contents ( $m^3/m^3$ ) using all available data for years 2009-2013 (ref. Figure 5) for (a) 5cm and (b) 100cm depths. .... 34

Figure 7 Locations of SCAN and CRN monitoring locations operational during at least a portion of 2006-2013. For the purposes of NLDAS-2 evaluation, the 12km domain (outlined in green) was sub-divided into two regions “East” and “West”. The division boundary is along 98°W longitude. .... 39

Figure 8 Comparison of observed and NLDAS-2 soil moisture at the in-situ SCAN/CRN measurement depths, averaged by Julian day during 2006-2013. Results are shown for the eastern (left) and western (right) portions of the 12km domain..... 46

Figure 9 Relative bias (%) of simulated soil moisture compared to observations for the eastern (left) and western (right) sub-regions at the in-situ measurement depths. The relative bias is calculated as:  $100 * (\text{modeled soil moisture} - \text{observed soil moisture}) / \text{observed soil moisture}$ . The error bars represent the 95% confidence interval for each model. Because the y-axis range is limited to -100% to 100%, VIC results >100% are not shown. .... 48

Figure 10 Observed and modeled daily soil moisture at in-situ measurements depths for the western and eastern sub-regions (ref. Figure 7) during 2006 to 2013. .... 51

Figure 11 As in Figure 10, but averaged by month..... 52

Figure 12 Observed and modeled daily soil moisture anomalies at in-situ measurements depths for the western and eastern sub-regions (ref. Figure 7) during 2006 to 2013. ... 53

Figure 13 As in Figure 12 but averaged by month..... 54

Figure 14 Simulation skill (correlation of daily soil moisture anomaly between model simulations and observations) at different depths for the West and East portions of the 12km domain. .... 55

Figure 15 Daily observed (in-situ) and NLDAS-2 (predicted) soil moisture at the Palestine monitoring location during 2011 at soil depths of (a) 5cm and (b) 100cm..... 61

Figure 16 Average seasonal observed (in-situ) and NLDAS-2 (predicted) soil moisture contents ( $m^3/m^3$ ) at selected soil depths during 2006-2013 for (a) Palestine, (b) Prairie View, (c) Port Aransas, (d) Austin, and (e) Durant (OK). Hourly observed and NLDAS-2 values were matched in space and time; seasonal averages were only calculated using hours with valid observations and a requirement of 75% data completeness by season. (spring==Mar/Apr/May; summer==Jun/Jul/Aug; fall==Sep/Oct/Nov; winter==Dec/Jan/Feb) ..... 63

Figure 17 Average seasonal observed and NLDAS-2 soil moisture contents ( $m^3/m^3$ ) at 5cm and 100cm soil depths based on all available data shown in Figure 16 for (a) Palestine and (b) Prairie View..... 70

Figure 18 Summer average 5cm soil moisture during all available years 2006-2013 at (a) Palestine, (b) Prairie View, and (c) Austin. Years are ordered by ascending observed values. .... 71

Figure 19 Summer average 50cm soil moisture during all available years 2006-2013 at (a) Palestine, and (b) Prairie View. Years are ordered by ascending observed values..... 73

Figure 20 The four sub-regions of the 12km grid domain (West, West Central, East Central, East) defined for the NLDAS-2 soil moisture inter-comparison. Analysis regions also include the five eastern Texas regions (North Central, South Central, East, Upper Coast, Edwards Plateau) as shown in Figure 2. .... 75

Figure 21 Simulated monthly NLDAS-2 soil moisture ( $m^3/m^3$ ) for the four 12km grid domain sub-regions and four soil layers. Each column presents a vertical profile of results for, from left to right: East, East Central, West Central, West; ref. Figure 20). Each

row displays a single soil layer; from top to bottom: 0-10cm, 10-40cm, 40-100cm, and 100-200cm. ....	78
Figure 22 Simulated monthly NLDAS-2 soil moisture ( $m^3/m^3$ ) for five eastern Texas climate divisions and four soil layers. Each column presents a vertical profile of results for, from left to right: East Texas, Upper Coast, North Central, South Central, and Edwards Plateau (within the 4km domain; ref. Figure 2). Each row displays a single soil layer; from top to bottom: 0-10cm, 10-40cm, 40-100cm, and 100-200cm. ....	79
Figure 23 Comparison of soil moisture anomaly ( $m^3/m^3$ ) for the top soil layer (0-10cm) simulated by NLDAS-2 models. The anomaly is relative to the 2006-2013 average.....	81
Figure 24 Similar to Figure 23 but for the bottom soil layer, i.e., 100-200cm. ....	82
Figure 25 Comparison of April-October anomalies for years 2007, 2011, and 2012 for 0-200cm NLDAS-2 (Mosaic, Noah, Noah-MP, and VIC LSMs) soil moisture and GRACE total water storage. Units are cm.....	84
Figure 26 Isoprene emission factors ( $kg/km^2/hr$ ). The boundaries of five Texas climate divisions are also shown. ....	88
Figure 27 Monthly PDSI for 2006-2014 for five Texas climate divisions: North Central, South Central, East, Upper Coast and Edwards Plateau. (Source: National Climatic Data Center; <a href="http://www.ncdc.noaa.gov/temp-and-precip/drought/historical-palmers/">http://www.ncdc.noaa.gov/temp-and-precip/drought/historical-palmers/</a> ).....	89
Figure 28 As presented in Table 6 but in graphical format. ....	91
Figure 29 Isoprene emissions as reported in Table 8 but in graphical format for (a) North Central, (b) Upper Coast, (c) South Central, (d) Edwards Plateau and (e) East. Note difference in y-axis scales between figures. ....	97
Figure 30 Isoprene emissions for summer 2007 predicted by MEGAN on the 4km grid domain (1km horizontal resolution) for the (a) basecase and (b) Mosaic simulations. Differences and percentage changes are shown in (c) and (d); refer to legend for changes in units and scale. ....	101
Figure 31 Area-averaged NLDAS-2 wilting point values by region. ....	103
Figure 32 NLDAS-2 wilting point values on the 4km grid domain for (a) Noah, (b) Noah-MP, (c) Mosaic and (d) VIC.....	107
Figure 33 A comparison of (a) STATSGO soil texture employed by NLDAS-2 and (b) percentage changes in predicted isoprene for the Mosaic simulation relative to the basecase for summer 2007.....	108

Figure 34 Average growing season (March-October) soil moisture during 2011 at Port Aransas and Prairie View for in-situ observations (Measured) and as simulated by Mosaic and Noah. .... 109

Figure 35 Total isoprene predicted for Mar-Oct 2011 at three Texas locations using observed, Noah, and Mosaic soil moisture databases. .... 110

Figure 36 As in Figure 35 but adding MEGAN simulations that utilized observed soil moisture and NLDAS-2 wilting points. .... 111

Table 1 Selected satellite missions (adapted directly from Ford et al., 2015). .....	15
Table 2 Abbreviated descriptions from Chapter 6 <i>The Categories of Soil Taxonomy</i> from “Soil Taxonomy A Basic System of Soil Classification for Making and Interpreting Soil Surveys” (USDA, 1999) for the chemical and physical properties of the seven Texas soil types (ref. Figure 3).....	26
Table 3 Summary of soil moisture measurements at selected monitors in eastern Texas and southeastern Oklahoma. ....	28
Table 4 Soil characterization data for selected Texas locations.....	33
Table 5 SCAN and CRN measurement locations used for NLDAS-2 evaluation.....	40
Table 6 Area-averaged isoprene emissions (kg/km <sup>2</sup> /day) predicted for five Texas climate regions during 2006, 2007, and 2011. ....	91
Table 7 Ratio of seasonal area-averaged isoprene emissions during 2006 and 2011 relative to 2007.....	92
Table 8 Predicted area-averaged isoprene emissions by season for five Texas climate regions during (a) 2006, (b) 2007, and (c) 2011. Results are shown for the basecase and each of the four soil moisture scenarios. The last four columns in Table 8 show the percentage changes in emissions relative to the basecase.....	94
Table 9 Predicted area-averaged summer isoprene emissions during 2006, 2007, and 2011 for three simulations: Noah-MP, Mosaic, and the Mosaic sensitivity run that used Mosaic soil moisture values and Noah-MP wilting points. The final two columns show the ratio of Mosaic predictions to the Noah-MP values. ....	104
Table 10 Average wilting points (0-200cm) at Palestine, Port Aransas, and Prairie View. ....	110
Table 11 Predicted isoprene (kg/m <sup>2</sup> /day) for summer 2007 and summer 2011 by region for the Noah-MP and Mosaic simulations. ....	115

## **1.0 Introduction**

The role of isoprene and other biogenic volatile organic compounds (BVOCs) in the formation of tropospheric ozone has been recognized as critical for air quality planning in Texas. In the southwestern United States (U.S.), drought has become a recurring phenomenon and, in addition to other extreme weather events, can impose profound and complex effects on human populations and the environment. Understanding these effects on vegetation and biogenic emissions is important as Texas concurrently faces requirements to achieve and maintain attainment with the National Ambient Air Quality Standard (NAAQS) for ozone in several large metropolitan areas. Previous research has indicated that biogenic emissions estimates are influenced by potentially competing effects in model input parameters during drought and that uncertainties surrounding several key input parameters remain high. The primary objective of the project is to evaluate and inform improvements in the representation of one of these key input parameters, soil moisture, through the use of simulated and observational datasets. The Model of Emissions of Gases and Aerosols from Nature (MEGAN) will be used to explore the sensitivity of isoprene emission estimates to alternative soil moisture representations.

### **1.1 Technical Context and Motivation**

Isoprene and monoterpenes are quantitatively among the most important BVOCs emitted globally from vegetation (Fehsenfeld et al., 1992; Guenther et al., 1995; Guenther et al., 2006). Average Texas statewide daily BVOC emissions were approximately 11,650 tons per day and ranked first within the continental U.S. in the 2011 National Emission Inventory (NEI) version 1 (EPA, 2014). Recognition of the role of BVOCs in tropospheric ozone and organic aerosol formation has been critical for air quality planning efforts in the state.

Recent air quality modeling for attainment demonstrations in Texas has relied on estimates of biogenic emissions from the Global Biosphere Emissions and Interactions System (GloBEIS; Yarwood et al., 2010); MEGAN (Guenther et al., 2012) has been utilized widely for estimating biogenic emissions throughout the U.S. as well as globally. Differences exist between the pathways and representations of input parameters that could be expected to influence biogenic emissions estimates. As an example, GloBEIS uses the Palmer Drought Severity Index (PDSI) as the basis for a drought activity factor. MEGAN instead employs an activity factor based on soil moisture and wilting point. Guenther and Sakulyanontvittaya (2011) suggest that the use of soil moisture in MEGAN offers advantages over the use of the PDSI in GloBEIS, including the ability to utilize observations from field measurement and laboratory studies or model-based predictions.

## 1.2 Objective

The primary objective of this work is to evaluate and inform improvements in the representation of soil moisture through the use of simulated and observational datasets. MEGAN is used to explore the sensitivity of biogenic emission estimates to alternative soil moisture representations. This work is a collaboration between two research teams at The University of Texas at Austin: Dr. Elena McDonald-Buller's at the Center for Energy and Environmental Resources and Dr. Rong Fu's of the Jackson School of Geosciences.

The geographic region of focus is the multi-state 12-km domain shown in Figure 1, with an emphasis on datasets available for the eastern half of Texas. The National Oceanic and Atmospheric Administration, National Climatic Data Center (NOAA - NCDC) divides Texas into 10 climate regions. Most large metropolitan areas in the state are located within one of four climate regions, shown in Figure 2: North Central Texas (Dallas-Fort Worth; sub-tropical steppe or semi-arid savanna), South Central Texas (Austin and San Antonio; sub-tropical sub-humid mixed prairie, savanna and woodlands), East Texas (sub-tropical humid mixed evergreen-deciduous forestland) and Upper Coast (Houston; sub-tropical humid marine prairies and marshes) (Texas Water Development Board, 2012). ([http://climatexas.tamu.edu/images/files/fnep\\_climdiv.txt](http://climatexas.tamu.edu/images/files/fnep_climdiv.txt)).

**Figure 1 The analysis of soil moisture will be conducted for regions within the 12-km (blue) grid domain; MEGAN simulations to predict isoprene concentrations will be focused on eastern Texas regions within the 4-km (green) grid domain (Source: <http://www.tceq.texas.gov/airquality/airmod/rider8/modeling/domain>).**

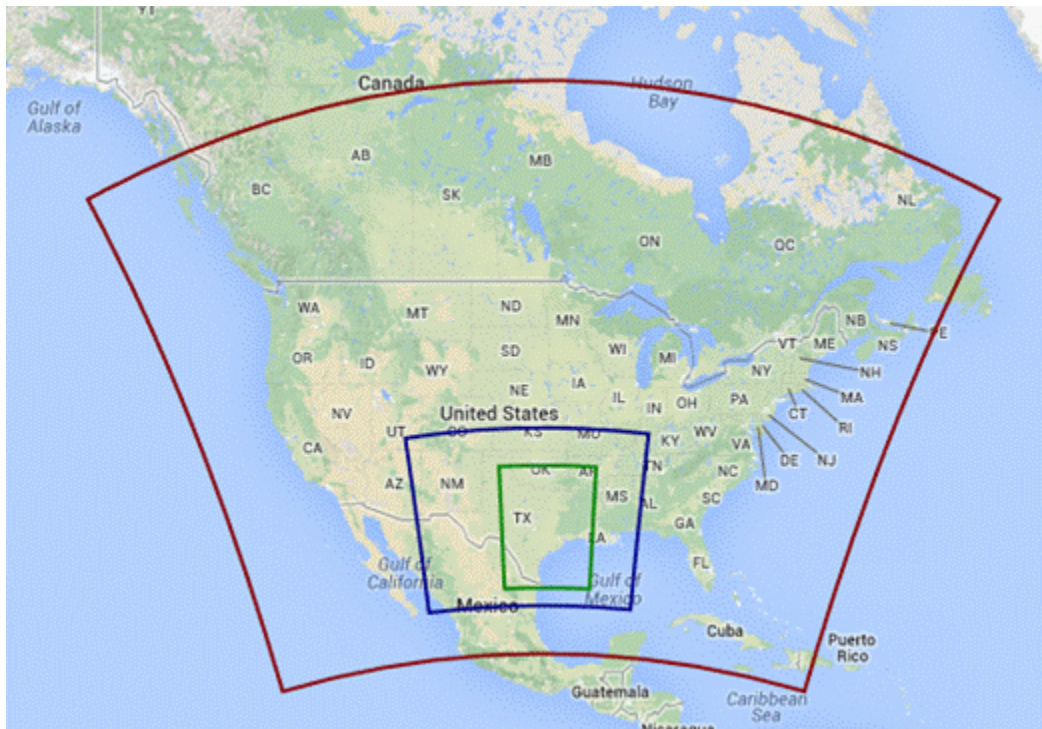
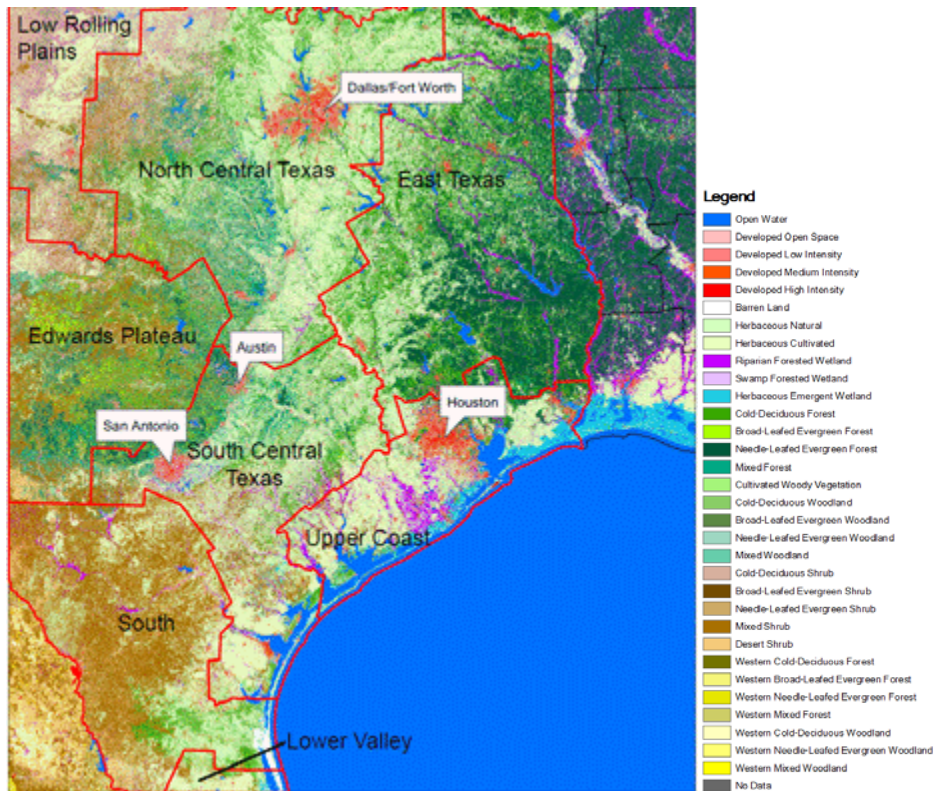


**Figure 2 Thirty-six land cover/land use types in eastern Texas (Source: Popescu et al., 2011) with boundaries of Texas climate divisions (Source: National Oceanic and Atmospheric Administration) and developed metropolitan areas shown in red.**



### 1.3 Report overview

This report is organized into the following sections. Section 2 provides an overview of the soil moisture databases available for Texas and surrounding states. A discussion of in-situ (observational) soil moisture measurements available in Texas is presented in Section 3. A regional inter-comparison of observed and North American Land Data Assimilation System Phase 2 (NLDAS-2) predicted soil moisture contents is provided in Section 4. A comparison of the eastern Texas in-situ and NLDAS-2 datasets is provided in Section 5. Section 6 investigates the spatial and temporal variability of NLDAS-2 soil moisture. Isoprene emission estimates using MEGAN and soil moisture databases during representative wet and dry years in Texas are presented in Section 7. Discussion and Recommendations for Future Work are provided in Sections 8 and 9, respectively.

## 1.4 References

EPA, 2014. 2011 National Emission Inventory, version 1 Technical Support Document Draft. Retrieved from [http://www.epa.gov/ttn/chief/net/2011nei/2011\\_nei\\_tsdv1\\_draft2\\_june2014.pdf](http://www.epa.gov/ttn/chief/net/2011nei/2011_nei_tsdv1_draft2_june2014.pdf) (accessed on February 19, 2015)

Fehsenfeld, F., Calvert, J., Fall, R., Goldan, P., Guenther, A. B., Hewitt, C. N., Lamb, B., et al., 1992. Emissions of volatile organic compounds from vegetation and the implications for atmospheric chemistry. *Global Biogeochemical Cycles*, 6(4), 389–430.

Guenther, A. B., Jiang, X., Heald, C. L., Sakulyanontvittaya, T., Duhl, T., Emmons, L. K., & Wang, X., 2012. The Model of Emissions of Gases and Aerosols from Nature version 2.1 (MEGAN2.1): an extended and updated framework for modeling biogenic emissions. *Geoscientific Model Development*, 5(6), 1471–1492. doi:10.5194/gmd-5-1471-2012

Guenther, A., and Sakulyanontvittaya, T., 2011. Improved biogenic emission inventories across the West. Prepared for the Western Governors' Association.

Guenther, A., Karl, T., Harley, P., Wiedinmyer, C., Palmer, P. I., & Geron, C., 2006. Estimates of global terrestrial isoprene emissions using MEGAN (Model of Emissions of Gases and Aerosols from Nature). *Atmospheric Chemistry and Physics*, 6(1), 107–173. doi:10.5194/acpd-6-107-2006.

Guenther, Alex, Nicholas, C., Fall, R., Klinger, L., Mckay, W. A., and Scholes, B., 1995. A global model of natural volatile organic compound emissions. *Journal of Geophysical Research*, 100(D5), 8873–8892.

Houborg, R., M. Rodell, B. Li, R. Reichle, and B. F. Zaitchik, 2012. Drought indicators based on model-assimilated Gravity Recovery and Climate Experiment (GRACE) terrestrial water storage observations. *Water Resources Research*, 48, W07525.

Lawrence, D. M., Oleson, K. W., Flanner, M. G., Thornton, P. E., Sean, C., Lawrence, P. J., Zeng, X., et al. (2010). Parameterization Improvements and Functional and Structural Advances in Version 4 of the Community Land Model, 1–29.

Popescu, S. C., Stuke, J., Mutlu, M., Zhao, K., Sheridan, R., Ku, N.-W., & Harper, C., 2011. Expansion of Texas Land Use / Land Cover through Class Crosswalking and Lidar Parameterization of Arboreal Vegetation Secondary Investigators : Retrieved September 17, 2013. [http://www.tceq.texas.gov/assets/public/implementation/air/am/contracts/reports/ot/h/5820564593FY0925-20110419-tamu-expension\\_tx\\_lulc\\_arboreal\\_vegetation.pdf](http://www.tceq.texas.gov/assets/public/implementation/air/am/contracts/reports/ot/h/5820564593FY0925-20110419-tamu-expension_tx_lulc_arboreal_vegetation.pdf)

Texas Water Development Board, 2012. 2012 State Water Plan. Retrieved September 17, 2013 from [http://www.twdb.state.tx.us/publications/state\\_water\\_plan/2012/04.pdf](http://www.twdb.state.tx.us/publications/state_water_plan/2012/04.pdf)

Yarwood, G., Shepard, S., Sakulyanontvittaya, T., Piyachaturawat, P., and Guenther, A., 2010. User's Guide to The Global Biosphere Emissions and Interactions System (GloBEIS3) Version 3.5.

## **2.0 Overview of soil moisture databases**

Methods used to measure soil moisture have been recently and thoroughly reviewed elsewhere, (e.g., Wagner et al, 2007; Robinson et al., 2008; Seneviratne et al., 2010; Dobriyal et al., 2012; Oschner et al., 2013). This section provides a brief summary of ground-based, satellite-based, and model-based methodologies and introduces the primary soil moisture datasets utilized for our work.

### **2.1 Ground-based**

In-situ soil moisture measurements can be made directly and indirectly as well as destructively and non-destructively. An example of a direct and destructive method is gravimetric, which involves oven drying a sample of known volume; the water content is the difference between the pre- and post-dried soil weights (Dobriyal et al., 2012). The gravimetric method is often used in support of constructing calibration curves for indirect methods (Kutilek and Nielsen, 1994). An example of a non-destructive method is the neutron probe (Zreda et al., 2008; 2012). A radioactive source is used to release high energy, fast moving neutrons. These neutrons are slowed by collisions with nuclei in the atoms of the surrounding soil including within water molecule hydrogen atoms. The output from the neutron probes can be directly related to volumetric soil water content via site-specific calibration curves (Oschner et al., 2013).

Indirect methodologies measure some property of the soil that is dependent on soil water content (Kutilek and Nielsen, 1994). Capacitance techniques typically employ buried metal plates or rods that are connected to an electric oscillator. When an electric circuit is applied, changes in the frequency of the circuit are related to changes in volumetric soil moisture so that a soil-specific calibration is required. Another methodology is time domain reflectometry that measures the time it takes for a pulse of energy to move through a transmission line buried in the soil; travel time is greater (i.e., slower velocity) in wetter soils. The pulse velocity is correlated to soil moisture and no soil specific calibration is required (Dobriyal et al., 2012).

In order to control for variations in salinity that can impact the electrical properties of soils, volumetric soil moisture can also be estimated using the gypsum block method. Gypsum is saturated with a calcium sulfite solution and the block, which is buried in the soil, absorbs moisture. Electrodes in the block are used to measure conductance, which increases with increasing moisture content. Other ground-based methods used to estimate soil moisture include tensiometers that measure the suction force of water and ground penetrating radar, among others (Dobriyal et al., 2012). Additional information on in-situ ground-monitoring networks currently operating in Texas and surrounding states is provided in Section 3.0 of this report.

## 2.2 Satellite-based

Satellite-based active and passive microwave instrumentation allows for frequent (e.g., every few days) and global observations that can be used to estimate soil moisture. The surface emissivity is substantially affected by the dielectric constant of water making the microwave portion of the electromagnetic spectrum most suitable for quantitative estimates (e.g., Wagner et al., 2007; Seneviratne et al., 2010). Radiation at specific frequencies is sensed by the satellite instrumentation as brightness temperatures that are affected by a variety of surface and atmospheric physical properties via scattering, absorption, and emission processes. In order to relate brightness temperatures to soil moisture, a retrieval algorithm is typically employed to simulate the impacts of relevant environmental variables at the specific radiation frequency. The lower microwave frequencies (<10 GHz) such as L-band (1-2 GHz) and C-band (4-8 GHz) are optimal for soil moisture retrievals because of reduced atmospheric interactions, better transparency to vegetation, and greater sensitivity to soil moisture compared to higher frequencies; however, microwave sensing can only measure water within the top few centimeters of soil (e.g., Oschner et al., 2013; Nghiem et al., 2012).

Since the 1970s, remote sensing approaches have typically used C-band microwave frequencies from available satellite-based observations to investigate soil moisture. For example, several retrieval algorithms have been developed using the passive Advanced Microwave Scanning Radiometer for the Earth Observing System (AMSR-E) that flew aboard the NASA Aqua satellite and collected dual-polarized brightness temperatures at 6.9 and 10.6 GHz from 2002 through October 2011. Active systems such as radars and scatterometers emit at a higher frequency and so have finer spatial resolution compared to microwave sensors. The Advanced SCATterometer (ASCAT) launched by European Space Agency (ESA) in 2006 aboard the MetOP-A meteorological satellite (as well as a previous iteration that flew aboard the European Remote Sensing) collects data at 5.26 GHz and can provide daily soil moisture retrievals at 50 (nominal) and 25 km spatial resolutions (Wagner et al., 2013). Another continuing active C-band radiometer is the Advanced Microwave Scanning Radiometer-2 (AMSR-2) on Japanese Aerospace Exploration Agency Global Change Observation Mission-Water (GCOM-W) that includes data collection at 6.95 and 7.3 GHz since May 2012 ([http://global.jaxa.jp/projects/sat/gcom\\_w/index.html](http://global.jaxa.jp/projects/sat/gcom_w/index.html)).

Although soil moisture retrievals have been performed using sub-optimal observations such as those previously discussed, the L-band wavelength is preferred because of better penetration through vegetation (e.g., Jackson and Schmugge, 1989, 1991). The first satellite dedicated to soil moisture sensing is the Soil Moisture and Ocean Salinity (SMOS) mission by ESA launched in November 2009. Dual polarization observations at 1.4 GHz are achieved using 69 small antennae resulting in a ground resolution of 50 km (Kerr et al., 2010, 2012) with repeat coverage every 2-3 days. NASA's Aquarius sensor, operational since August 2011, is equipped with a quad-polarized scatterometer at 1.26 GHz and a dual-pol radiometer at 1.41 GHz; the mission is intended primarily to map

ocean salinity as well as soil moisture, at a spatial resolution of 100 km with weekly repeat coverage (<http://podaac.jpl.nasa.gov/aquarius>). Microwave emissions measured passively are more robust but provide a coarser resolution compared to backscatter (measured actively) that provides greater spatial resolution but is more sensitive to soil roughness and vegetation. The most recent mission specifically designed to measure soil moisture is NASA’s Soil Moisture Active Passive (SMAP), launched in January 2015, which also combines active and passive observations at 1.26 and 1.41 GHz, respectively, to provide global soil moisture at an unprecedented spatial (9km/36km for active/passive) and temporal (2-3 days) resolutions (<http://smap.jpl.nasa.gov/>).

Table 1 summarizes currently operational satellite missions that collect data that have been used to retrieve soil moisture. Although the above satellite datasets can provide crucial information on the spatial and temporal variations of soil moisture that assist studies of land-atmospheric-hydrological processes such as the assessment of drought, the microwave frequencies are only sensitive to soil moisture within the near-surface layer (typically 0-5cm) and cannot directly provide information on water contents for deeper layers. Root zone moisture is essential for studies of plant processes such as biogenic emissions; the root zone is usually found within the 25-60cm soil layer but can extend to depths of 2 meters dependent on the predominant vegetation. Recent studies have estimated root zone water contents from satellite observations (e.g., Ford et al., 2015); however, evaluation is difficult given the temporal and spatial variability of soil moisture. In recognition of the importance of deep soil moisture, SMAP mission will specifically develop model-based estimates of soil moisture to a depth of 1 meter that are consistent with the assimilated SMAP observations (Oschner et al., 2013).

**Table 1 Selected satellite missions (adapted directly from Ford et al., 2015).**

Satellite	Temporal Resolution	Spatial Resolution (km)	Passive (P) or Active (A)	C-Band or L-Band
SSM/I	Daily	25	P	C
TRMM TM	Daily	50-56	P	C
Aqua AMSR-E	Daily	56	P	C
ERS 1-2 SCAT	35 days	25-50	A	C
SMOS	3 days	50	P	L
SMAP	2-3 days	10-40	Both	L
MetOp ASCAT	29 days	50	A	C

Because the drought response of plants is dependent, in part, on soil moisture within the root zone, we did not utilize satellite-based soil moisture estimates in our work. In future, continuing research to extend satellite estimates of near-surface soil moisture to deeper depths will likely provide beneficial insight to vegetation studies especially when the data are combined with additional observations such as in-situ measurements and/or model-based predictions.

## 2.3 Model-based

Most land surface models (LSMs) track soil moisture as a prognostic (state) variable. Given the lack of in-situ large-scale observations of soil moisture, model-generated predictions driven by meteorological forcings have been produced as a data product (Koster et al., 2009; Dirmeyer et al., 2004) for the scientific community. LSMs are commonly coupled to an atmospheric general circulation model or run uncoupled (i.e., offline) using near-surface meteorological analyses as the upper boundary condition (Dirmeyer et al., 2004). The soil moisture simulation is strongly impacted by the characteristics of the LSM as well as the quality of the meteorological datasets (Dirmeyer et al., 1999). Different LSMs may provide very different estimates of soil moisture, even when driven by identical atmospheric datasets (Entin et al., 1999; Xia et al., 2014). Nonetheless, the LSM approach represents the current state of the art for producing global long-term analyses of soil moisture (Dirmeyer et al., 2004; Xia et al., 2014).

LSMs that simulate soil moisture can be classified into different basic categories. For example, LSMs can use a simple water-budget model (or “bucket” model) or a complicated parameterization that fully represents the water and energy budget and the impact of vegetation on these budgets explicitly (Dirmeyer et al., 2004). These LSMs can also be run as coupled and uncoupled (offline) models based on how the meteorological forcings are used to drive the simulation of soil moisture.

Coupled land-atmosphere surface models include general circulation models such as those evaluated for the Atmospheric Model Intercomparison Project (AMIP; Robock et al., 1998; Srinivasan et al., 2000) and the fully coupled ocean-atmosphere-land-sea ice models such as Coupled Model Intercomparison Project (CMIP5) CMIP5 (Taylor et al., 2012). The more commonly used predictions of soil moisture come from the utilization of reanalysis models that assimilate available observations for atmospheric variables. These models also dynamically simulate the interactions and feedbacks between the land and atmosphere. These reanalysis products include the National Center for Environmental Prediction-National Center for Atmospheric Research (NCEP-NCAR, Kalnay et al., 1996), the NCEP-Department of Energy (NCEP-DOE; Kanamitsu et al., 2002), the 40-yr European Centre for Medium-Range Weather Forecasts (ECMWF) Reanalysis (ERA-40, Simmons and Gibson 2002), and the more recent ERA-Interim, NASA’s Modern-Era Retrospective Analysis for Research and Applications (MERRA) (Reichle et al., 2011). These reanalysis models produce global soil moisture products and have been widely evaluated (e.g., Dirmeyer et al., 2004, 2006; Li et al., 2005; Lu et al., 2005). Similar reanalysis efforts have been made at regional scales, for example, the NCEP North American Regional Reanalysis (NARR) provides soil moisture at a high spatial resolution (32km). The coupled models also produce weather forecasts (e.g., Global Forecast System, GFS) and seasonal forecast (e.g., Climate Forecast System Version 2, CFSv2) which typically include soil moisture prediction.

In order to remove the impact of biases in meteorological predictions often inherent to a specific atmospheric model, LSMs can be run offline using reanalysis meteorological forcings as input. One such effort is the Global Land Data Assimilation System (GLDAS, Rodell et al., 2004), which provides real-time estimates of soil moisture fields. Observation-based precipitation and downward radiation products and the best available analyses from atmospheric data assimilation systems are employed. The GLDAS provides high resolution soil moisture products including 1-degree and 0.25-degree resolution for 1979-present simulations using the Noah, CLM, VIC, and Mosaic land surface models. A regional analog is the North American Land Data Assimilation System (NLDAS; Mitchell et al., 2004). This system aims to reduce errors in soil moisture and energy storage, which are often present in numerical weather prediction models and degrade the accuracy of weather forecasts. NLDAS is currently running in near real-time on a 1/8th-degree grid over central North America; retrospective NLDAS datasets and simulations also extend back to 1979. To-date, NLDAS (version 2) provides long-term soil moisture at varying depths with the highest spatial resolution and highest quality of atmospheric forcing over U.S.

## **2.4 Soil moisture datasets employed in our study**

In support of our project, we investigate available in-situ monitoring data collected at Soil Climate Analysis Network (SCAN) and Climate Research Network (CRN) locations within the 12km grid domain (ref. Section 3). These measurements are collected at depths ranging between 5cm and 100cm that span the root zone; however, these observations are sparse and cannot be used to represent regional soil moisture conditions throughout eastern Texas. We employ the North American Land Data Assimilation System Phase 2 (NLDAS-2) dataset to provide the estimates of soil moisture required to support BVOC modeling in the 4km grid domain. The NLDAS-2 data provide gridded soil moisture estimates encompassing the time period of interest (i.e., 2006-2013) using consistent and high quality meteorological forcings. NLDAS-2 has been reasonably evaluated across the South Central U.S. (Xia et al., 2012, 2014; Cai et al., 2014ab) including studies focused on 2011 drought conditions in Texas. Subsequent sections of this report evaluate the NLDAS-2 datasets in conjunction with observations (ref. Sections 4 and 5) as well as independently (ref. Section 6) and in support of MEGAN modeling of isoprene emissions (Section 7.0).

## **2.5 References**

Cai, X., Z.-L. Yang, C. H. David, G.-Y. Niu, and M. Rodell, 2014a. Hydrological evaluation of the Noah-MP land surface model for the Mississippi River Basin, *J. Geophys. Res. Atmos.*, 119, 23–38, doi:10.1002/2013JD020792.

Cai, X., Z.-L. Yang, Y. Xia, M. Huang, H. Wei, L. R. Leung, and M. B. Ek, 2014b. Assessment of simulated water balance from Noah, Noah-MP, CLM, and VIC over CONUS using the

NLDAS test bed, *J. Geophys. Res. Atmos.*, 119, 13,751–13,770, doi:10.1002/2014JD022113.

Dee, DP, SM Uppala, and AJ Simmons, 2011. The ERA-Interim reanalysis: Configuration and performance of the data assimilation system. *Quarterly Journal of the Royal Meteorological Society*, doi:10.1002/qj.828. <http://onlinelibrary.wiley.com/doi/10.1002/qj.828/full>.

Dirmeyer, PA, Z Guo, and X Gao, 2004: Comparison, validation, and transferability of eight multiyear global soil wetness products. *Journal of Hydrometeorology*, <http://journals.ametsoc.org/doi/abs/10.1175/JHM-388.1>.

Dirmeyer, PA, and F. J. Zeng, 1999: An update to the distribution and treatment of vegetation and soil properties in SSiB. COLA Tech. Rep. 78, 25 pp. [Available from the Center for Ocean–Land–Atmosphere Studies, 4041 Powder Mill Road, Suite 302, Calverton, MD 20705.]

Dobriyal, P., A. Qureshi, R. Badola, and S.A. Hussain. 2012. A review of the methods available for estimating soil moisture and its implications for water resource management. *J. Hydrol.* 458–459:110–117. doi:10.1016/j.jhydrol.2012.06.021

Entin, J. K., A. Robock, K. Ya. Vinnikov, V. Zabelin, S. Liu, and A. Namkhai, 1999: Evaluation of Global Soil Wetness Project soil moisture simulations. *J. Meteor. Soc. Japan*, 77, 183–198.

Ford, T. W., Harris, E., and Quiring, S. M., 2014. Estimating root zone soil moisture using near-surface observations from SMOS, *Hydrol. Earth Syst. Sci.*, 18, 139-154, doi:10.5194/hess-18-139-2014, 2014.

Jackson, T.J., and T.J. Schmugge, 1989. Passive microwave remote-sensing system for soil-moisture: Some supporting research. *IEEE Trans. Geosci. Remote Sens.* 27:225–235. doi:10.1109/36.20301

Jackson, T.J., and T.J. Schmugge, 1991. Vegetation effects on the microwave emission of soils. *Remote Sens. Environ.* 36:203–212. doi:10.1016/0034-4257(91)90057-D  
Kalnay, E., and Coauthors, 1996: The NCEP/NCAR 40-Year Reanalysis Project. *Bull. Amer. Meteor. Soc.*, 77, 437–471.

Kanamitsu, M., W. Ebisuzaki, J. Woollen, S.-K. Yang, J. J. Hnilo, M. Fiorino, and G. L. Potter, 2002. NCEP-DOE AMIP-II Reanalysis (R-2). *Bull. Amer. Meteor. Soc.*, 83, 1631–1643.

Kerr, Y.H., P. Waldteufel, P. Richaume, J.P. Wigneron, P. Ferrazzoli, A. Mahmoodi, et al., 2012. The SMOS soil moisture retrieval algorithm. *IEEE Trans. Geosci. Remote Sens.* 50:1384–1403. doi:10.1109/TGRS.2012.2184548

Kerr, Y.H., P. Waldteufel, J.P. Wigneron, S. Delwart, F. Cabot, J. Boutin, et al., 2010. The SMOS mission: New tool for monitoring key elements of the global water cycle. *Proc. IEEE* 98:666–687. doi:10.1109/JPROC.2010.2043032

Koster, R.D., Z. Guo, P.A. Dirmeyer, R. Yang, K. Mitchell, and M.J. Puma, 2009: On the nature of soil moisture in land surface models. *J. Climate*, 22, 4322–4335, doi:10.1175/2009JCLI2832.1.

Kutilek M., Nielsen D.R., 1994. *Soil Hydrology*. Catena Verlag, Cremlingen.

Li, H. B., A. Robock, S. Liu, X. Mo, and P. Viterbo, 2005: Evaluation of reanalysis soil moisture simulations using updated Chinese soil moisture observations. *J. Hydrometeor.*, 6, 180– 193.

Lu, C. H., M. Kanamitsu, J. O. Roads, W. Ebisuzaki, K. E. Mitchell, and D. Lohmann, 2005. Evaluation of soil moisture in the NCEP–NCAR and NCEP–DOE global reanalyses. *J. Hydrometeor.*, 6, 391–408.

Mitchell, KE, D Lohmann, and PR Houser, 2004. The multi-institution North American Land Data Assimilation System (NLDAS): Utilizing multiple GCIP products and partners in a continental distributed hydrological modeling system. *Journal of Geophysical Research Atmospheres*, doi:10.1029/2003JD003823.  
<http://onlinelibrary.wiley.com/doi/10.1029/2003J>

Nghiem, S.V., Brian D. Wardlow, David Alured, Mard D. Svoboda, Doug LeComte, Matthew Rosencrans, Steven K. Chan, and Gregory Neumann, 2012. Microwave Remote Sensing of Soil Moisture Science and Applications, in "Remote Sensing of Drought: Innovative Monitoring Approaches", B. Wardlow, M. Anderson and J. Verdin (eds.), p. 270, Taylor and Francis, London, United Kingdom.

Ochsner, Tyson E.; Cosh, Michael H.; Cuenca, Richard H.; Dorigo, Wouter A.; Draper, Clara S.; Hagimoto, Yutaka; Kerr, Yann H.; Njoku, Eni G.; Small, Eric E.; Zreda, Marek, 2013. State of the art in large-scale soil moisture monitoring. *Soil Science Society of America Journal*, 77(6), 1888–1919. doi:10.2136/sssaj2013.03.0093

Reichle, R. H., R. D. Koster, G. J. M. De Lannoy, B. A. Forman, Q. Liu, S. P. P. Mahanama, and A. Toure, 2011. Assessment and enhancement of MERRA land surface hydrology estimates, *Journal of Climate*, 24, 6322–6338, doi:10.1175/JCLI-D-10-05033.1.

Robinson, D.A., C.S. Campbell, J.W. Hopmans, B.K. Hornbuckle, S.B. Jones, R. Knight, et al., 2008. Soil moisture measurement for ecological and hydrological watershed-scale observatories: A review. *Vadose Zone J.* 7:358–389. doi:10.2136/vzj2007.0143

Robock, A., C. A. Schlosser, K. Ya. Vinnikov, N. A. Speranskaya, J. K. Entin, and S. Qiu, 1998. Evaluation of the AMIP soil moisture simulations. *Global Planet. Change*, 19, 181–208.

Rodell, M, PR Houser, and U Jambor, 2004. The global land data assimilation system. *Bulletin of the American Meteorological Society*.  
<http://journals.ametsoc.org/doi/abs/10.1175/BAMS-85-3-381>.

Seneviratne, S.I., Corti, T., Davin, E.L., Hirschi, M., Jaeger, E.B., Lehner, I., Orlowsky, B., Teuling, A.J., 2010. Investigating soil moisture–climate interactions in a changing climate: A review. *Earth-Science Rev.* 99, 125–161.

Simmons, A. J., and J. K. Gibson, 2000. The ERA-40 Project Plan. ERA-40 Project Report Series 1, 63 pp.

Srinivasan, G., A. Robock, J. K. Entin, L. Luo, K. Ya. Vinnikov, and P. Viterbo, 2000. Soil moisture simulations in revised AMIP models. *J. Geophys. Res.*, 105 (D21), 26 635–26 644.

Taylor, K. E., R. J. Stouffer, G. A. Meehl, 2012. An overview of CMIP5 and the experiment design. *Bull. Am. Meteorol. Soc.* 93, 485–498.

Wagner, W., S. Hahn, R. Kidd, T. Melzer, Z. Bartalis, S. Hasenauer, et al., 2013. The ASCAT soil moisture product: A review of its specifications, validation results, and emerging applications. *Meteorol. Z.* 22:5–33. doi:10.1127/0941-2948/2013/0399  
doi:10.1016/j.earscirev.2010.02.004

Xia, Y., K. Mitchell, M. Ek, J. Sheffield, B. Cosgrove, E. Wood, L. Luo, C. Alonge, H. Wei, J. Meng, B. Livneh, D. Lettenmaier, V. Koren, Q. Duan, K. Mo, Y. Fan, and D. Mocko, 2012. Continental-scale water and energy flux analysis and validation for the North American Land Data Assimilation System project phase 2 (NLDAS-2): 1. Intercomparison and application of model products, *J. Geophys. Res.*, 117, D03109, doi:10.1029/2011JD016048.

Xia, Y., J. Sheffield, M. B. Ek, J. Dong, N. Chaney, H. Wei, J. Meng, and E. F. Wood, 2014. Evaluation of multi-model simulated soil moisture in NLDAS-2, *J. Hydrol.*, 512, 107–125, doi:10.1016/j.jhydrol.2014.02.027.

Zreda, M., D. Desilets, T.P.A. Ferré, and R.L. Scott, 2008. Measuring soil moisture content non-invasively at intermediate spatial scale using cosmic-ray neutrons. *Geophys. Res. Lett.* 35:L21402.. doi:10.1029/2008GL035655

Zreda, M., W.J. Shuttleworth, X. Zeng, C. Zweck, D. Desilets, T. Franz, and R. Rosolem, 2012. COSMOS: The COsmic-ray Soil Moisture Observing System. *Hydrol. Earth Syst. Sci.* 16:4079–4099. doi:10.5194/hess-16-4079-2012

### 3.0 In-situ soil moisture monitoring

There are a variety of networks currently operating in the U.S. at both the state and national levels. A comprehensive review of monitoring networks with spatial extents greater than  $100^2 \text{ km}^2$  has recently been provided by Ochsner et al. (2013). This section provides information on networks operating within Texas and surrounding states as well as a summary of observations at monitoring stations in eastern Texas.

#### 3.1 Overview of large-scale networks

The Illinois Water Survey began one of the first long-term programs in 1981 using neutron probes to measure soil moisture as frequently as twice monthly (Hollinger and Isard, 1994). In 1998, the stations were converted to dielectric sensors to provide continuous monitoring currently at depths of 5, 10, 20, and 50 cm at 19 individual locations (<http://www.isws.illinois.edu/warm/soil/>).

A second pioneering soil monitoring initiative was begun in 1991 by University of Oklahoma and Oklahoma State University; by 1994, the Oklahoma Mesonet consisted of 120 automated stations with at least one in each county (<https://www.mesonet.org/index.php/site/about>). The Oklahoma Mesonet hosts a suite of meteorological measurements (e.g., air and soil temperature, winds, pressure, precipitation) that provides data for mesoscale weather studies and climate research (Brock et al., 1995; McPherson et al., 2007). Heat dissipation sensors are used to measure soil moisture at 5, 25, 60, and (at some locations) 75 cm; network-wide accuracy of the soil moisture observations has been estimated at  $\pm 0.053 \text{ m}^3/\text{m}^3$  (Scott et al., 2013).

In Texas, Texas Tech University initiated West Texas Mesonet measurements in 2000 with a mission to provide meteorological data to support operational meteorology, agriculture and farming, research, and media (<http://www.mesonet.ttu.edu/who.htm>). Currently, the network consists of 84 surface stations (including 3 in far southeastern New Mexico), one radar wind profiler, seven boundary-layer SONIC Detection And Ranging (SODAR) instruments, and one upper-air sounding (rawinsonde) system. The surface stations collect soil moisture and meteorological measurements (e.g., winds, pressure, solar radiation, soil temperature, precipitation, leaf wetness). Soil moisture is measured at depths of 5, 20, 60, and 75 cm using water content reflectometers (Schroeder et al., 2005). The density of monitors is greatest in portions of northwestern Texas south of the Texas Panhandle.

With regard to Texas stations that are part of nationwide soil moisture monitoring, the Soil Climate Analysis Network (SCAN), Climate Research Network (CRN), and Cosmic Ray Soil Moisture Observing System (COSMOS) operate fourteen, eight, and two stations, respectively. SCAN originated in the 1990s from a pilot soil moisture-soil temperature program initiated by the National Resources Conservation Service (NRCS) to measure

these parameters at a national scale (Ochsner et al., 2013). Currently, SCAN consists of 200 U.S. stations located in 40 states; soil moisture monitoring is conducted at depths of 5, 10, 20, 50, and 100 cm (where possible) using dielectric constant instrumentation (<http://www.wcc.nrcs.usda.gov/scan/scan%20brochure.pdf>). Archived hourly and daily soil moisture observations are publicly available from the NRCS SCAN website (<http://www.wcc.nrcs.usda.gov/scan/>).

The U.S. Climate Reference Network (CRN) consists of 114 stations in the conterminous U.S. (with additional stations in Alaska and Hawaii) developed and maintained by the National Oceanic and Atmospheric Administration (NOAA) for the purpose of weather and climate monitoring. The monitoring locations are sited in pristine environments expected to be free of human disturbance and development for many decades and parameters such as temperature and precipitation are measured in triplicate to support maintenance and continuity of record (<http://www.ncdc.noaa.gov/crn>). Soil moisture sensors are being added at CRN stations based on the SCAN configuration (Ochsner et al. (2013)). The archived quality-assured sub-hourly, hourly, daily, and monthly soil moisture datasets are publicly available from the NOAA CRN website (<http://www.ncdc.noaa.gov/crn/qcdatasets.html>).

The most recent national-scale monitoring network is the Cosmic Ray Soil Moisture Observing System (COSMOS) consisting of 67 individual locations in 2013 (Ochsner et al., 2013) with additional locations planned (<http://cosmos.hwr.arizona.edu/Docs/ProjectSummary.pdf>). COSMOS has the aim to provide area-averaged soil moisture data for atmospheric applications. Cosmic-ray protons impinging on the top of the atmosphere trigger a self-propagating cascade of secondary neutrons leading to the creation of fast neutrons; because fast neutrons are strongly affected by hydrogen, their measured intensity is impacted by variations in soil moisture (Zreda et al., 2008; 2012). Stationary probes installed above the surface to measure and transmit neutron intensity have a footprint of hundreds of meters and an effective depth that varies from ~70 cm in dry soils to ~12 cm in saturated soils (Zreda et al, 2008). Site-specific calibration is required to correct for ancillary effects such as surface water (including snow), soil type, lattice water and organic matter, vegetation, and atmospheric water vapor (Ochsner et al., 2013). Franz et al. (2012) found a root mean square error of 0.017 m<sup>3</sup>/m<sup>3</sup> for a well-calibrated probe at a desert site in Tucson, Arizona.

Beginning in late 2014, the Texas Soil Observation Network (TxSON) provides intensive monitoring for soil moisture within a 500 square mile area located near Fredericksburg, Texas, along the Pedernales River within the Colorado River Basin. TxSON was designed by researchers at The University of Texas at Austin in collaboration with NASA; the network currently consists of 36 soil moisture monitoring stations and 7 Lower Colorado River Authority (LCRA) Hydromet stations supplemented with soil moisture sensors. One of the goals of TxSON is to assist in the validation and refinement of satellite and land surface model products produced by programs such as NASA's Soil Moisture Active Passive (SMAP). Hourly measurements (soil moisture and temperature, rainfall, air

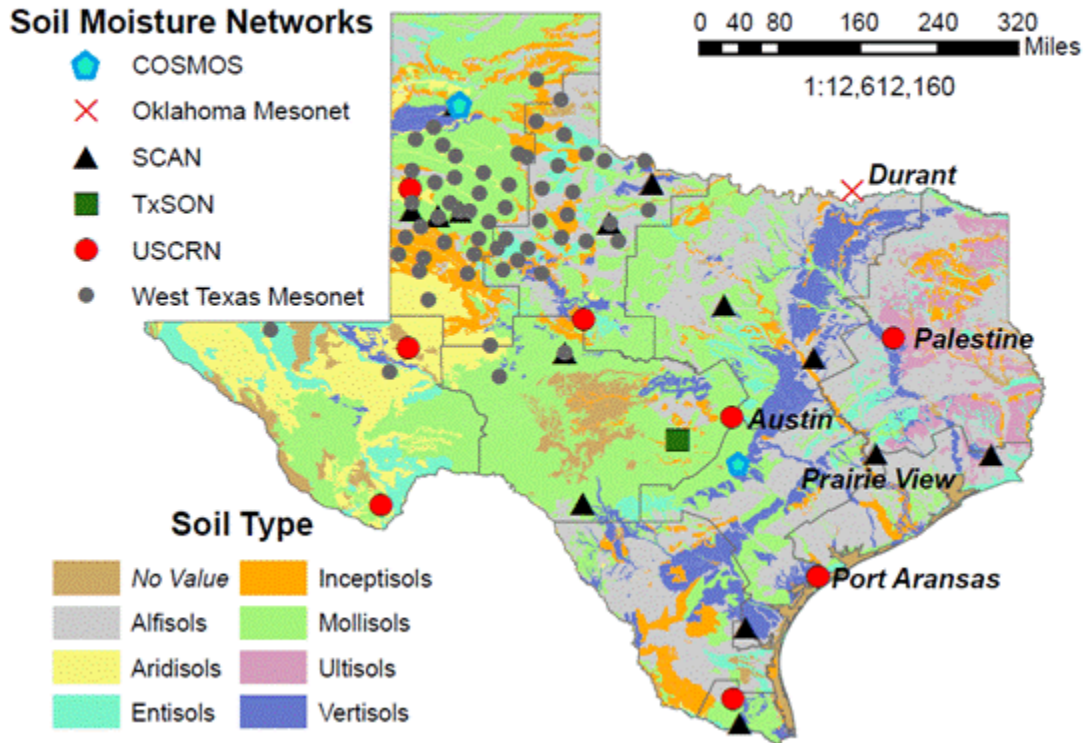
temperature and humidity) are available in near real-time via the TxSON website (<http://www.beg.utexas.edu/txson/>).

Figure 3 shows the locations of Texas soil monitors overlain on a soil types map. The TxSON intensive monitoring region is shown using a dark green square. The soil types map was constructed using datasets provided by the National Resource Conservation Service (NRCS) of the U.S. Department of Agriculture (USDA) distributed in U.S. Geological Survey (USGS) Digital Line Graph (DLG-3) Optional Distribution Format ([http://www.ctre.iastate.edu/research/bts\\_wb/cd-rom/spatial/dlg.htm](http://www.ctre.iastate.edu/research/bts_wb/cd-rom/spatial/dlg.htm)). The Soil Survey Geographic Data Base (SSURGO), which is created using field methods and aerial photos, provides the most detailed level of soil information. The detailed SSURGO soil survey maps, or if unavailable data on geology, topography, vegetation, and climate together with satellite images, are generalized to create the State Soil Geographic Data Base (STATSGO). STATSGO is mapped on USGS 1:250,000-scale topographic quadrangle series and is the source of the USDA soil taxonomy classification mapping shown in Figure 3. Table 2 provides technical summaries of selected chemical and physical soil characteristics for the seven Texas soil types according to USDA (1999).

As demonstrated in Figure 3, soil moisture monitoring has historically been sparse throughout much of Texas; the four stations labeled in Figure 3 (“Palestine”, “Austin”, “Prairie View”, “Port Aransas”) are the only monitors in eastern Texas that collected soil moisture measurements at multiple depths for one or more years during 2006-2013. Soil moisture observations from these four locations, in addition to measurements at one Oklahoma Mesonet station (“Durant” also shown in Figure 3), are the focus of analyses presented in the following section of this report.

**Figure 3** Locations of soil moisture observation stations in Texas overlain on a soils type map. The boundaries show the ten Texas climate divisions. The intensive TxSON monitoring area is shown by the dark green square. A summary of soil moisture measurements during 2006-2013 collected at the four labeled locations in eastern Texas (and one additional location in southeastern Oklahoma) are presented in the Section 3.2 of this report.

## Locations of Soil Moisture Observation Stations



**Table 2 Abbreviated descriptions from Chapter 6 *The Categories of Soil Taxonomy* from “Soil Taxonomy A Basic System of Soil Classification for Making and Interpreting Soil Surveys” (USDA, 1999) for the chemical and physical properties of the seven Texas soil types (ref. Figure 3).**

Soil Type	Description (abbreviated from USDA, 1999)
Alfisols	Properties include a combination of ochric or umbric epipedon, an argillic or natric horizon, a medium to high supply of bases in the soils, and water available to mesophytic plants more than half the year or more than 3 consecutive months. Because these soils have water and bases, they are, as a whole, intensively used.
Aridisols	Properties include one or more pedogenic horizons, a surface horizon or horizons not significantly darkened by humus, and an absence of deep, wide cracks (see Vertisols) and andic soil properties. Aridisols are primarily soils of arid areas; if irrigated, many are suitable for a wide variety of crops.
Entisols	Properties include dominance of mineral soil materials and absence of distinct pedogenic horizons. Entisols support plants and may occur in any climate and under any vegetation.
Inceptisols	Inceptisols have a wide range in characteristics and occur in a wide variety of climates formed in any environment except arid, with comparable differences in vegetation. Properties include a combination of water available to plants for more than half the year or more than 3 consecutive months and one or more pedogenic horizons of alteration or concentration with little accumulation of translocated materials other than carbonates or amorphous silica.
Mollisols	Mollisols have a combination of very dark brown to black surface horizon (mollic epipedon), a dominance of calcium, crystalline clay minerals, and <30% clay in some horizon above 50 cm if the soils have deep wide cracks (>1 cm). Mollisols typically form under grass in climates that have a moderate to pronounced soil moisture deficit, but can also form under a forest ecosystem and sometimes in marshes or in mals in humid climates.
Ultisols	Utisols have markers of clay translocation like Alifols but have markers of intensive leaching absent in Alfisols. Properties include argillic horizon and a low supply of bases, particularly in the lower horizons. Cation exchange is moderate or low; in uncultivated soils the highest base saturation is a few cm beneath the surface. Because they are commonly warm and moist, they can be made highly productive if fertilizer is applied.
Vertisols	Properties include a high bulk density when the soils are dry, low or very low hydraulic conductivity when soils are moist, an appreciable rise and fall of the soil when the soils are moist, and then dry and rapid drying as a result of open cracks. Unique preopertys are high content of clay, cracks that open and close periodically, and evidence of soil movement in the form of slickensides and of wedge-shaped structural aggregates that are tilted at an angle from the horizontal.

### 3.2 Eastern Texas in-situ data during 2006-2013

Because this project investigates the impact of soil moisture variability on the prediction of biogenic emissions within eastern portions of Texas, analyses of in-situ soil moisture data are focused on the four labeled Texas sites in Figure 3 (i.e., “Palestine”, “Austin”, “Prairie View”, “Port Aransas”) in addition to the one Oklahoma Mesonet station (intended to represent conditions in northeastern Texas) adjacent to the Red River in southeastern Oklahoma (“Durant”). A summary of the available soil moisture observations at each of these five monitoring locations is provided in Table 3. The measurements for Texas stations were retrieved directly from the SCAN and CRN websites; daily data for the Durant Oklahoma Mesonet station were retrieved from the North American Soil Moisture Database (NASMD; <http://soilmoisture.tamu.edu/>) and were only available (at the time of this data analysis) through September 2012.

#### *Example daily data (year 2011 at Palestine)*

To demonstrate the range of variability of soil moisture at a relatively high temporal resolution, Figure 4 presents daily average soil moisture values (5/10/20/50/100cm) during 2011 at the Palestine CRN station in addition to daily total precipitation measured at this location. Soil moisture values at each depth during 2011, a year characterized by all-time record heat and drought in Texas, are greatest during portions of the winter months, likely associated, in part, to periodic rainfall events as well as relatively cooler temperatures. Minimum soil moisture contents at any given depth occurred during wide portions of March through November. Moisture availabilities were characterized by a general increase with increasing depth; for example, 5cm soil moisture during February ranged 0.17-0.28 m<sup>3</sup>/m<sup>3</sup> compared to nearly constant values of 0.43 m<sup>3</sup>/m<sup>3</sup> at 100cm. Soil moisture availability diminished substantially by March, reaching lows of nearly zero and 0.1 m<sup>3</sup>/m<sup>3</sup> at 5cm and 100cm, respectively, for much of the summer and fall.

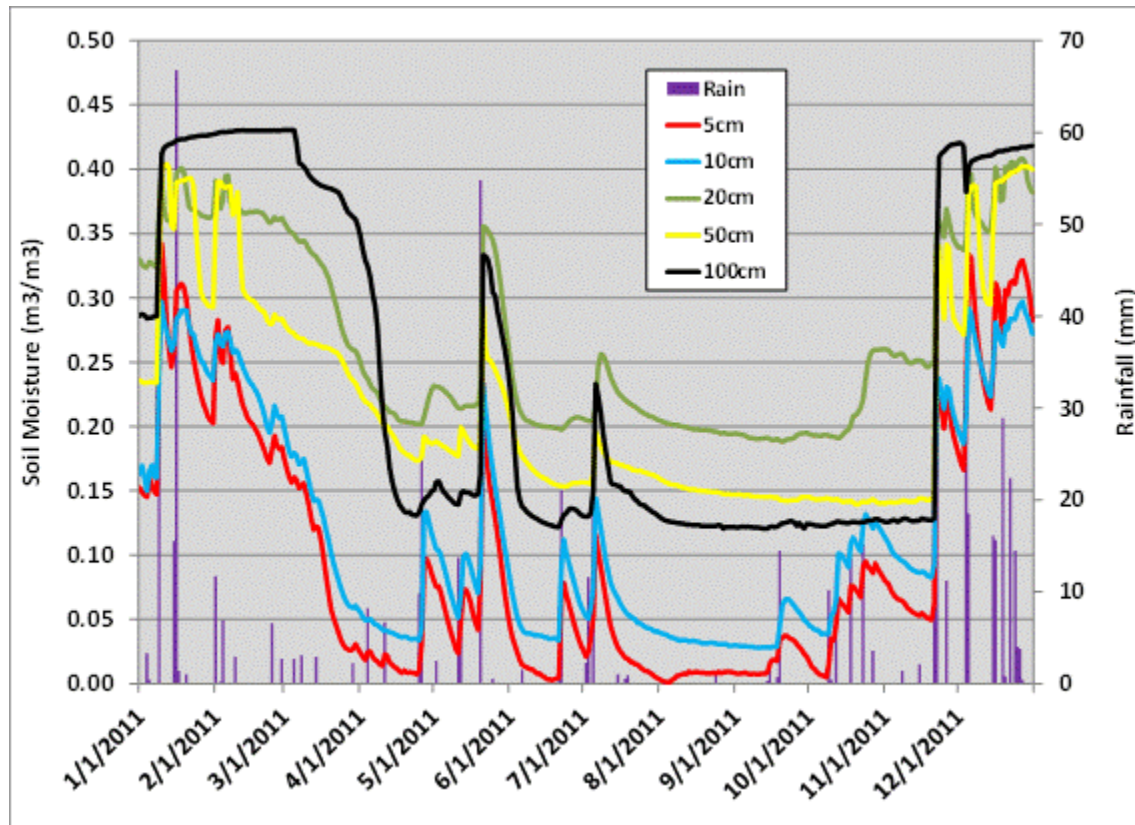
Figure 4 clearly demonstrates the impact of sporadic rainfall events on soil moisture during the growing season (March-October). The penetration of these periodic wetting events is partially dependent on the magnitude and intensity of rainfall. For example, a light precipitation episode on May 2<sup>nd</sup> (2.5 mm or 0.1 in.) is associated with a quick increase in 5cm soil moisture from 0.01 to 0.13 m<sup>3</sup>/m<sup>3</sup>; the impact on deeper soil layers is comparatively modest. Several low magnitude rainfall events occurred May 11<sup>th</sup>-12<sup>th</sup> followed by rainfall of 55 mm (2.2 in.) on May 20<sup>th</sup>. This relatively heavy precipitation day was associated with a substantial and rapid increase in soil moisture at all depths; for example, 5cm soil moisture spiked to 0.23 m<sup>3</sup>/m<sup>3</sup> from 0.04 m<sup>3</sup>/m<sup>3</sup> on May 20<sup>th</sup> while 100cm soil moisture more than doubled from 0.15 m<sup>3</sup>/m<sup>3</sup> on May 19<sup>th</sup> (prior to the rain event) to 0.33 m<sup>3</sup>/m<sup>3</sup> on May 21<sup>st</sup> (one day following the rain event). The return to pre-May 20<sup>th</sup> soil moisture contents was slightly quicker within the near-surface levels compared to the deeper soil layers; for example, 5cm soil moisture is nearly zero by

June 1<sup>st</sup> while 100cm soil moisture remained greater than the 0.15 m<sup>3</sup>/m<sup>3</sup> May 19<sup>th</sup> values until June 5<sup>th</sup>.

**Table 3 Summary of soil moisture measurements at selected monitors in eastern Texas and southeastern Oklahoma.**

Site Name (ref. Figure 3)	Network	Measurement Availability (during 2006-2013)	Measurement Depths (cm)	Notes
Austin	CRN	Beginning late Apr 2010	5, 10	
Palestine	CRN	Beginning Jul 2009	5, 10, 20, 50, 100	Potential missing data beginning late Nov 2013
Prairie View	SCAN	2006-2013	5.1, 10.2, 20.3, 50.6, 101.7	Missing data: 5.1cm (Aug 2010-early Apr 2011 ); 10.2cm (Mar 2011-2013); 50.6cm (early Mar 2012-2013); 101.7cm (early Sept 2013–mid Oct 2013)
Port Aransas	CRN	Beginning Apr/May 2011	5, 10, 20, 50, 100	
Durant	Oklahoma Mesonet	2006-2013	5, 25, 60, 75	Missing data: 75cm (mid Sept 2009-2013); most recent NASMD archive has no data beginning late Sept 2012

**Figure 4 Daily average soil moisture and rainfall at the Palestine monitoring location during 2011.**



*Seasonal soil moisture*

In order to provide an overview of the seasonal patterns in soil moisture values at the stations shown in Table 3, Figure 5(a-e) presents average seasonal values by location and year using all available data during 2006-2013. Data completeness criteria were applied so that at least 2 of 3 months had 60% valid observations based on hourly measurements. As visually demonstrated in Figure 5, all sites exhibit a similar tendency towards maximum soil moisture availability during winter and minimum values during summer and/or fall. The annual patterns are strongest for Palestine, Austin, and Durant and somewhat less consistent at Prairie View and, especially, Port Aransas. As demonstrated previously in Figure 4 for Palestine using daily values for 2011, there is a general tendency at all monitoring locations for increasing soil moisture with increasing depth across all sampling years.

Differences in interannual seasonal variability are driven, in part, by variations in environmental drivers such as precipitation and temperature. For example, year 2010 in eastern Texas had temperature and rainfall conditions generally representative of 30-year averages compared to all-time record drought and heat during 2011. At Palestine (ref. Figure 4), the 5cm and 100cm soil moisture values for summer of 2010 were 0.12

$m^3/m^3$  and  $0.27 m^3/m^3$ , respectively, compared to  $0.02 m^3/m^3$  and  $0.14 m^3/m^3$  for 2011. The directional variability of differences in seasonal averages between 2010 and 2011 at the other monitoring locations is often similar to that for Palestine, although the magnitudes of the differences vary.

**Figure 5 Average seasonal soil moisture contents ( $m^3/m^3$ ) during 2006-2013 for (a) Palestine, (b) Prairie View, (c) Port Aransas, (d) Austin, and (e) Durant (OK). Data completeness criteria were applied so that at least 2 of 3 months had 60% valid data based on hourly observations. (spring==Mar/Apr/May; summer==Jun/Jul/Aug; fall==Sep/Oct/Nov; winter==Dec/Jan/Feb).**

(a) Palestine (summer 2009 – fall 2013)

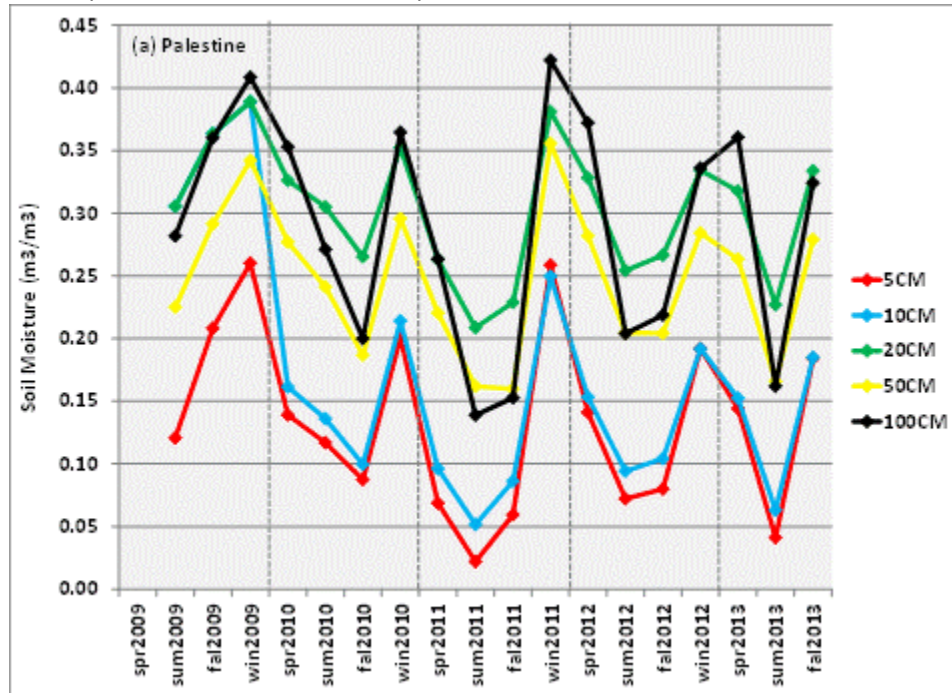
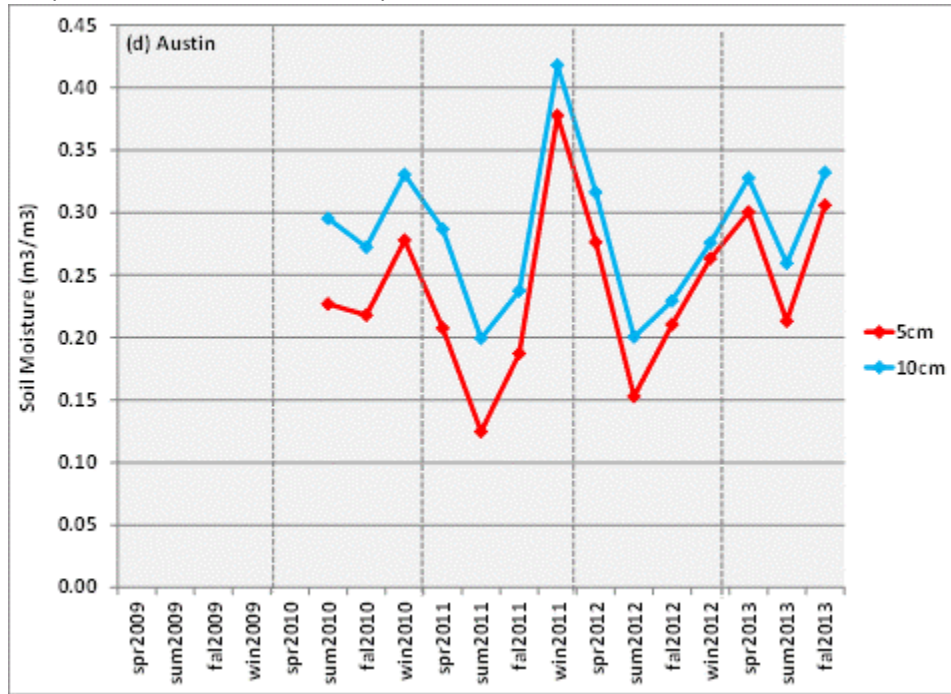


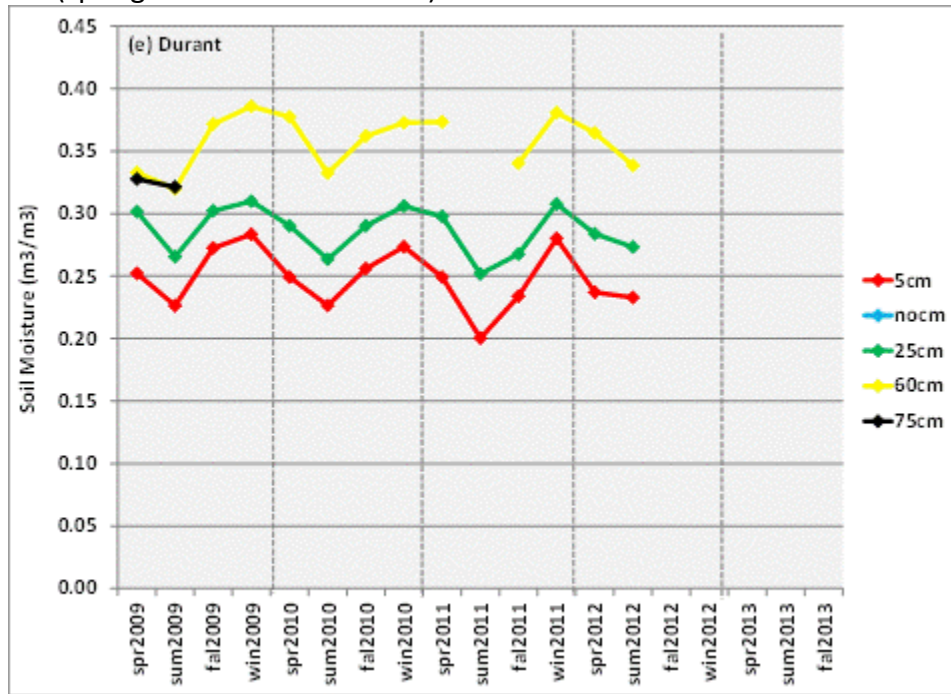


Figure 5 (continued).

(d) Austin (summer 2010 – fall 2013)



(e) Durant (spring 2009 – summer 2012)



For ease of visual comparison of seasonal trends among the monitoring locations, the available seasonal averages for years 2009-2013 shown in Figure 5 were averaged by site for the 5cm (ref. Figure 6a) and 100cm (ref. Figure 6b) depths. The strongest differences in seasonal soil water contents are observed at Austin and Palestine with relatively weaker seasonality at Durant and Port Aransas. Figure 6 also demonstrates that the absolute soil moisture values differ substantially between locations; for example, Port Aransas has low water contents for all years (e.g., 0.02-0.04 m<sup>3</sup>/m<sup>3</sup> at 5cm) compared to other locations such as Austin (0.18-0.31 m<sup>3</sup>/m<sup>3</sup> at 5cm).

The absolute soil moisture contents and variability among the monitoring locations are affected by a wide range of factors, including climate, land cover, and soil properties that impact water flux and water storage. Table 4 summarizes basic soil types, as a function of depth, at each of the four Texas monitoring locations. The soil type is generally established by the relative composition of sand, silt, and clay that determine properties such as porosity, storage capacity, and hydraulic conductivity. For example, Port Aransas has roughly similar annual precipitation compared to the other monitoring locations but has consistently low soil moisture. As shown in Table 4, Port Aransas is dominated by sandy soils, which have substantially poorer water retention and field capacity compared to the soils at the other locations such as Austin, which has clay soils characterized by relatively high storage and water holding capacity.

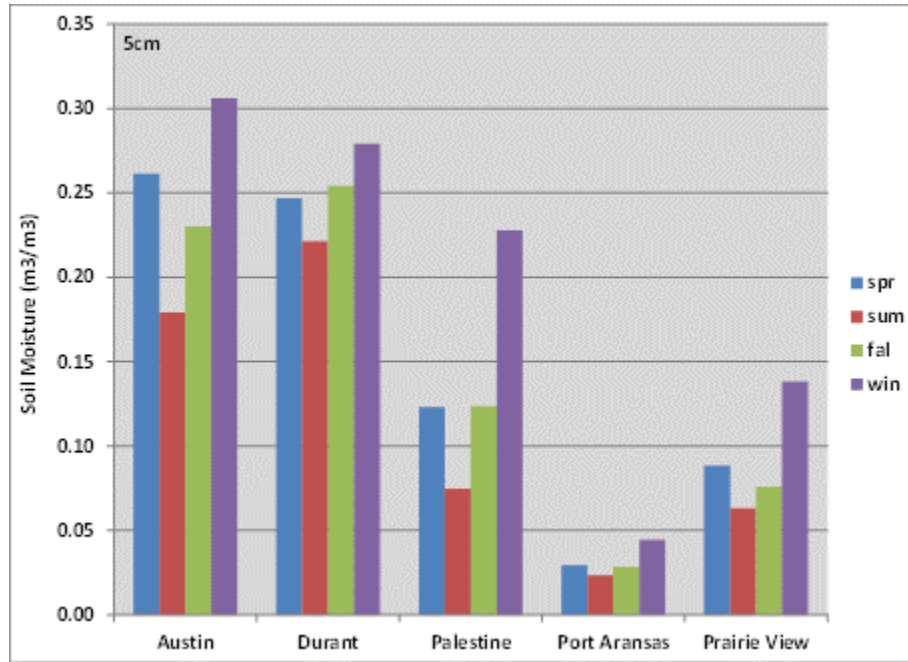
**Table 4 Soil characterization data for selected Texas locations.**

Depth	Austin*	Port	Palestine**	Prairie View**
0-5cm	Silty Clay	Sand	Sandy/Clay	Sandy loam
5-10cm	Silty Clay	Sand	Clay	Sandy loam
10-20cm	NA	Sand	Clay	Sandy loam
20-30cm	NA	Sand	Clay	Sandy loam
30-40cm	NA	Sand	Clay	Sandy loam
40-60cm	NA	Sand	Clay	Sandy loam
60-80cm	NA	Sand	Clay	Sandy clay loam
80-100cm	NA	Sand	Clay	Sandy clay loam

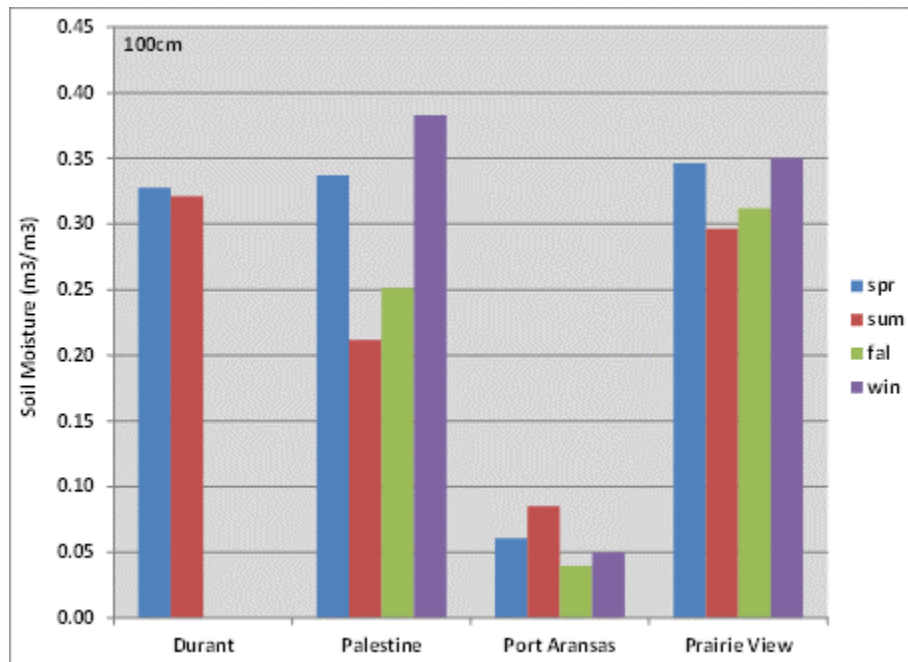
\*Source for Austin: NASMD; \*\*Source: SCAN or CRN metadata.

**Figure 6 Average seasonal soil moisture contents ( $m^3/m^3$ ) using all available data for years 2009-2013 (ref. Figure 5) for (a) 5cm and (b) 100cm depths.**

(a)



(b)



As shown previously in Figure 4, Palestine is unique among the five monitoring locations in that the greatest soil moisture values are commonly observed at 20cm rather than at 100cm. The soil types shown in Table 4 offer a potential explanation; the near-surface layer at Palestine is sandy compared to clay at deeper depths. The underlying clay layers would be expected to act as an impediment to vertical water movement and may explain why the highest soil moisture availabilities most commonly occur at 20cm at this specific location.

### 3.3 Summary

Direct soil moisture monitoring has historically been sparse in eastern Texas. A review of limited observations at four Texas locations demonstrates wide variability in volumetric water contents with near-surface values  $<0.05 \text{ m}^3/\text{m}^3$  at Port Aransas and  $>0.25 \text{ m}^3/\text{m}^3$  at inland locations where soil moisture increases with increasing depth. Soil moisture is generally highest in winter and lowest in summer. The lack of in-situ observations demonstrates the need for additional sources of information on the spatial and temporal variability of regional soil moisture throughout eastern Texas during 2006-2013.

### 3.4 References

- Brock, F.V., K.C. Crawford, R.L. Elliott, G.W. Cuperus, S.J. Stadler, H.L. Johnson, and M.D. Eilts, 1995. The Oklahoma Mesonet: A technical overview. *J. Atmos. Ocean. Technol.* 12:5–19.
- Franz, T.E., M. Zreda, R. Rosolem, and T.P.A. Ferré, 2012. Field validation of a cosmic-ray neutron sensor using a distributed sensor network. *Vadose Zone J.* vol. 11.(4). doi:10.2136/vzj2012.0046
- Hollinger, S.E., and S.A. Isard, 1994. A soil moisture climatology of Illinois. *J. Clim.* 7:822–833.
- McPherson, R.A., C.A. Fiebrich, K.C. Crawford, J.R. Kilby, D.L. Grimsley, and J.E. Martinez, 2007. Statewide monitoring of the mesoscale environment: A technical update on the Oklahoma Mesonet. *J. Atmos. Ocean. Technol.* 24:301–321. doi:10.1175/JTECH1976.1
- Ochsner, Tyson E.; Cosh, Michael H.; Cuenca, Richard H.; Dorigo, Wouter A.; Draper, Clara S.; Hagimoto, Yutaka; Kerr, Yann H.; Njoku, Eni G.; Small, Eric E.; Zreda, Marek, 2013. State of the art in large-scale soil moisture monitoring. *Soil Science Society of America Journal*, 77(6), 1888-1919. doi:10.2136/sssaj2013.03.0093

Schroeder, J.L., W.S. Burgett, K.B. Haynie, I. Sonmez, G.D. Skwira, A.L. Doggett, and J.W. Lipe, 2005. The West Texas Mesonet: A technical overview. *J. Atmos. Ocean. Technol.* 22:211–222. doi:10.1175/JTECH-1690.1

Scott, B.L., T.E. Ochsner, B.G. Illston, C.A. Fiebrich, J.B. Basara, and A.J. Sutherland, 2013. New soil property database improves Oklahoma Mesonet soil moisture estimates. *J. Atmos. Ocean. Tech.* (in press). doi:10.1175/JTECH-D-13-00084.1

USDA, 1999. *Soil Taxonomy: A Basic System of Soil Classification for Making and Interpreting Soil Surveys*, second edition, 1999, USDA Handbook 436, Soil Survey Staff, NRCS.

Zreda, M., D. Desilets, T.P.A. Ferré, and R.L. Scott, 2008. Measuring soil moisture content non-invasively at intermediate spatial scale using cosmic-ray neutrons. *Geophys. Res. Lett.* 35:L21402.. doi:10.1029/2008GL035655

Zreda, M., W.J. Shuttleworth, X. Zeng, C. Zweck, D. Desilets, T. Franz, and R. Rosolem, 2012. COSMOS: The COsmic-ray Soil Moisture Observing System. *Hydrol. Earth Syst. Sci.* 16:4079–4099. doi:10.5194/hess-16-4079-2012

## 4.0 Comparison of NLDAS-2 and in-situ soil moisture

This section presents an evaluation of seasonal and inter-annual variability of in-situ observations compared to North American Land Data Assimilation System Phase 2 (NLDAS-2) predictions.

### 4.1 NLDAS-2 datasets

NLDAS-2 provides high-resolution predictions of land surface variables, including soil moisture, beginning from January 1979 up to present (e.g., Mitchell et al., 2004; Xia et al., 2012). NLDAS-2 integrates a large quantity of observation-based and model reanalysis datasets to drive LSMs at hourly temporal and 1/8<sup>th</sup> degree latitude/longitude spatial resolutions over central North America (Rui et al., 2014). The simulated soil moisture datasets employed in our study covered years 2006–2013. With the exception of precipitation, the NLDAS-2 forcing fields are based on archived output from NCEP – NARR while the precipitation data are from gaged daily rainfall from NCEP/Climate Prediction Center (Rui et al., 2014). The original NLDAS-2 testbed included four LSMs: NASA’s Mosaic, NOAA’s Noah, Princeton’s Variable Infiltration Capacity (VIC), and the Sacramento Soil Moisture Accounting model (SAC-SMA) (Rui et al., 2014).

The Noah LSM is the land component of the NOAA NCEP mesoscale Eta model (Betts et al., 1997; Chen et al., 1997; Ek et al., 2003) as well as the evolving Weather Research and Forecasting (WRF) regional atmospheric model (Skamarock et al., 2008), the NOAA NCEP coupled Climate Forecast System (CFS) (Saha et al., 2010), and the Global Forecast System (GFS) (Yang et al., 2006). The Noah version 2.8 is used in the NLDAS-2 system. This version improves the snowpack simulation, snowmelt, and snow cover (Livneh et al., 2010). It also improves energy fluxes, streamflow, and land surface temperature simulations for warm seasons (Wei et al., 2011). These improved physics may ensure a more realistic soil moisture simulation. Noah has four soil layers with spatially invariant thicknesses of 10, 30, 60, and 100cm, representing the 0-10, 10-40, 40-100, and 100-200cm soil depths respectively. The top three layers form the root zone in non-forested regions, with the fourth layer included in forested regions (Rui 2014).

Mosaic was developed by Koster and Suarez (1994, 1996) to account for sub-grid vegetation variability. Mosaic employs a tiled approach, with each vegetation tile carrying its own energy and water balance. In NLDAS-2, all Mosaic tiles within a grid cell have a predominant soil type, and each tile has three soil layers with fixed thicknesses of 10, 30, and 160cm, corresponding to spatially non-varying soil layers of 0-10, 10-40 and 40-200cm. The first two layers are assumed to comprise the vegetation root zones (Rui 2014).

The Variable Infiltration Capacity (VIC) model was developed at the University of Washington and Princeton University as a macroscale, semi-distributed, grid-based, hydrologic model (Liang et al., 1994; Wood et al., 1997). The NLDAS-2 version of VIC

(4.0.5) employs the full water and energy balance modes and includes a two-layer energy balance model, which represents snow accumulation and ablation on the ground and in the forest canopy, as well as the impact of elevation on temperature, precipitation and snow (Cherkauer et al., 2003). VIC has three soil layers; the near-surface layer has a constant thickness of 10 cm while the two deeper soil layers have thicknesses that vary spatially throughout the grid domain. The root zone, which may span all three soil layers, is dependent on the vegetation and associated root distributions within each grid cell.

An additional LSM used for our work is an enhanced version of the original Noah LSM that incorporates improved physics and multi-parameterization options (Noah-MP; Niu et al., 2011; Yang et al., 2011). Noah-MP has not been officially incorporated by the NLDAS-2 system. The Noah-MP includes recent developments in the LSM community (e.g., prognostic leaf models, dynamic groundwater, multilayer snow; Cai et al., 2014a and b) that have also been incorporated into the Community Land Model version 4 (CLM4) (Lawrence et al., 2011). The Noah-MP LSM employs the same vertical soil structure as the standard Noah model, i.e., 0-10, 10-40, 40-100, and 100-200cm layers, and has recently been shown to provide good performance for soil moisture in Texas (Cai et al., 2014a and b).

The original NLDAS testbed includes another hydrological model, the Sacramento Soil Moisture Accounting model (SAC), that was not included in our work because the data output were not officially available at the time of analysis but would be interesting to investigate once it becomes publicly available in the future. Additionally, the Community Land Model (CLM) was used for hydrological evaluation together with the standard NLDAS-2 model outputs by Cai et al. (2014b), but was not included in our analyses because CLM has not been incorporated in the standard NLDAS-2 system and is the model output is not currently publicly available.

## **4.2 Methodology**

### *In-situ data*

The evaluation of NLDAS-2 soil moisture predictions (i.e., Noah, Noah-MP, Mosaic, and VIC) utilized in-situ soil moisture measurements collected by the SCAN and CRN networks (ref. Section 3). The soil moisture evaluation used all available observations collected during 2006-2013 at monitoring locations within the 12km domain (ref. Figure 7). During at least a portion of 2006-2013, in-situ soil moisture observations were collected at 84 locations (47 SCAN sites; 37 CRN sites); however, the data availability at monitoring locations is highly variable. In particular, the soil observation program of CRN was not commissioned until 2009 so monitoring at most stations was not initiated until late 2009 or early 2010. Given the general sparseness of monitoring data and a desire to maintain as much observational data as reasonable to support model

evaluation, sites were screened so that at least two years of measurements were available; these criteria identified the 36 SCAN and 20 CRN sites described in Table 5.

**Figure 7 Locations of SCAN and CRN monitoring locations operational during at least a portion of 2006-2013. For the purposes of NLDAS-2 evaluation, the 12km domain (outlined in green) was sub-divided into two regions “East” and “West”. The division boundary is along 98°W longitude.**

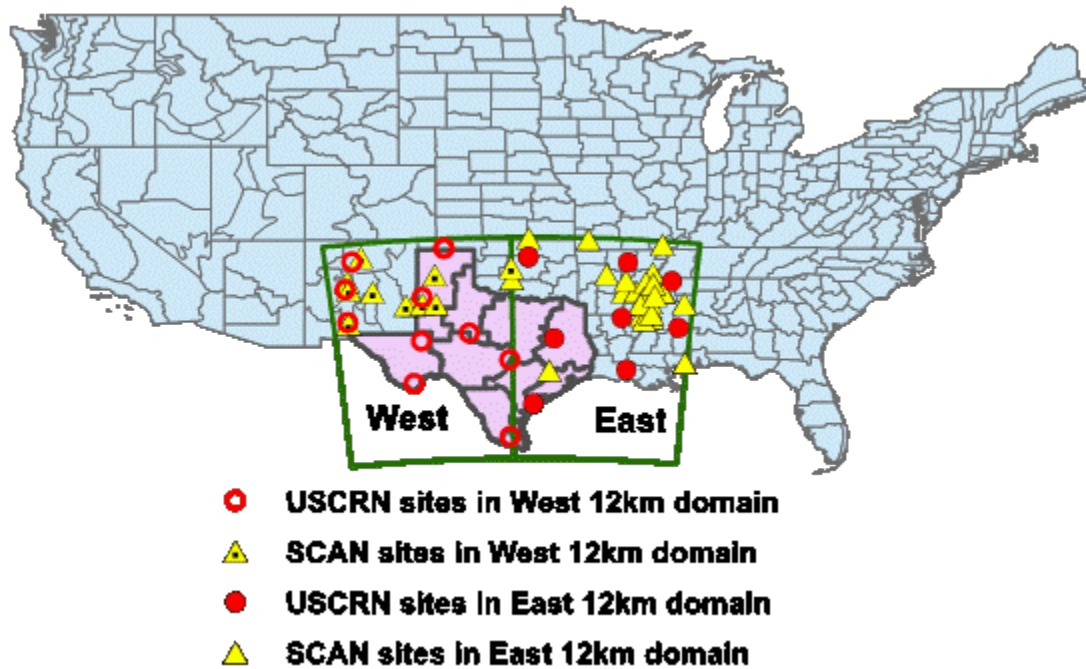


**Table 5 SCAN and CRN measurement locations used for NLDAS-2 evaluation.**

Region	State	Network	Site Name	Measurement Start Date (if later than 2006)
West	NM	SCAN	Adams_Ranch_#1	Jan 2006
	NM	SCAN	Alcalde	Mar 2010
	NM	SCAN	Crossroads	Jan 2006
	NM	SCAN	Jornada_Exp_Range	Oct 2009
	NM	SCAN	Los_Lunas_PMC	Oct 2009
	NM	SCAN	Sevilleta	Mar 2010
	NM	SCAN	Willow_Wells	Jan 2006
	OK	SCAN	Fort_Reno_#1	Jan 2006
	TX	SCAN	Bushland_#1	Jan 2006
	TX	SCAN	Lehman	Jan 2006
	TX	SCAN	Reese_Center	Jan 2006
	NM	USCRN	Socorro_20_N	Jun 2010
	NM	USCRN	Los_Alamos_13_W	Jan 2010
	NM	USCRN	Las_Cruces_20_N	Apr 2010
	OK	USCRN	Goodwell_2_E	Jul 2009
	OK	USCRN	Goodwell_2_SE	Aug 2011
	TX	USCRN	Monahans_6_ENE	Apr 2010
	TX	USCRN	Muleshoe_19_S	Jun 2010
	TX	USCRN	Bronte_11_NNE	Apr 2010
	TX	USCRN	Edinburg_17_NNE	Apr 2010
	TX	USCRN	Panther_Junction_2_N	Apr 2010
	TX	USCRN	Austin_33_NW	Apr 2010
East	AR	SCAN	Uapb_Campus_PB	Jan 2006
	AR	SCAN	Uapb_Dewitt	Jan 2006
	AR	SCAN	Uapb_Point_Remove	Jan 2006
	AR	SCAN	Uapb_Earle	Jan 2006
	AR	SCAN	Uapb_Lonoke_Farm	Jan 2006
	AR	SCAN	Uapb_Marianna	Jan 2006
	KS	SCAN	Abrams	Jan 2006
	MO	SCAN	Dexter	Jan 2006
	MO	SCAN	Mt_Vernon	Jan 2006
	MS	SCAN	Beasley_Lake	Jan 2006
	MS	SCAN	Goodwin_Ck_Pasture	Feb 2007
	MS	SCAN	Goodwin_Ck_Timber	Jan 2006
	MS	SCAN	Mayday	Jan 2006
	MS	SCAN	North_Issaquena	Jan 2006
	MS	SCAN	Onward	Nov 2006
	MS	SCAN	Perthshire	Jan 2006
	MS	SCAN	Sandy_Ridge	Jan 2006
	MS	SCAN	Scott	Jan 2006
	MS	SCAN	Silver_City	Jan 2006
	MS	SCAN	Starkville	Jan 2006
	MS	SCAN	Tnc_Fort_Bayou	Jan 2006
	MS	SCAN	Tunica	Jan 2006
	MS	SCAN	Vance	Jan 2006
	OK	SCAN	Little_Washita_#1	Jan 2006
	TX	SCAN	Prairie_View_#1	Jan 2006
	AR	USCRN	Batesville_8_WNW	Aug 2009
	LA	USCRN	Lafayette_13_SE	Jul 2009
	LA	USCRN	Monroe_26_N	Aug 2009
	MS	USCRN	Holly_Springs_4_N	Aug 2009
	MS	USCRN	Newton_5_ENE	Jul 2009
	OK	USCRN	Stillwater_2_W	Jul 2009
	OK	USCRN	Stillwater_5_WNW	Jul 2009
	TX	USCRN	Port_Aransas_32_NNE	Apr 2011
	TX	USCRN	Palestine_6_WNW	Jul 2009

The limited availability of monitoring locations precluded a detailed regional analysis; however, to examine the general east-to-west spatial gradient of soil moisture, the 12km domain was evenly split into two sub-regions “East” and “West” (ref. Figure 7). The eastern region included 25 SCAN and 9 CRN stations compared to 11 SCAN and 11 CRN sites in “West”. The boundary between the sub-regions is roughly along 98°W longitude and divides the 12km domain into regions with contrasting climatology and vegetation. The eastern region, on average, receives ~40 inches of rainfall annually compared to less than 20 inches in the west (Long et al., 2014, based on PRISM precipitation data). Additionally, “East” has relatively denser vegetation cover (e.g., forest, woodland, and cropland) compared to typically semi-desert western conditions (e.g., shrub and grassland). The east-to-west gradients in precipitation and vegetation generally lead to decreasing soil moisture.

#### *Processing of NLDAS-2 datasets*

NLDAS-2 soil moisture outputs were retrieved from <http://disc.sci.gsfc.nasa.gov/hydrology/data-holdings>; the data consisted of both monthly and hourly files. For the evaluation with observations, the hourly values were averaged to generate daily values. All hourly datasets are in gridded format with 1/8 degree resolution; each grid cell has equal latitude and longitude intervals.

The soil predictions among the four NLDAS-2 datasets were processed to a consistent vertical structure. The Noah layer structure was adopted as the target because: (1) soil layers are uniform throughout the entire domain, making it convenient to compare model simulations with measurements; and (2) the full resolution of Noah/Noah-MP predictions (4 fixed layers) is preserved compared to Mosaic (3 fixed layers) and VIC (3 spatial varying layers). For the purposes of vertical interpolation, the volumetric soil moisture contents were assumed constant across each layer for Mosaic and VIC. A simple linear interpolation was used to convert the Mosaic and VIC predictions to match the four Noah soil layers (0-10, 10-40, 40-100, and 100-200cm). The VIC soil moisture data were converted to the Noah model layers by calculating the weighted average of soil moisture in each of the three VIC layers that intersected each of the four Noah layers. For grid cells where the bottom VIC layer is shallower than the lowest Noah layer, the VIC soil moisture value is assumed to be uniform down to the depth of the bottom of the Noah layer. This procedure is similar to that employed by Xia et al. (2014) for the multi-model evaluation of soil moisture with SCAN, Oklahoma Mesonet, and Illinois network observations.

A direct comparison of soil moisture between the in-situ measurements and NLDAS-2 model simulations is not possible because the measurements are made at specific depths that differ from the models’ layered vertical configuration. The SCAN/CRN measurements are collected at 5 distinct depths across the soil profile, i.e., 5, 10, 20, 50, and 100cm wherever possible. In contrast, NLDAS-2 predicts total water availability in each vertical model layer. To address this inconsistency in the vertical model-

measurement structures, a linear interpolation technique was used to transform the four NLDAS-2 layers to the in-situ measurement depths. For the purposes of interpolation, the NLDAS-2 values were assumed to represent conditions at the center of each layer, i.e. 5, 25, 70, and 150cm for the 0-10, 10-40, 40-100, and 100-200cm layers, respectively. For the inter-comparison of regional NLDAS-2 predictions provided in Section 6, this latter interpolation step to measurement depths was not performed.

### *Temporal and spatial aggregation of in-situ and simulated soil moisture*

To compare simulated (NLDAS-2) and observed (in-situ) soil moisture values, the NLDAS-2 predictions were extracted at the 1/8<sup>th</sup> degree grid cells that contained the in-situ monitoring locations. The in-situ point measurements and gridded NLDAS-2 predictions have different spatial scales; using the NLDAS-2 grid resolution (~12.5km) inherently assumes that the spatial resolution is sufficiently small to represent the soil moisture in the surroundings of the measurement locations. This assumption is associated with numerous uncertainties because, for example, the land and vegetation properties are often characterized by substantial horizontal and vertical heterogeneity over even short distances.

The comparison between model predictions and in-situ measurements was performed at a daily timescale. The daily in-situ datasets were retrieved directly from the SCAN (<http://www.wcc.nrcs.usda.gov/scan/>) and CRN (<http://www.ncdc.noaa.gov/crn/qcdatasets.html>) websites; hourly NLDAS-2 predictions were averaged over 24 hours. The daily observed/modeled data were paired in space and time at each monitoring site; NLDAS-2 results were only maintained if matching in-situ measurements were available. In order to address uncertainties arising from the scaling mismatch between the NLDAS-2 simulation and in-situ measurements, spatial averaging of data at all sites within each sub-region was performed similar to the methodology for other studies (e.g., Xia et al., 2014; Robock et al., 2003).

### *Model performance*

Model performance was evaluated using calculations that quantify bias (i.e., comparison of absolute values) as well as skill at capturing observed temporal variations of soil moisture (i.e., anomalies). Bias (%) is computed as  $100 * (\text{modeled soil moisture} - \text{observed soil moisture}) / \text{observed soil moisture}$  and describes how much the NLDAS-2 predictions deviate from observations in an “absolute” sense. A second metric aims to assess model skill in simulating the relative temporal variations in observations at time scales ranging from seasonal to annual. A soil moisture anomaly is first calculated by subtracting a reference value that represents the baseline climatological soil moisture. This “reference” is taken as the mean for each Julian day across all years (2006-2013). A positive anomaly indicates above-normal water availability compared to the reference period while a negative anomaly may indicate conditions of drought. The correlation

coefficient (“R”) between the simulated and observed anomalies is then considered to be representative of model skill.

Bias and anomalies are generated for each of the examined NLDAS-2 models (i.e., Mosaic, Noah, VIC, and Noah-MP) and used to assess the relative performance for the East and West sub-regions. For a visual comparison, time series graphs of measured and modeled values are shown at daily and monthly time scales.

### *Sources of uncertainty*

The inter-comparison of in-situ measurements and NLDAS-2 predictions are affected by a number of uncertainties, including (but not limited to):

- 1) **The in-situ observations are a point measurement whereas the NLDAS-2 simulations represent average conditions over a larger area` (i.e., 1/8 degree horizontal spatial resolution).** For example, soil type is critical in determining the capacity water content and actual soil properties within a given grid cell that are typically highly spatially heterogeneous (both horizontally and vertically) even in the immediate vicinity of the measurement location.
- 2) **The site-specific soil type differs from NLDAS-2 descriptions.** The models are often applied in regions where detailed soil surveys are not available; therefore, soil parameters are estimated from relatively coarse datasets (e.g., STATSGO). For example, the soil texture in the upper one-meter at Palestine is specified by the Climate Research Network (CRN) as “Clay” whereas the NLDAS-2 grid cell that contains the Palestine monitoring location is characterized as “Sandy”.
- 3) **Uncertainties in the NLDAS-2 model structure and parameterizations.** The NLDAS-2 configurations use the same atmospheric forcing data/soil texture/vegetation types; however, the physics, structure and other soil parameterizations are model-specific. For example, the vegetation characterization that establishes density, seasonality and root fraction as a function of depth can vary substantially. These differences can impact maximum total water storage capacities, infiltration and drainage, interaction of evapotranspiration and soil moisture, and seasonality of processes associated with soil moisture dynamics.
- 4) **There may be crucial processes that are not directly considered by NLDAS-2 but impact soil moisture at specific locations.** Examples include irrigation at agricultural sites or ground water pumping.
- 5) **There are uncertainties in the meteorological forcing data that drives the NLDAS-2 simulations.** For NLDAS-2, the forcing data (e.g., temperature, precipitation, radiation, etc.) are generated primarily from the North American Regional Reanalysis (NARR), which is also an assimilated product with its own set of assumptions and uncertainties.
- 6) **Interpolation-induced bias.** For our current analysis, a linear relationship was inherently assumed in interpolating the NLDAS-2 layer values to the in-situ depths.

However, soil properties can vary dramatically over even short vertical distances often related to site-specific hydrological variability.

### 4.3 Results

#### *Daily averaged soil moisture during 2006-2013*

Figure 8 compares the observed and NLDAS-2 soil moisture values averaged by Julian day across the 8-year period from 2006-2013. Results are shown for each in-situ measurement depth for the eastern and western sub-regions.

For all depths, observed soil moisture in the eastern region is relatively high in winter and spring with low water availability during summer (e.g., June through September); the seasonal magnitude is greatest for the near-surface layer. Superimposed on the seasonal variability are daily fluctuations, which are more evident in the top soil layers and tend to diminish with depth. This behavior likely reflects the fast response of shallow soil layers to rainfall events while deep soils are less influenced by atmospheric perturbations. Compared to the eastern values, observed soil moisture in the western sub-region is substantially lower and characterized by weak seasonal variability across all depths.

Overall, the Noah, Noah-MP, and Mosaic models show relatively best agreement with observations in the near-surface layers and exhibit a consistent dry bias at greater depths in the east with good performance in the west. At 5cm in the eastern sub-region, Noah-MP best resembles the observed seasonal pattern while Mosaic and Noah have a dry winter bias ( $\sim 0.05 \text{ m}^3/\text{m}^3$ ) and a slower water restoration rate with respect to observations during the transition from summer to winter. In the western region, Mosaic best replicates observed soil moisture in the top layers above 20cm except for an underestimation during spring (February, March, and April); Noah and Noah-MP have wet biases.

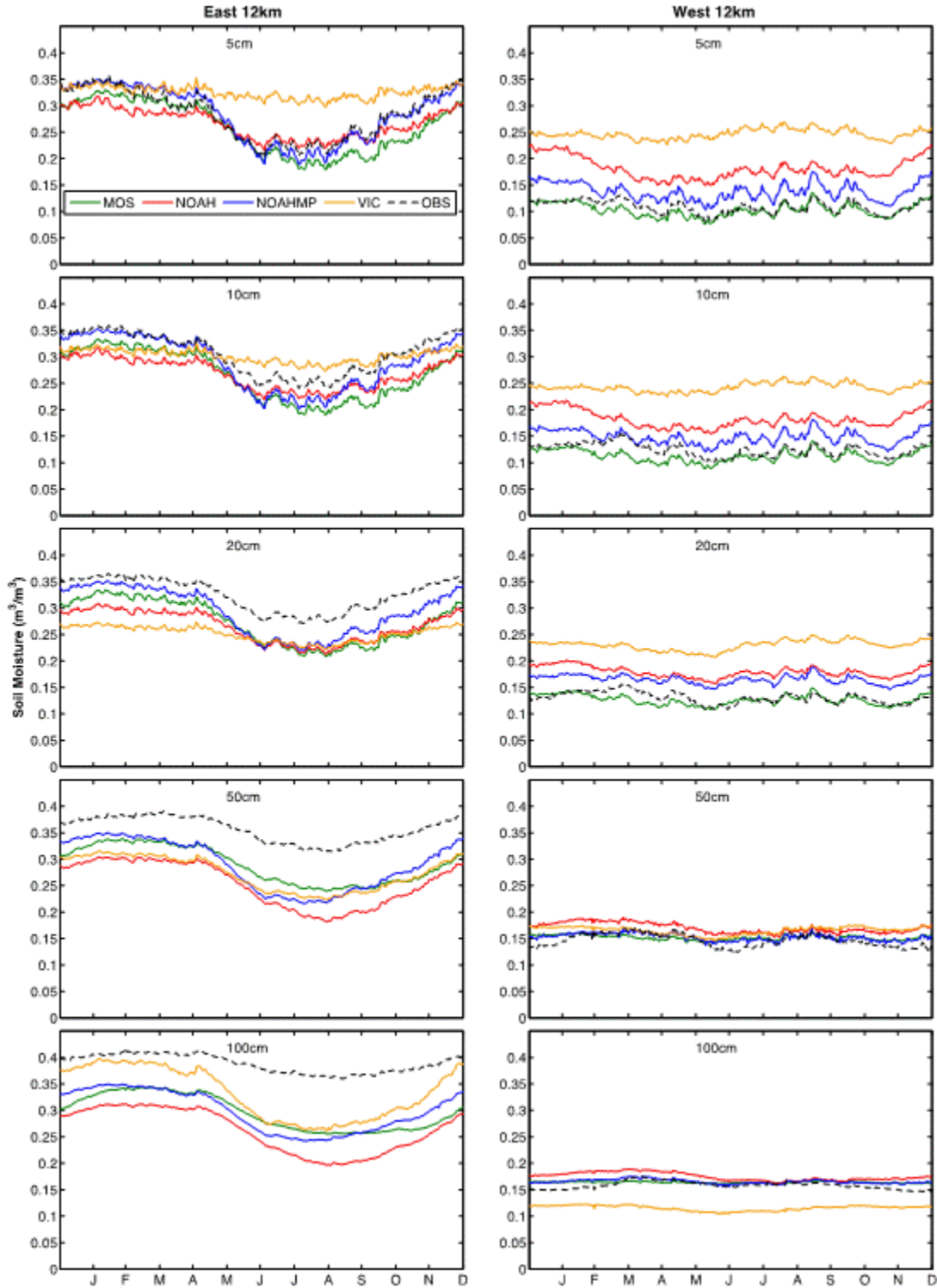
With the exception of the eastern cool seasons, VIC has a substantial wet bias in the near-surface layers. In the VIC LSM, evaporation from soils can only occur from bare soils and not from vegetation even if the canopy is sparse. Xia et al. (2014) found that increasing the fraction of bare soil in VIC resulted in improved seasonal performance via enhanced evaporation.

For deeper soil layers models show a strong dry bias compared to observations in the eastern region, while the models converge to observed soil moisture at 50cm and 100cm in the western region (with the exception of VIC at 100cm that has a dry bias). The eastern NLDAS-2 predictions have substantial dry biases below 10cm, with roughly  $0.1 \text{ m}^3/\text{m}^3$  underestimation in winter and  $0.2 \text{ m}^3/\text{m}^3$  in summer across all models at 100cm. The dry bias increases for deeper layers with a largest bias at 100cm simulated by Noah. In the east, VIC simulates weak seasonal variation in the top soil layers

changing to strong seasonal variations for the deeper soil layers. VIC has the best agreement with observed soil moisture at 100cm during winter.

Within both the eastern and western regions, there is a small increase in observed soil moisture with increasing depth ( $\sim 0.05 \text{ m}^3/\text{m}^3$  between 5 and 100cm). However, modeled soil moisture values tend to remain unchanged with respect to depth resulting in the consistent dry bias for the deep layers in the eastern sub-region. The seasonal variation of observed soil moisture dampens with increasing soil depth; this tendency is not captured by the models.

**Figure 8 Comparison of observed and NLDAS-2 soil moisture at the in-situ SCAN/CRN measurement depths, averaged by Julian day during 2006-2013. Results are shown for the eastern (left) and western (right) portions of the 12km domain.**

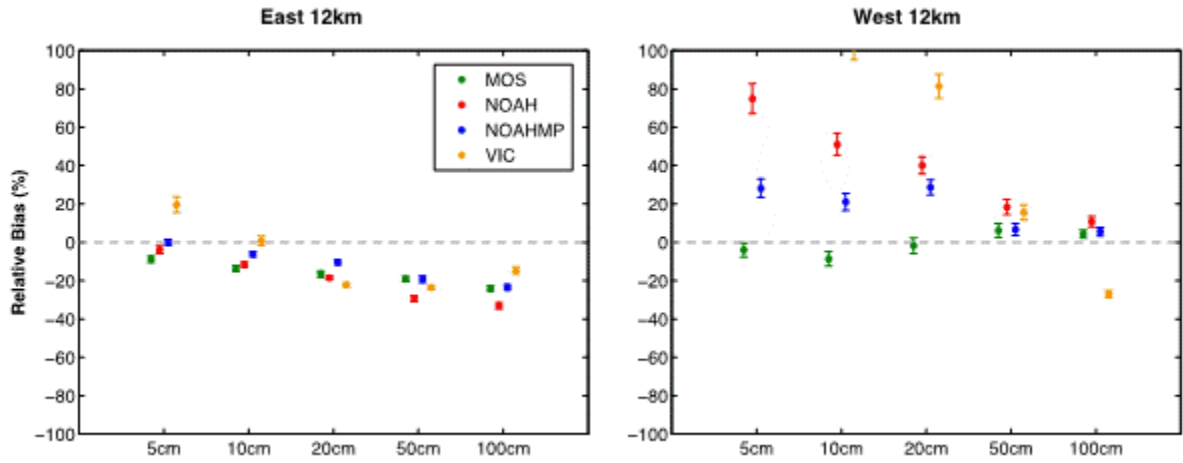


Using all paired observations/predictions throughout 2006-2013, the percentage bias by soil depth is shown in Figure 9. Within the eastern sub-region, the NLDAS-2 LSMs have a dry bias with the exception of VIC at 5cm. The dry bias generally increases with increasing soil depth, ranging from <10% at 5/10cm to 20-30% at 50/100cm. This variation is robust in this region, because the 95% error bars are quite narrow. The VIC model initially shows a 20% positive bias at 5cm, zero bias at 10cm (caused by an offset of negative predictions relative to observations during winter and the opposite tendency during summer), and negative biases at 20/50cm improving to <20% at 100cm.

The western sub-region has a more divergent bias across models. Mosaic has a neutral bias relative to observation at all depths indicating an overall excellent agreement with observations. The Noah and Noah-MP LSMs simulate a consistent wet bias across the entire soil column with a magnitude that decreases with soil depth. For example, Noah predicts a ~80% overestimation of soil moisture compared to observations at 5cm decreasing to ~8% at 100cm. Noah-MP overpredicts by ~30% above 20cm. The VIC model has the largest positive bias within the top soil layers (e.g., exceeding 200% at 5cm, not shown) decreasing to negative values at 100cm. The relatively wider error bars indicate greater uncertainty compared to the eastern region.

Overall, the bias results shown in Figure 9 (dry in the east; wet in the west) are qualitatively consistent with the tendencies shown in Figure 8 (i.e., time series of predicted and observed soil moisture) and with the findings in previous studies (e.g., Xia et al., 2014). The dry bias in the eastern sub-region might be related to a lack of irrigation processes and/or suggests an overestimation of runoff and evapotranspiration by the NLDAS-2 LSMs. The large wet bias in the western sub-region is probably caused by the relatively large maximum water holding and field capacities assumed by the models.

**Figure 9** Relative bias (%) of simulated soil moisture compared to observations for the eastern (left) and western (right) sub-regions at the in-situ measurement depths. The relative bias is calculated as:  $100 * (\text{modeled soil moisture} - \text{observed soil moisture}) / \text{observed soil moisture}$ . The error bars represent the 95% confidence interval for each model. Because the y-axis range is limited to -100% to 100%, VIC results >100% are not shown.



### *Annual average daily soil moisture during 2006-2013*

Figure 10 shows the time series of daily soil moisture for the in-situ observations and NLDAS-2 predictions by depth; monthly averages are shown in Figure 11. The eastern domain consistently shows a stronger and more consistent seasonal signal compared to the western region. The model tendencies for wet/dry biases shown in Figure 8 and Figure 9 generally reappear every year in the same season, suggesting a systematic model deficiency in simulating the absolute soil moisture magnitudes. The generally poor performance of VIC in predicting near-surface soil moisture relative to the other models is clearly evident in Figure 11.

For the eastern sub-region, observed seasonal variability is stronger than variability between years. For both regions, years 2010-2013 have slightly lower soil moisture compared to prior years; this might be related, in part, to differences in available monitoring locations between the two periods (e.g., recall most CRN stations were not operational until 2010). Observations show that differences between 2006-2009 and 2010-2013 diminish with depth. Overall, Noah-MP and Mosaic show the best visual agreement with observations across both the eastern and western sub-regions compared to Noah and, especially, VIC.

To remove the impact of systematic model bias and seasonality in the comparison of observed and predicted soil moisture, the anomalies of soil moisture are shown in Figures 12 (daily) and 13 (monthly). Positive values represent above-average soil moisture while negative values represent drier conditions. Overall, the results suggest very similar model skill at replicating the observations. Note, for example, the strongly negative values for all models indicative of drought conditions during 2011. The previously noted difference in soil moisture between 2006-2009 and 2010-2013 is apparent in the anomalies; note the positive values for the prior period and generally negative values thereafter. There was a sharp decline of soil moisture in late 2010 from a positive anomaly to a negative one. This condition persists throughout 2011 with a slow recovery afterwards and is found in both observations and all NLDAS-2 models.

The anomalies also highlight the periodic impact of higher frequency rain events (i.e., spikes in soil moisture) that are more pronounced for the near-surface layers and generally simulated by all models except VIC. VIC is similar to the other models in over-predicting the deeper soil variations. An interesting feature is that the Mosaic model sometimes shows a slower drawdown and recovery of soil moisture compared to the other models and observations, especially at 50 and 100cm. This might be caused, in part, to the relatively larger water holding capacity in Mosaic compared to the other models. The maximum active water holding capacity is the portion of water that can be absorbed by plant roots and is the amount of water available, stored, or released between field capacity and the permanent wilting point dependent on soil type. The slow recovery of Mosaic from a negative anomaly is probably due to its no-limit

extraction of water from below the wilting point for a dry anomaly recovery (e.g., Schaake et al., 2004).

In the western sub-region, the soil moisture deficit was very evident in 2011 and a strong surplus is shown for both 2007 and early 2010. This pattern is consistent between simulations and observations. The magnitude of predicted fluctuations is larger than observed, especially for the top soil layers. However, the timing of wet and dry events is generally well-handled with the exception of deep layers during 2011. For example, at 100cm, the maximum observed soil moisture deficit occurred in spring compared to fall for the simulations. This feature might be caused, in part, by a lack of measurements at deep soil layers. Another possible cause is a relatively slower simulated penetration rate associated with various assumed soil properties in the NLDAS-2 LSMs.

The apparent temporal shift was also observed in eastern sub-region; note maximum observed soil water depletion in late 2010 compared to early 2011 in the simulations. This might be partially caused by the inclusion of states that were less affected by drought during spring and summer of 2011, which would partially offset the drying signal.

**Figure 10** Observed and modeled daily soil moisture at in-situ measurements depths for the western and eastern sub-regions (ref. Figure 7) during 2006 to 2013.

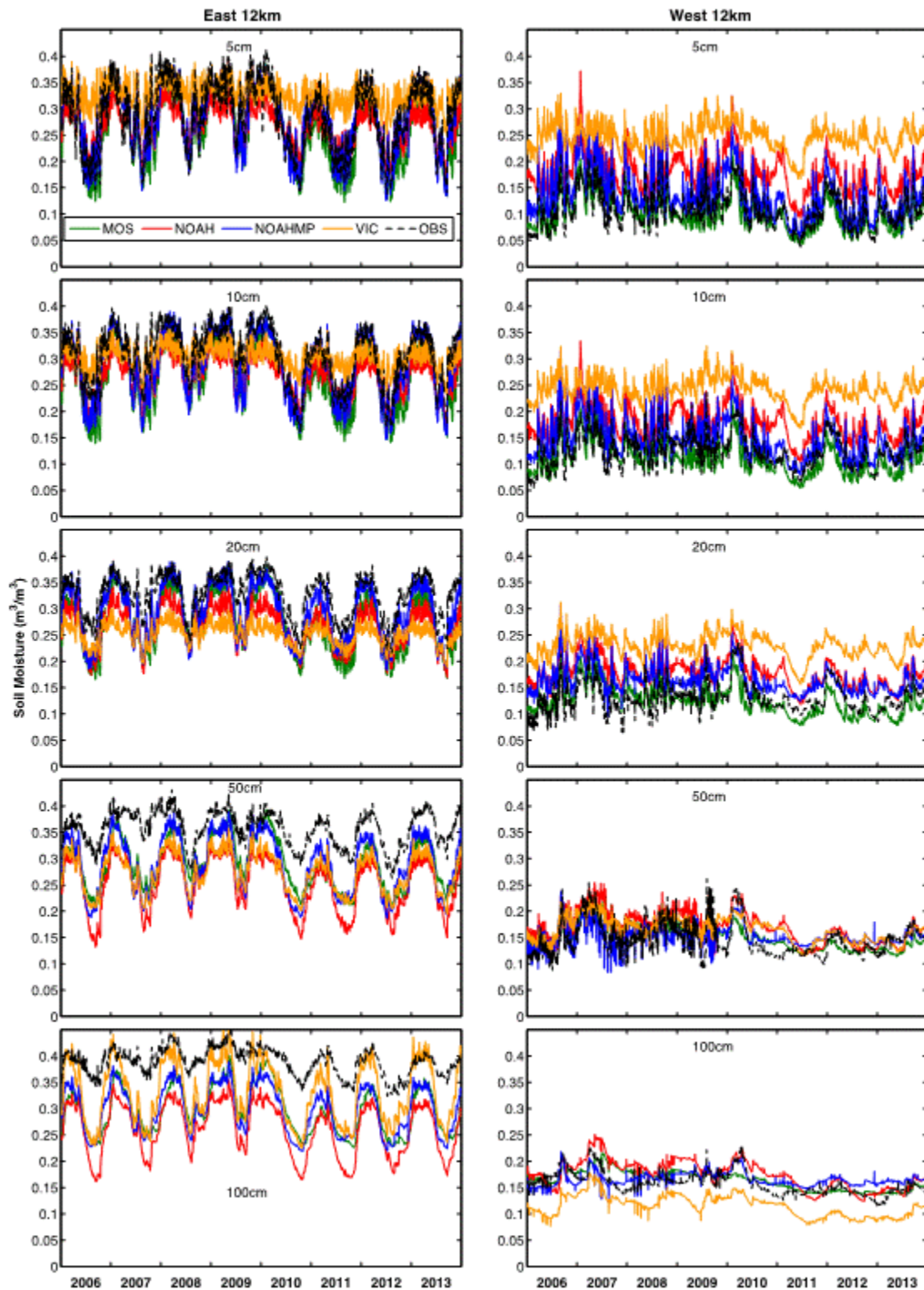
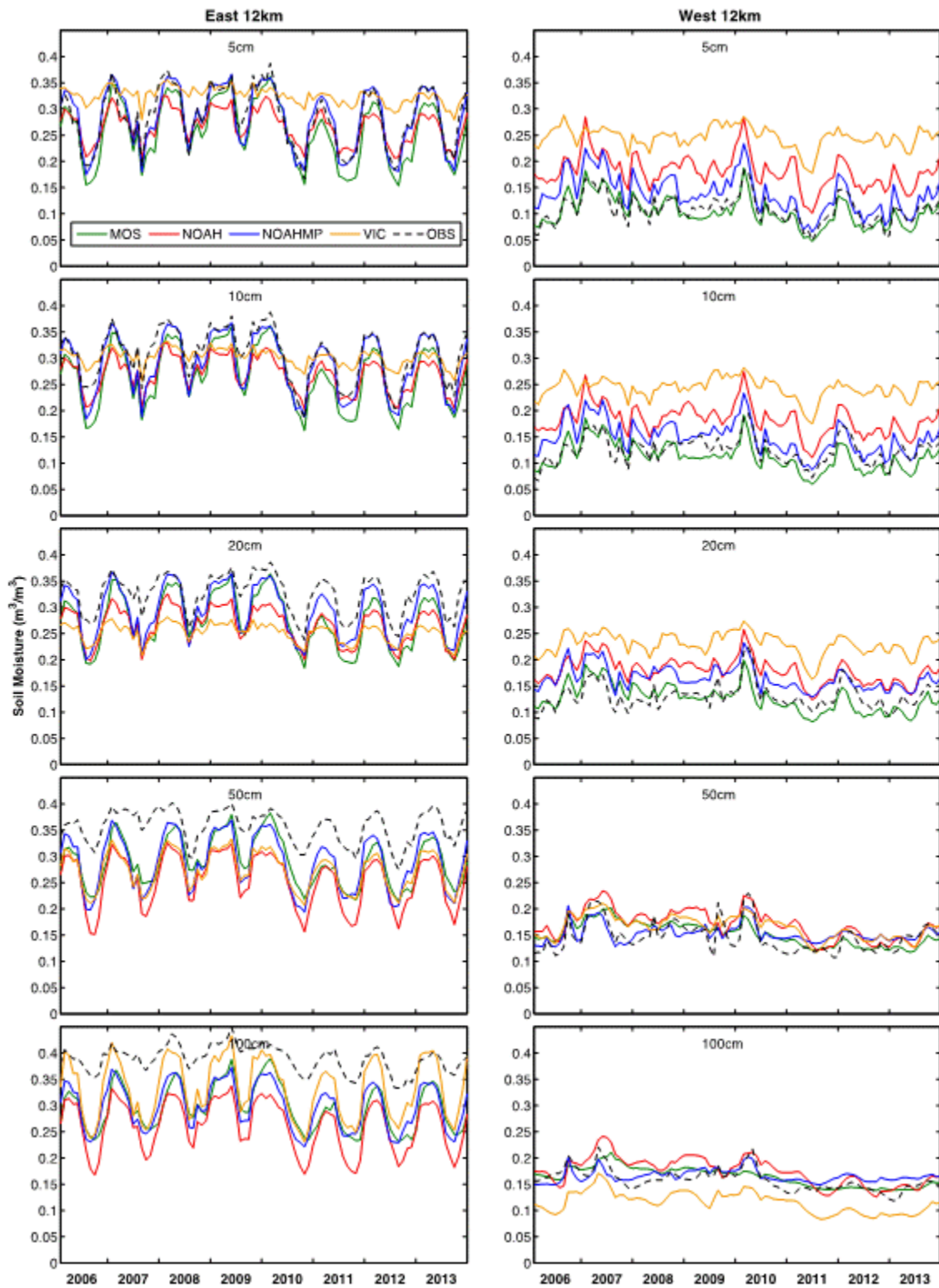


Figure 11 As in Figure 10, but averaged by month.



**Figure 12** Observed and modeled daily soil moisture anomalies at in-situ measurements depths for the western and eastern sub-regions (ref. Figure 7) during 2006 to 2013.

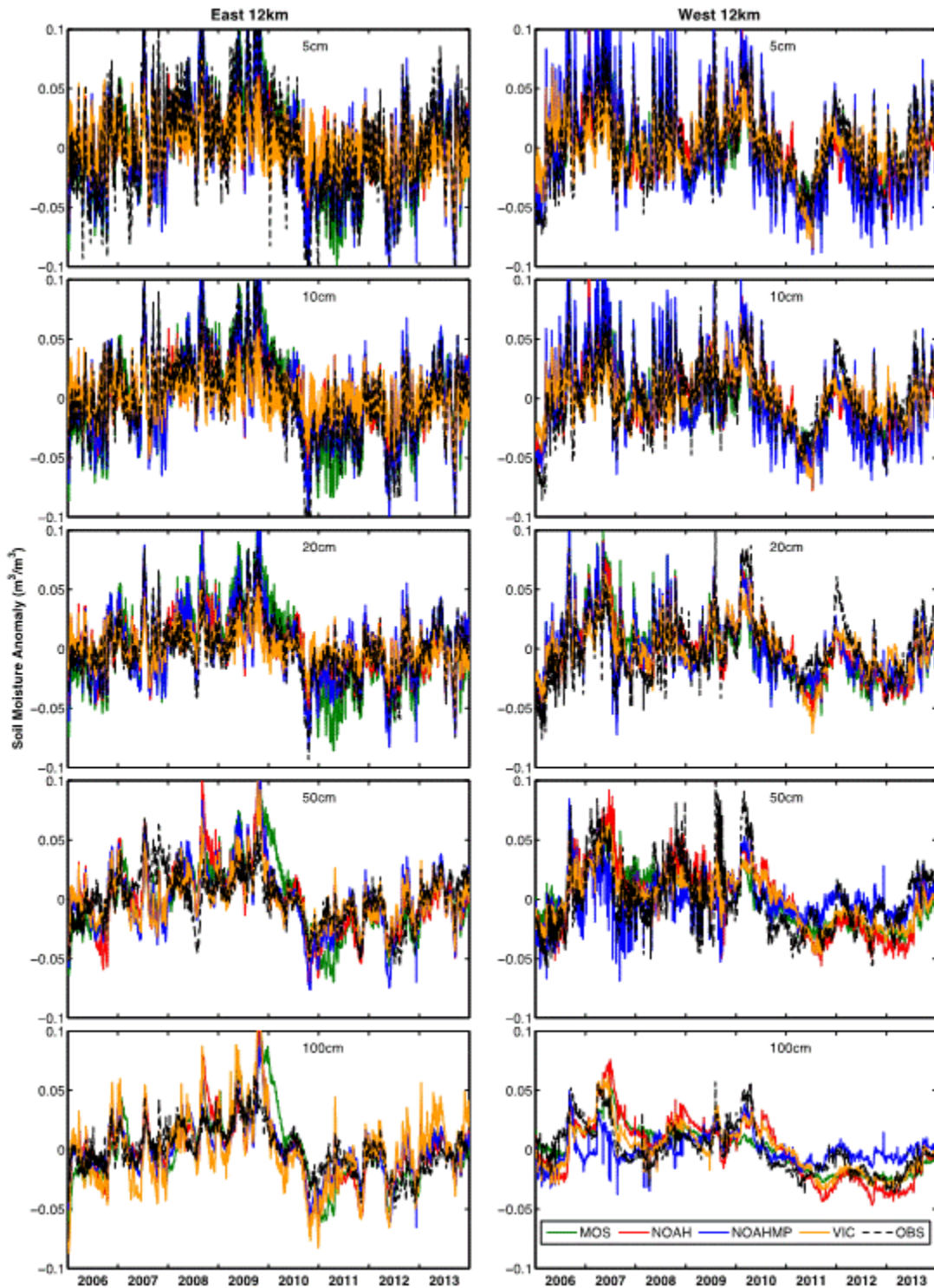
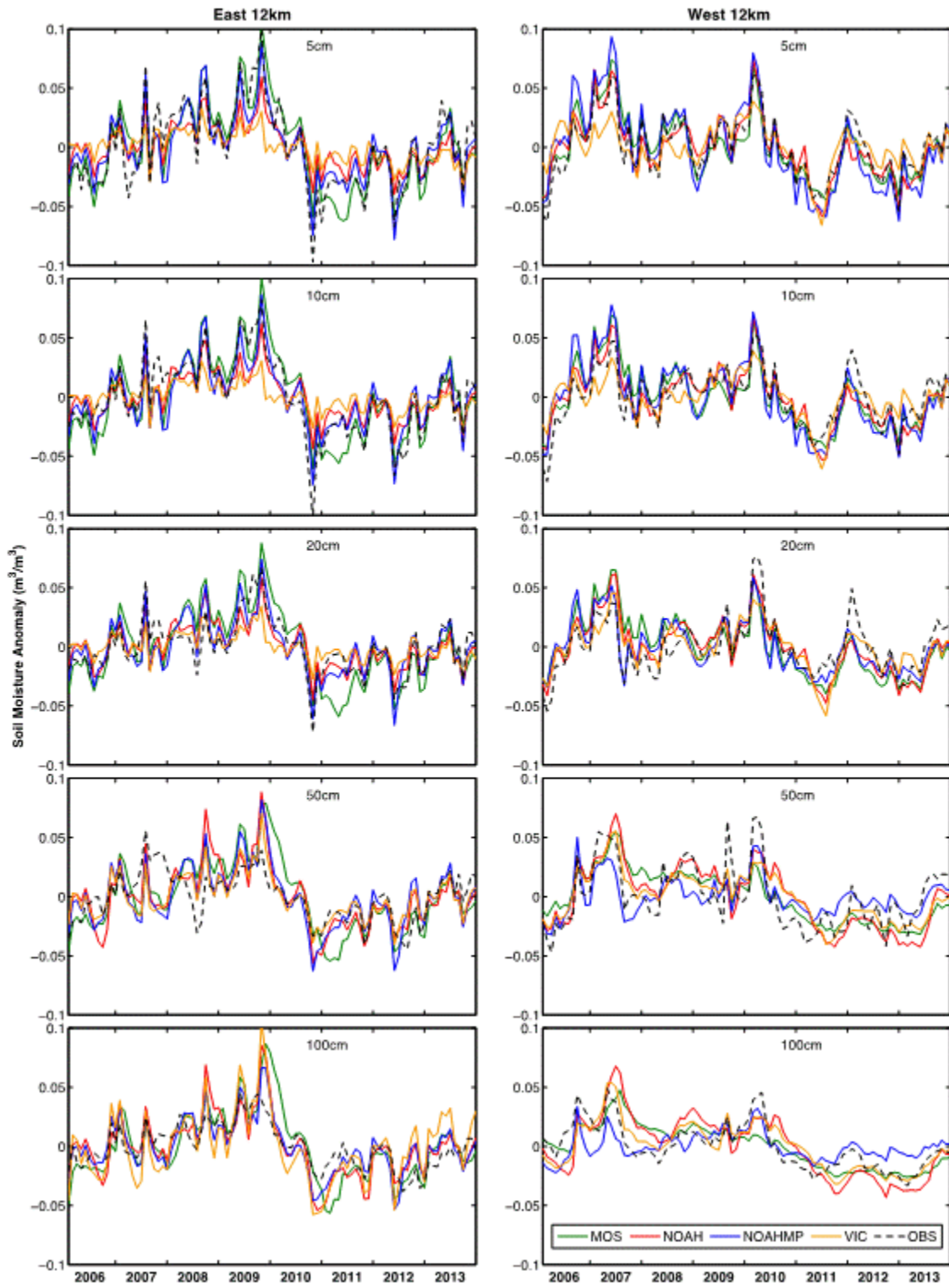


Figure 13 As in Figure 12 but averaged by month.

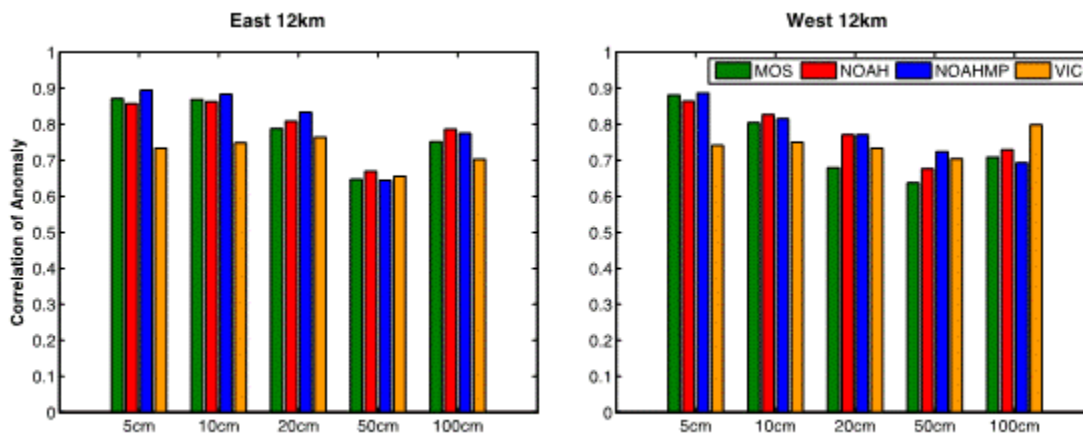


### Model skill

Simulation skill was quantified by calculating the correlation coefficient between the observed and predicted daily soil moisture anomalies using all data during 2006-2013. A higher value of the correlation coefficient indicates relatively better skill in capturing soil moisture variability and vice versa.

As shown in Figure 14, simulation skill generally decreases with increasing soil depth for all models. All datasets except VIC show high correlation coefficients ( $\sim 0.85-0.9$ ) with best values for Noah-MP at 5cm. All models show lowest correlations at 50cm ( $\sim 0.6-0.7$ ). Results for VIC show the least variability across depths and generally range 0.65-0.75. Results for Mosaic demonstrate significantly lower skill compared to Noah/Noah-MP for the 20cm and 50m western soil depths. For the western region at 100cm, VIC exhibits larger correlation values compared to the other models but are much lower for the 5cm results. The relative trends in correlation coefficients among the LSMs and regions are generally consistent with the visual differences in the anomaly time series (e.g., ref. Figure 7).

**Figure 14 Simulation skill (correlation of daily soil moisture anomaly between model simulations and observations) at different depths for the West and East portions of the 12km domain.**



### 4.4 Summary

Overall, the NLDAS-2 LSMs capture the broad features of observed soil moisture variations, including seasonal evolution, interannual differences, and the general east-to-west spatial gradients. The impacts of the precipitation events and drought are often well-reproduced at different depths; however, absolute soil moisture values are consistently predicted too high by VIC for the near-surface layers while all models tend to be drier compared to observations at deeper depths throughout the eastern region.

Statistically, the four LSMs show high simulation skill, with correlation coefficients greater than 0.7 at all soil depths. These results indicate that the NLDAS-2 LSMs are good at capturing the relative changes in the general spatial and temporal variations such as the extent and evolution of drought potentially important for BVOC emission modeling. However, the absolute model biases may be large with the magnitude partially dependent on LSM, soil depth, and location. In particular, the negative biases for deep soil moisture suggest that NLDAS-2 might consistently overestimate drought impacts at 50 and 100cm.

#### 4.5 References

- Betts, A., F. Chen, K. Mitchell, and Z. Janjic, 1997. Assessment of the land surface and boundary layer models in two operational versions of the NCEP Eta model using FIFE data, *Mon. Weather Rev.*, 125, 2896-2916, doi:10.1175/1520-0493(1997)125<2896:AOTLSA>2.0.CO;2.
- Cai, X., Z.-L. Yang, C. H. David, G.-Y. Niu, and M. Rodell, 2014a. Hydrological evaluation of the Noah-MP land surface model for the Mississippi River Basin, *J. Geophys. Res. Atmos.*, 119, 23–38, doi:10.1002/2013JD020792.
- Cai, X., Z.-L. Yang, Y. Xia, M. Huang, H. Wei, L. R. Leung, and M. B. Ek, 2014b. Assessment of simulated water balance from Noah, Noah-MP, CLM, and VIC over CONUS using the NLDAS test bed, *J. Geophys. Res. Atmos.*, 119, 13,751–13,770, doi:10.1002/2014JD022113.
- Chen, F., Z. Janjic, and K. Mitchell, 1997. Impact of atmospheric surface-layer parameterizations in the new land-surface scheme of the NCEP mesoscale Eta model, *Boundary Layer Meteorol.*, 85, 391-421, doi:10.1023/A:1000531001463.
- Cherkauer, K. A., L. C. Bowling, and D. P. Lettenmaier, 2003. Variable infiltration capacity cold land process model updates, *Global Planet. Change*, 38(1–2), 151–159, doi:10.1016/S0921-8181(03)00025-0.
- Ek, M. B., K. E. Mitchell, Y. Lin, E. Rodgers, P. Grunman, V. Koren, G. Gayno, and J. D. Tarpley, 2003. Implementation of Noah land surface model advances in the National Centers for Environmental Prediction operational mesoscale Eta model, *J. Geophys. Res.*, 108(D22), 8851, doi:10.1029/2002JD003296.
- Livneh, B., Y. L. Xia, K. E. Mitchell, M. B. Ek, and D. P. Lettenmaier, 2010. Noah LSM snow model diagnostics and enhancements, *J. Hydrometeorol.*, 11(3), 721–738, doi:10.1175/2009jhm1174.1.

Lawrence, D. M., et al., 2011. Parameterization improvements and functional and structural advances in version 4 of the Community Land Model, *J. Adv. Model. Earth Sy.*, 3, doi:10.1029/2011ms000045.

Liang, X., D.P. Lettenmaier, E.F. Wood, and S.J. Burges, 1994: A simple hydrologically based model of land surface water and energy fluxes for GCMs. *J. Geophys. Res.*, 99, 14415–14428, doi:10.1029/94JD00483.

Niu, G.-Y., et al., 2011. The community Noah land surface model with multiparameterization options (Noah-MP): 1. Model description and evaluation with local-scale measurements, *J. Geophys. Res.*, 116, doi:10.1029/2010jd015139.

Livneh, B., Y.L. Xia, K.E Mitchell, M.B. Ek, and D.P. Lettenmaier, 2010. Noah LSM snow model diagnostics and enhancements, *J. Hydrometeorology*, 11(3), 721-738, doi:10.1175/2009jhm1174.1

Mitchell, K.E., D. Lohmann, P.R. Houser, E.F. Wood, J.C. Schaake, A. Robock, B.A. Cosgrove, J. Sheffield, Q. Duan, L. Luo, R.W. Higgins, R.T. Pinker, J.D. Tarpley, D.P. Lettenmaier, C.H. Marshall, J.K. Entin, M. Pan, W. Shi, V. Koren, J. Meng, B.H. Ramsay, and A.A. Bailey, 2004. The multi-institution North American Land Data Assimilation System (NLDAS): Utilizing multiple GCIIP products and partners in a continental distributed hydrological modeling system, *J. Geophys. Res.*, 109, D07S90, doi:10.1029/2003JD003823.

Rui, Hualan, and David Mocko, 2014. Readme document for North American Land Data Assimilation System Phase 2 (NLDAS-2).Goddard Earth Sciences Data and Information Services Center.

Saha, Suranjana, and Coauthors, 2010. The NCEP Climate Forecast System Reanalysis. *Bull. Amer. Meteor. Soc.*, 91, 1015-1057. doi: 10.1175/2010BAMS3001.1

Skamarock, W. C., J. B. Klemp, J. Dudhia, D. O. Gill, M. Barker, K. G. Duda, Y. Huang, W. Wang, and J. G. Powers, 2008. A description of the Advanced Research WRF version 3, Tech. Note NCAR/TN-475 + STR, 113pp., Natl. Cent. for Atmos. Res., Boulder, Colo.

Wei, H., Y. Xia, K. E. Mitchell, and M. B. Ek, 2011. Improvement of Noah land surface model for warm season processes: Evaluation of water and energy flux simulation, *Hydrol. Processes*, doi:10.1002/hyp.9214.

Wood, E.F., D.P. Lettenmaier, X. Liang, B. Nijssen, and S.W. Wetzel, 1997. Hydrological modeling of continental-scale basins. *Annu. Rev. Earth Planet. Sci.*, 25, 279–300, doi:10.1146/annurev.earth.25.1.279.

Xia, Y., K. Mitchell, M. Ek, J. Sheffield, B. Cosgrove, E. Wood, L. Luo, C. Alonge, H. Wei, J. Meng, B. Livneh, D. Lettenmaier, V. Koren, Q. Duan, K. Mo, Y. Fan, and D. Mocko, 2012. Continental-scale water and energy flux analysis and validation for the North American Land Data Assimilation System project phase 2 (NLDAS-2): 1. Intercomparison and application of model products, *J. Geophys. Res.*, 117, D03109, doi:10.1029/2011JD016048.

Xia, Y., J. Sheffield, M. B. Ek, J. Dong, N. Chaney, H. Wei, J. Meng, and E. F. Wood, 2014b. Evaluation of multi-model simulated soil moisture in NLDAS-2, *J. Hydrol.*, 512, 107–125, doi:10.1016/j.jhydrol.2014.02.027.

Yang, Fanglin, Hua-Lu Pan, Steve Krueger, Shrinivas Moorthi, Stephen Lord, 2006. Evaluation of the NCEP Global Forecast System at the ARM SGP Site. *Monthly Weather Review*. 134, No. 12, 3668-3690.

Yang, Z.-L., et al., 2011. The community Noah land surface model with multiparameterization options (Noah-MP): 2. Evaluation over global river basins, *J. Geophys. Res.*, 116, doi:10.1029/2010jd015140.

## 5.0 Comparison of in-situ and NLDAS-2 soil moisture at eastern Texas locations

### 5.1 Methodology

The in-situ soil moisture measurements during 2006-2013 at the four eastern Texas and one Oklahoma locations (ref. Table 3 and analyses presented in Section 3) are compared to predictions from the NLDAS-2 datasets (Mosaic, Noah, Noah-MP, VIC). The NLDAS-2 dataset are the predictions for the 1/8 degree grid cell that contains each monitoring location; the primary focus is on seasonally-averaged values.

A direct comparison between in-situ measurements and NLDAS-2 model simulations is not possible because the measurements are made at depths that differ from the model configuration. The SCAN and CRN networks collect measurements at five distinct vertical depths, i.e., 5, 10, 20, 50, and 100cm wherever possible, while the Oklahoma Mesonet collects observations at 5, 25, 60, and 75cm. The NLDAS-2 models simulate average water availability within multiple vertical soil layers, e.g., 0-10, 0-100, 0-200, 10-40, 40-100, and 100-200cm for Noah. To overcome this inconsistency between measurements and model simulations, the NLDAS-2 datasets were linearly interpolated to the in-situ measurement depths at each location. The modeled average soil moisture was assumed as the value at the middle of each layer, i.e. 5, 25, 70, and 150cm for 0-10, 10-40, 40-100, and 100-200cm layers, respectively. Because the thicknesses of VIC soil layers vary spatially, a vertical interpolation was performed to convert them into four uniform soil depths as in Noah model, following the protocol of Xia et al. (2014). This was achieved by calculating the weighted average of soil moisture in each VIC layer that intersected each of the Noah model layers. For grid cells where the lowest VIC layer was shallower than the lowest Noah layer, the VIC soil moisture value was assumed to be uniform down to the depth of the bottom of the Noah layer, i.e., 200cm.

### 5.2 Results

#### *Example daily data (year 2011 at Palestine)*

To demonstrate an example comparison of soil moisture contents at a relatively high temporal resolution, Figure 15 presents daily Palestine 2011 values at the 5cm and 100cm soil depths (ref. Figure 4 for daily total precipitation measured at this location and time period.) Observed 5cm soil moisture exceeded  $0.25 \text{ m}^3/\text{m}^3$  during winter compared to nearly zero during much of the April-October growing season. During the winter months, all NLDAS-2 models predict lower soil moisture compared to observations; the lowest NLDAS-2 predictions are by Mosaic. VIC, which has relatively little seasonal variability, has substantially greater soil moisture values during the growing season compared to observations as well as the other NLDAS-2 models. The observed extremely low soil moisture values during summer and early fall are often

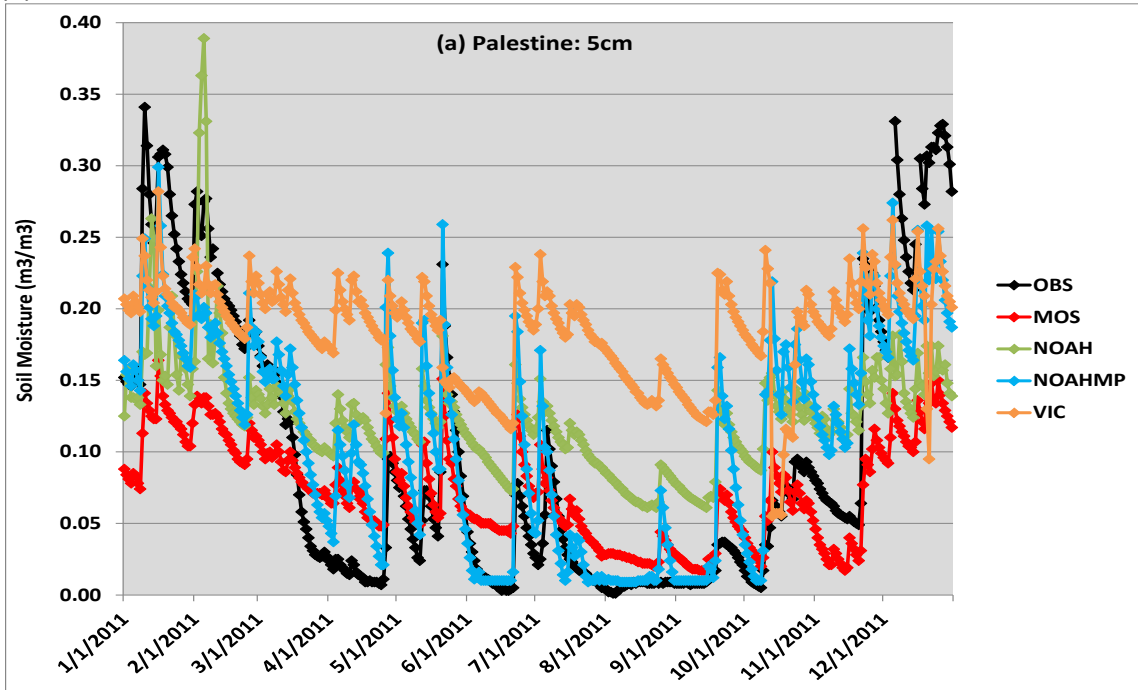
well-captured by Noah-MP compared to slightly greater moisture predictions by Mosaic; Noah predicts higher values roughly halfway between the Noah-MP and VIC simulations. Although the predicted changes in Noah-MP soil moisture displayed visually in Figure 15 appear to best capture the overall magnitude of observed changes during the spring and fall transition seasons, the observed seasonal values are often closer in magnitude to the Mosaic predictions that are characterized by a relatively flatter temporal profile compared to Noah-MP. Periodic spikes in soil moisture values associated with episodic rain events are often predicted by all models; Noah-MP typically simulates greater magnitude increases within these soil moisture spikes than observed.

Soil moisture observations at 100cm indicate consistently high winter values ( $\sim 0.42 \text{ m}^3/\text{m}^3$ ) compared to much lower baseline values of approximately  $0.125 \text{ m}^3/\text{m}^3$  for the majority of May through November. Compared to the predicted variability in soil moisture values at 5cm, the 100cm NLDAS-2 predictions are rather similar among the four models and do not temporally replicate the magnitude of marked and abrupt changes in observed soil moisture during March and late November. All NLDAS-2 soil moisture values are substantially lower compared to observations during the winter and spring months; VIC and Mosaic are in good agreement with observations during May through November with slightly drier values predicted by Noah and Noah-MP. Although coincident minor spikes in soil moisture associated with an early June precipitation event are noted, the magnitudes of increases in NLDAS-2 soil moisture in response to at least two obvious rain events are far less than observed.

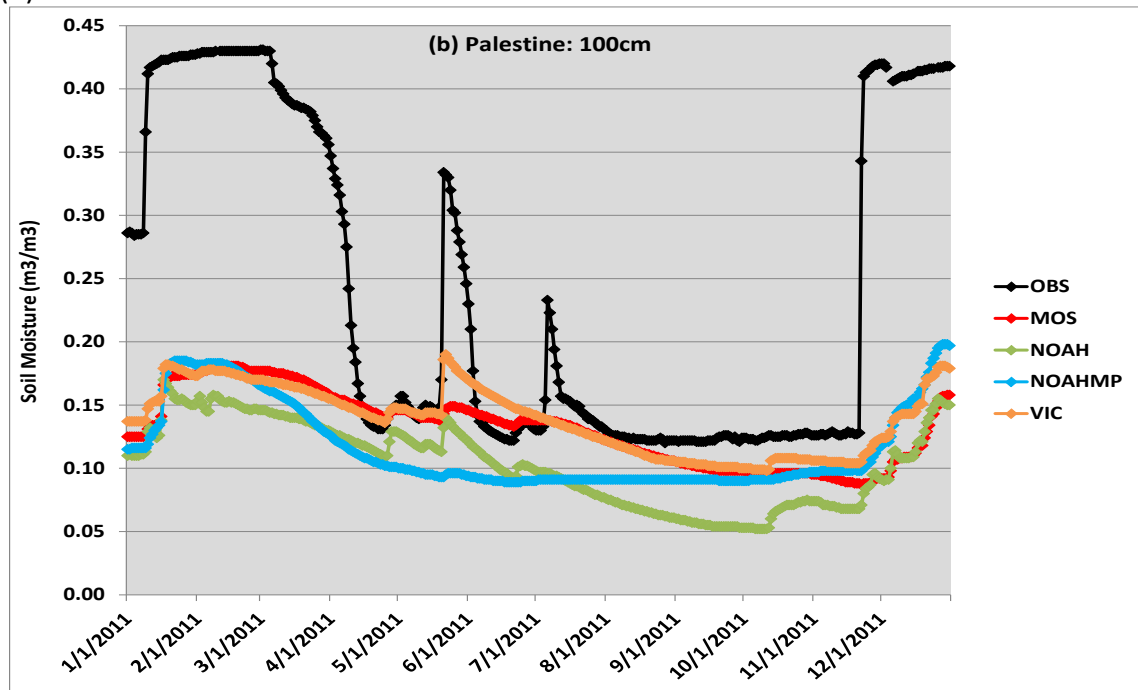
Overall, the NLDAS-2 datasets generally capture the broad seasonal variations of observed soil moisture in addition to responses during specific precipitation events. These comparisons demonstrate that although the majority of precipitation events are often well-captured, there is often a large bias in the baseline soil moisture. The finding of bias is common to other studies (e.g., Xia et al., 2014; Cai et al., 2014) and may be due, in part, to the previously mentioned sources of uncertainties (ref. uncertainties discussion in Section 4.2).

Figure 15 Daily observed (in-situ) and NLDAS-2 (predicted) soil moisture at the Palestine monitoring location during 2011 at soil depths of (a) 5cm and (b) 100cm.

(a) 5cm



(b) 100cm



### *Seasonal soil moisture*

In order to provide an overview of the seasonal trends in soil moisture values, Figure 16 presents average seasonal values by location and year. Daily NLDAS-2 predictions and observations were paired in space and time; seasonal averages were computed if at least 59 observations were available. Across all locations at 5cm depth, VIC most often predicts soil moisture values that are too wet compared to observations as well as the other NLDAS-2 models. VIC, and to a lesser extent Noah, tend to exhibit lower seasonal variability compared to Mosaic and Noah-MP. Across the monitoring locations, seasons, and depths, there is wide variability in the model that best represents observations. For example, the observed year-to-year seasonal magnitude and inter-annual differences at Palestine are best captured by Noah-MP; Mosaic predictions agree well with the very low observed soil moisture conditions at Port Aransas, while Noah shows the best agreement with 5cm observations at Austin and Durant. At deeper soil depths at Prairie View and Palestine, all models are substantially drier compared to observations while the opposite trend is noted at Port Aransas.

In a demonstration of the variability of model predictions with respect to depth, the strong and relatively consistent magnitude of observed seasonal variations at 60cm at Durant are generally well-captured by Noah-MP. However, the Noah-MP 5cm predictions are substantially too moist with greatly exaggerated seasonal variability while Noah shows excellent agreement with observations.

**Figure 16 Average seasonal observed (in-situ) and NLDAS-2 (predicted) soil moisture contents ( $m^3/m^3$ ) at selected soil depths during 2006-2013 for (a) Palestine, (b) Prairie View, (c) Port Aransas, (d) Austin, and (e) Durant (OK). Hourly observed and NLDAS-2 values were matched in space and time; seasonal averages were only calculated using hours with valid observations and a requirement of 75% data completeness by season. (spring==Mar/Apr/May; summer==Jun/Jul/Aug; fall==Sep/Oct/Nov; winter==Dec/Jan/Feb)**

(a) Palestine (summer 2009 – fall 2013); (1) 5cm, (2) 20cm, and (3) 100cm soil depths

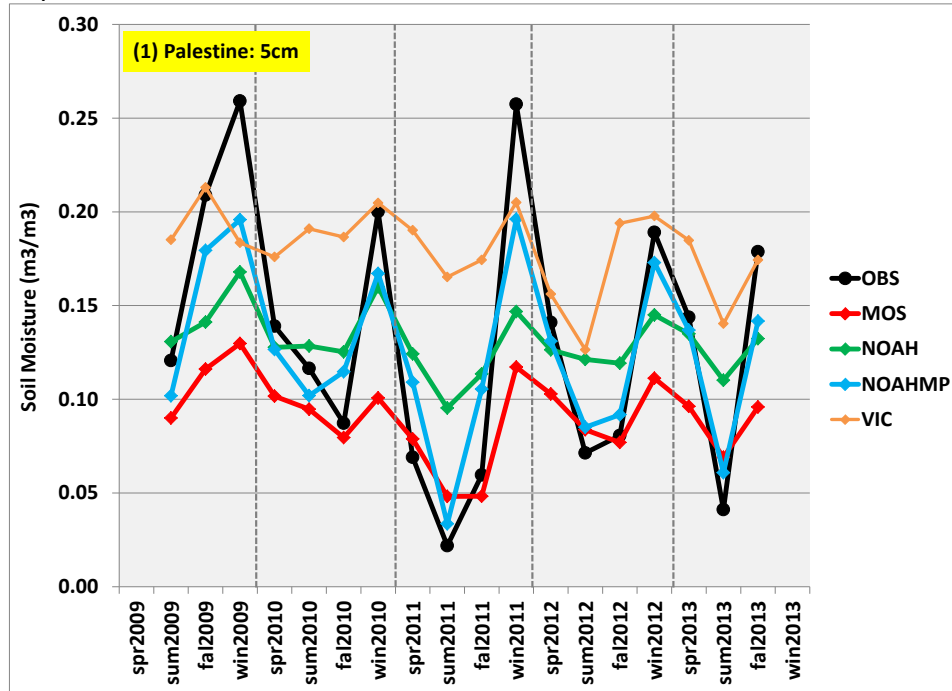


Figure 16 (continued)

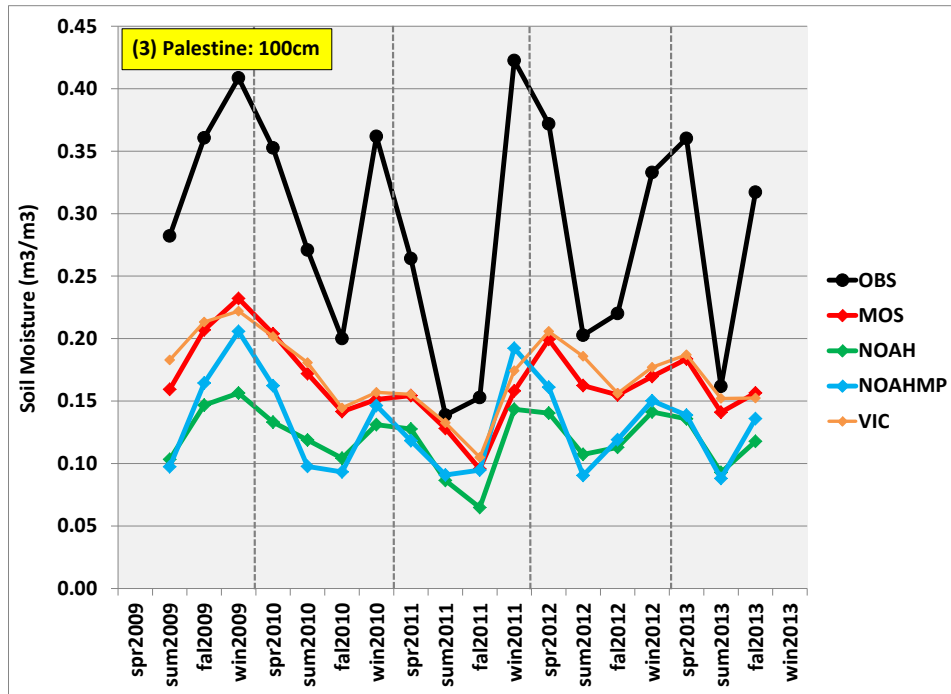
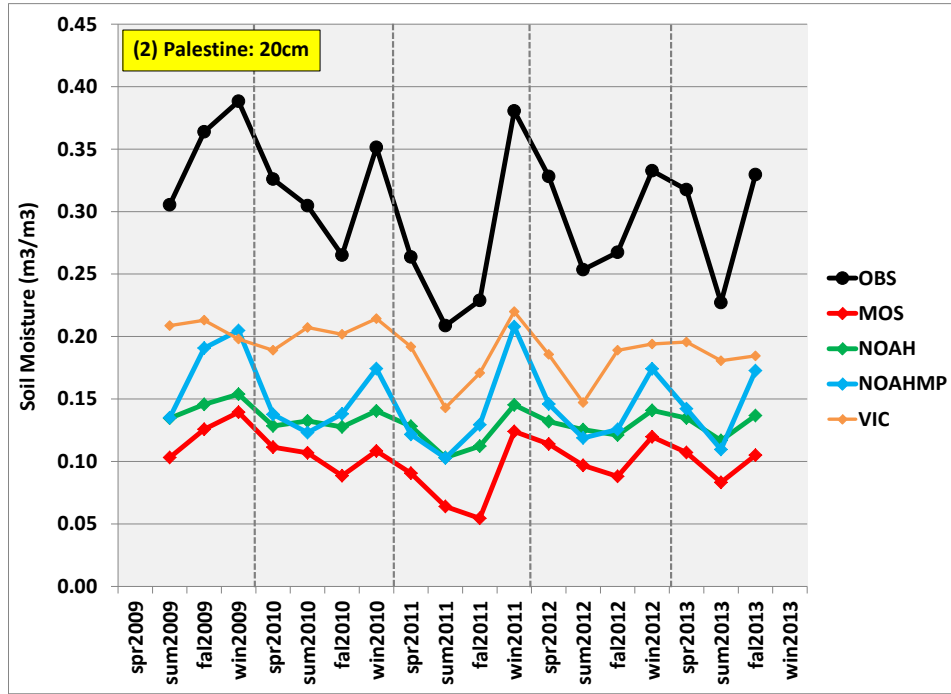


Figure 16 (continued)

(b) Prairie View (winter 2006 – fall 2013); (1) 5cm, (2) 20cm, and (3) 100cm soil depths

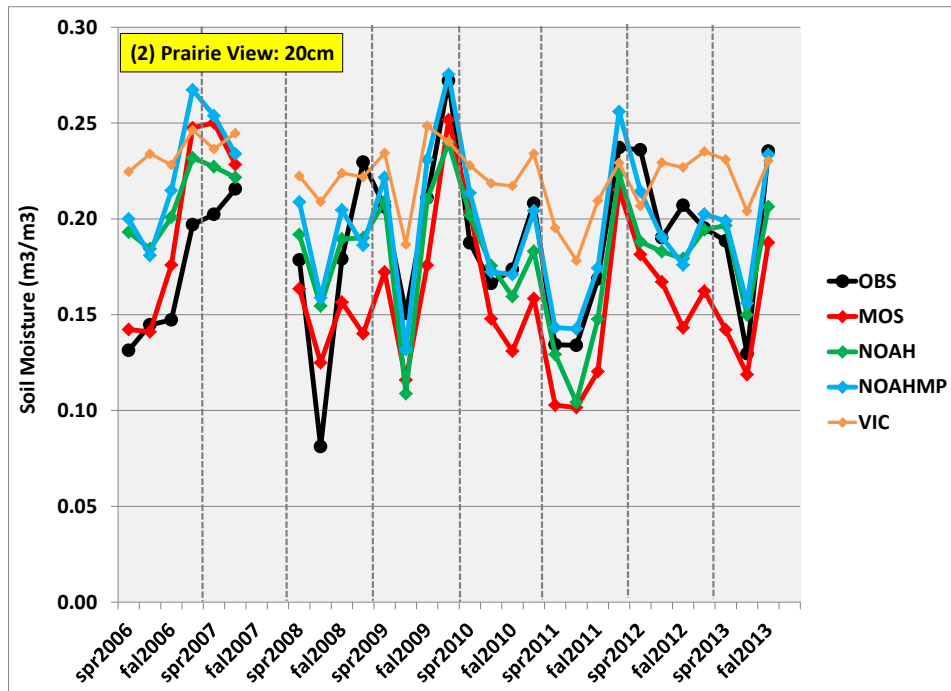
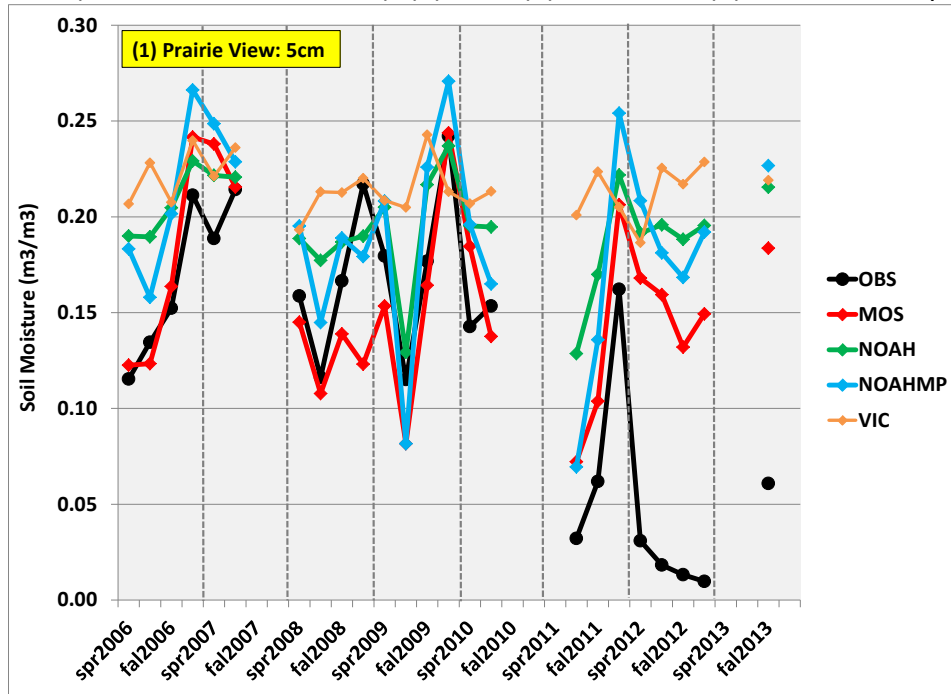
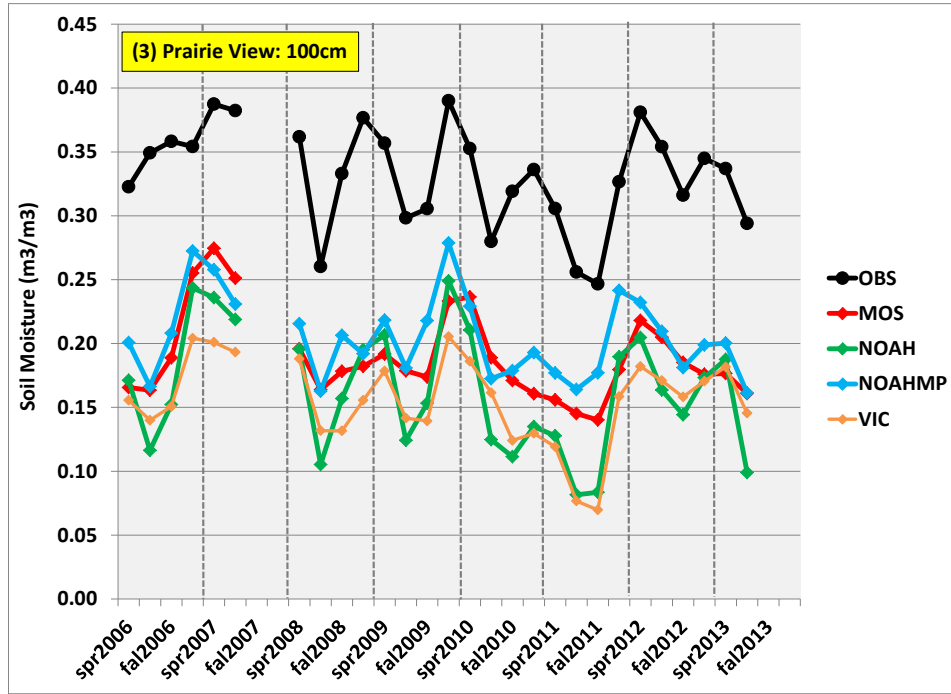


Figure 16 (continued)



(c) Port Aransas (summer 2011 – fall 2013), (1) 5cm and (2) 100cm soil depths

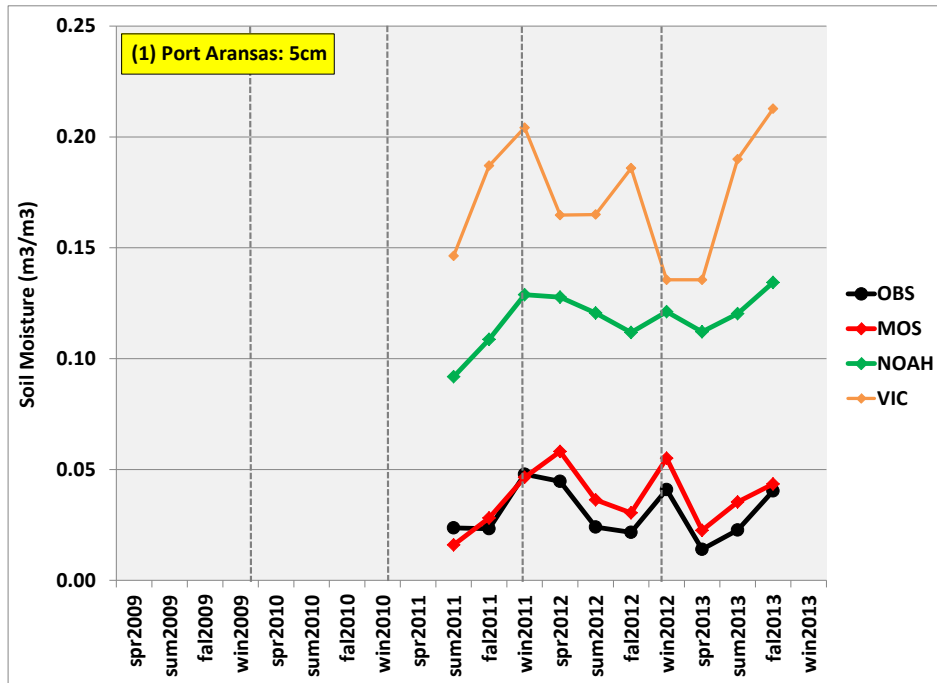
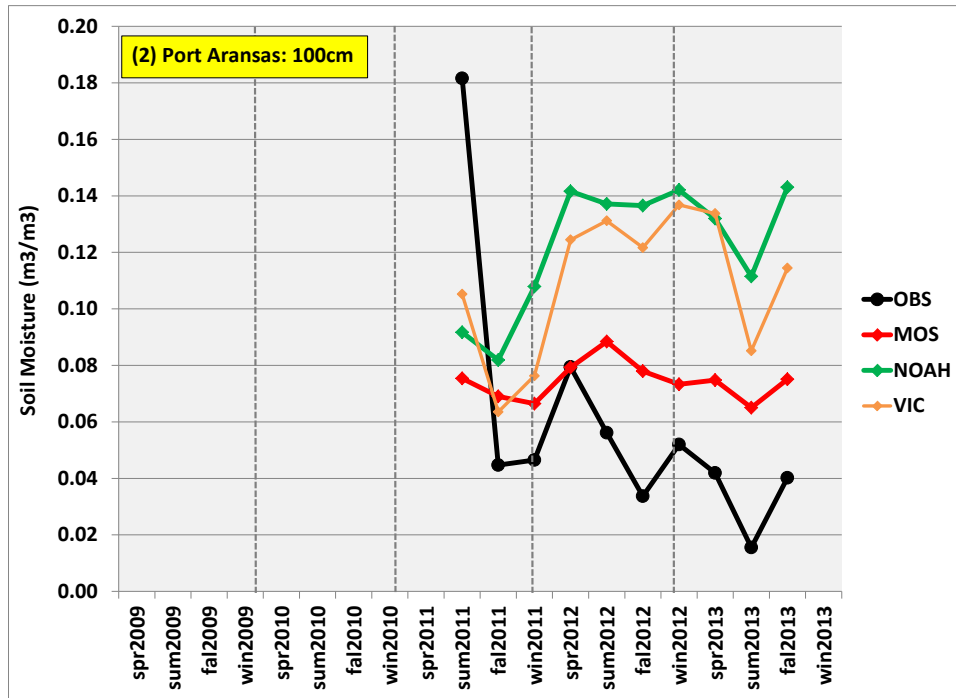


Figure 16 (continued)



(d) Austin (summer 2010 – fall 2013), (1) 5cm soil depth

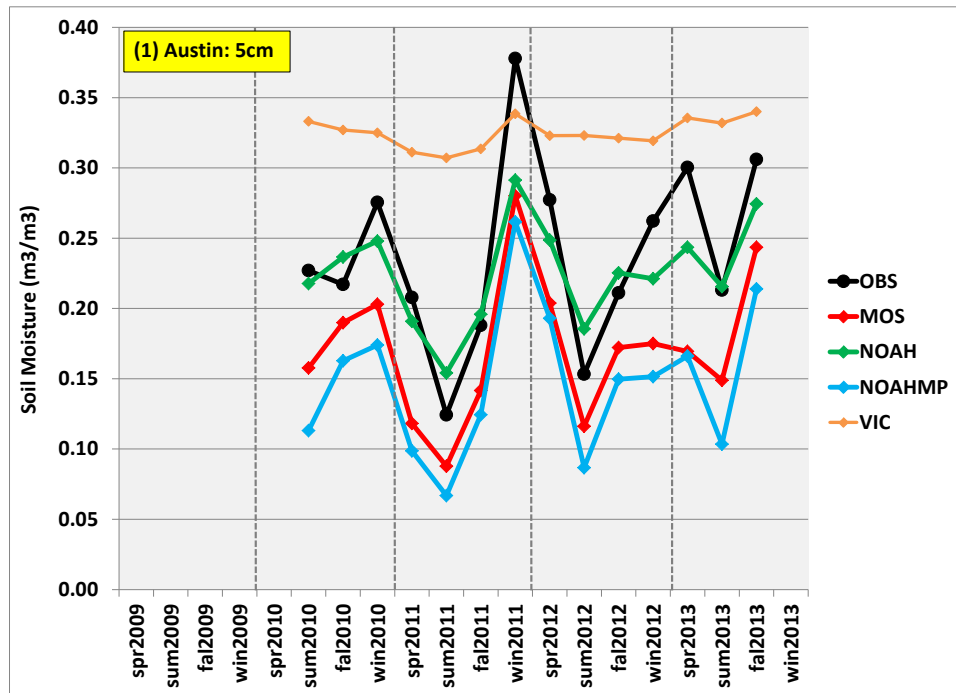
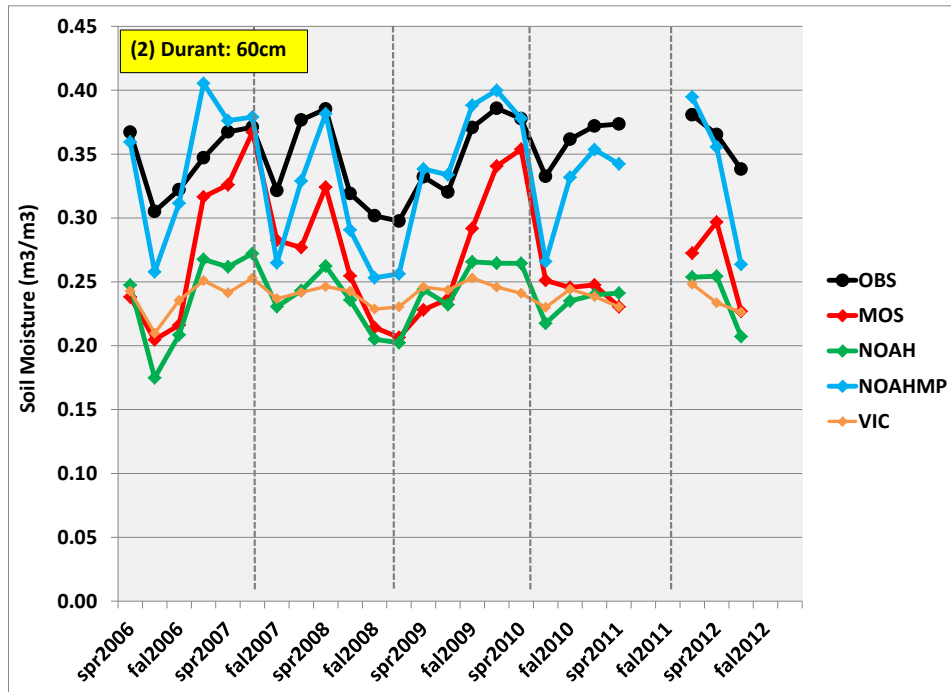
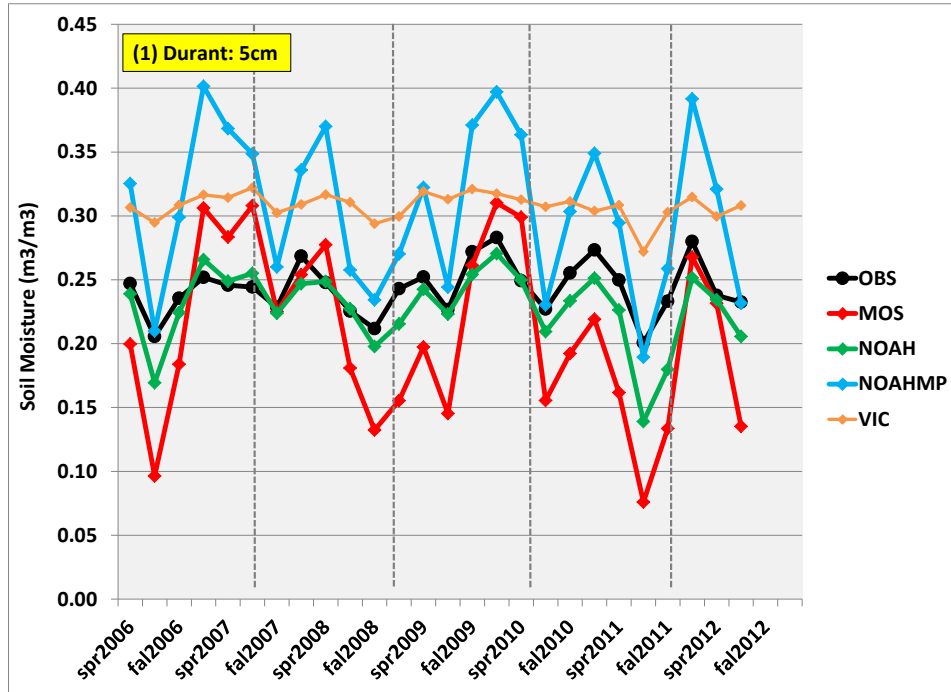


Figure 16 (continued)

(e) Durant (spring 2009 – summer 2012), (1) 5cm and (2) 60cm soil depths

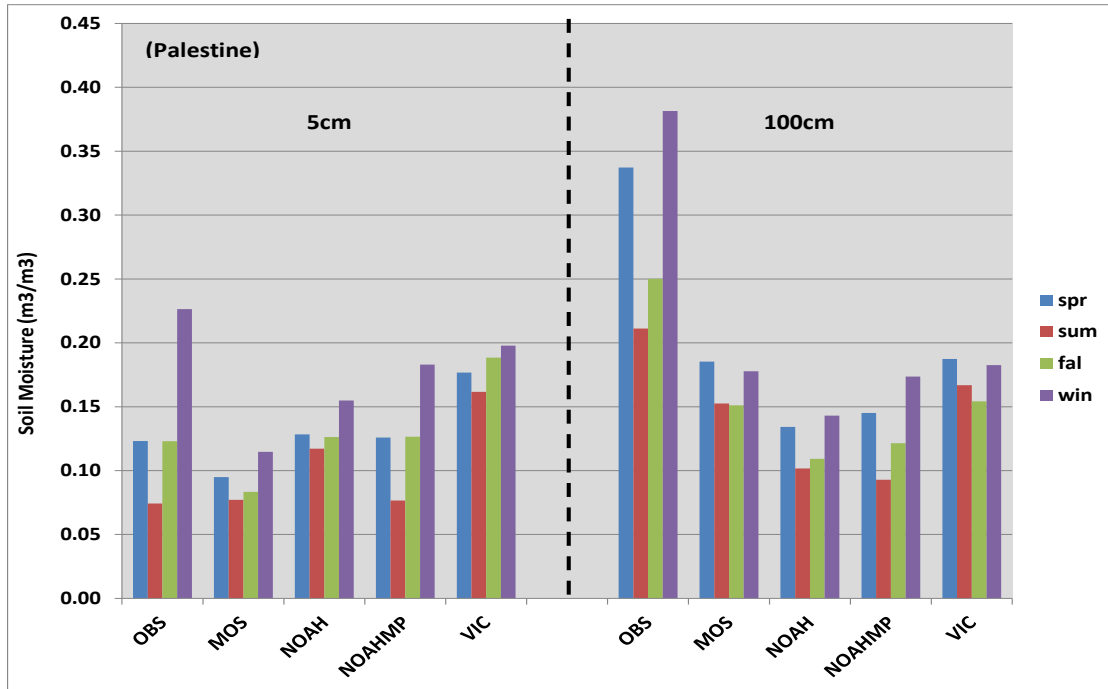


Compared to the other monitoring locations, Palestine and Prairie View show substantial differences in inter-annual seasonal variability. For ease of visual comparison of the overall seasonal trends, the available seasonal values for years 2006-2013 shown for Palestine (ref. Figure 16a) and Prairie View (ref. Figure 16b) are averaged and provided in Figure 17 for the 5cm and 100cm soil depths. At 5cm, both Mosaic and Noah-MP capture the summer minimum at Palestine; the Mosaic average spring and fall values are too low compared to observations but well-predicted by both Noah-MP and Noah while the relatively wettest winter prediction for Noah-MP is closest, but still lower than, the observed wintertime peak. Overall across all seasons, Noah-MP best simulates the observed seasonality at 5cm. At 100cm, slightly greater soil moisture values predicted by Mosaic compared to other models are closer to observations but still more similar to the other model predictions than the observed (wetter) seasonal averages.

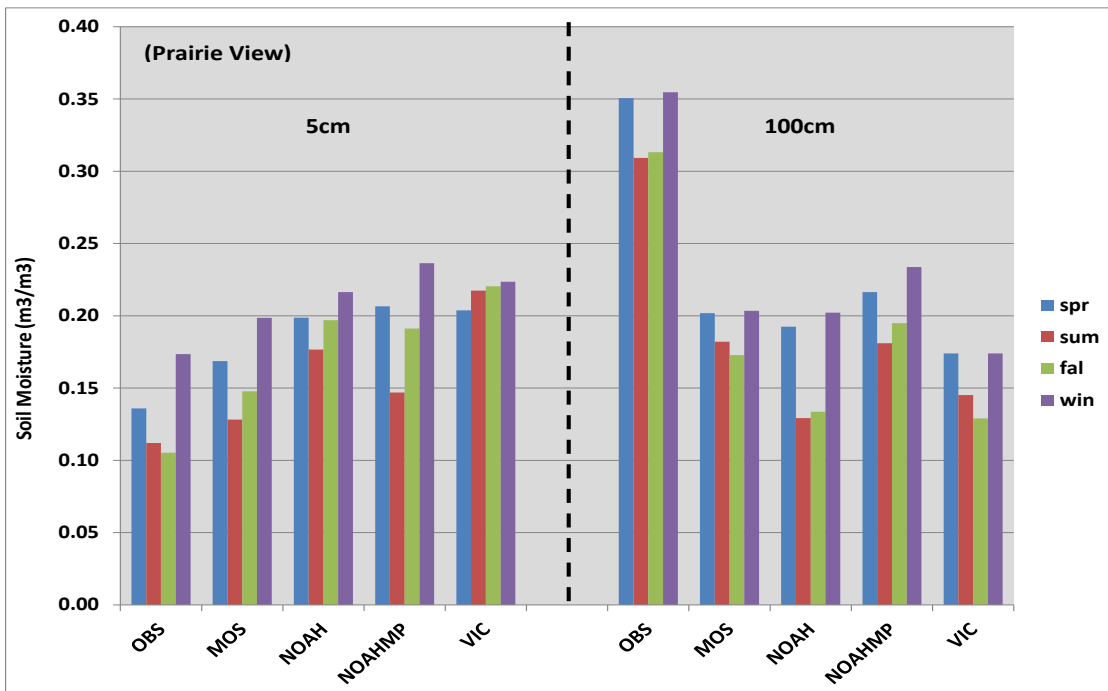
At 5cm at Prairie View, the average seasonal trends predicted by Mosaic are most similar to observations while other models show slightly greater soil moisture values. As for Palestine at 100cm, the NLDAS-2 predictions at Prairie View are substantially lower than observations but with slightly higher predictions for Noah-MP not Mosaic.

**Figure 17 Average seasonal observed and NLDAS-2 soil moisture contents (m<sup>3</sup>/m<sup>3</sup>) at 5cm and 100cm soil depths based on all available data shown in Figure 16 for (a) Palestine and (b) Prairie View.**

(a) Palestine



(b) Prairie View



*Inter-annual season variability during summer*

In order to directly compare inter-annual variations in seasonal soil moisture values between observations and NLDAS-2 predictions, summer soil moisture values at Palestine, Prairie View, and Austin at 5cm (ref. Figure 18) and 50cm (ref. Figure 19) depths for all years. The years are presented in ascending order of observed soil moisture values. VIC often shows little interannual variability compared to Noah, Noah-MP, and Mosaic. Although there are relative differences in the magnitude of year-to-year differences for the NLDAS-2 datasets compared to observations, the directional changes are often well-captured; for example, both observed and NLDAS-2 soil moisture values are relatively low for drought year 2011 compared to other years. At 5cm, an obvious exception is for year 2012 at Prairie View that was extremely dry according to measurements; in contrast, all models predict moist conditions compared to other years.

**Figure 18 Summer average 5cm soil moisture during all available years 2006-2013 at (a) Palestine, (b) Prairie View, and (c) Austin. Years are ordered by ascending observed values.**

(a) Palestine

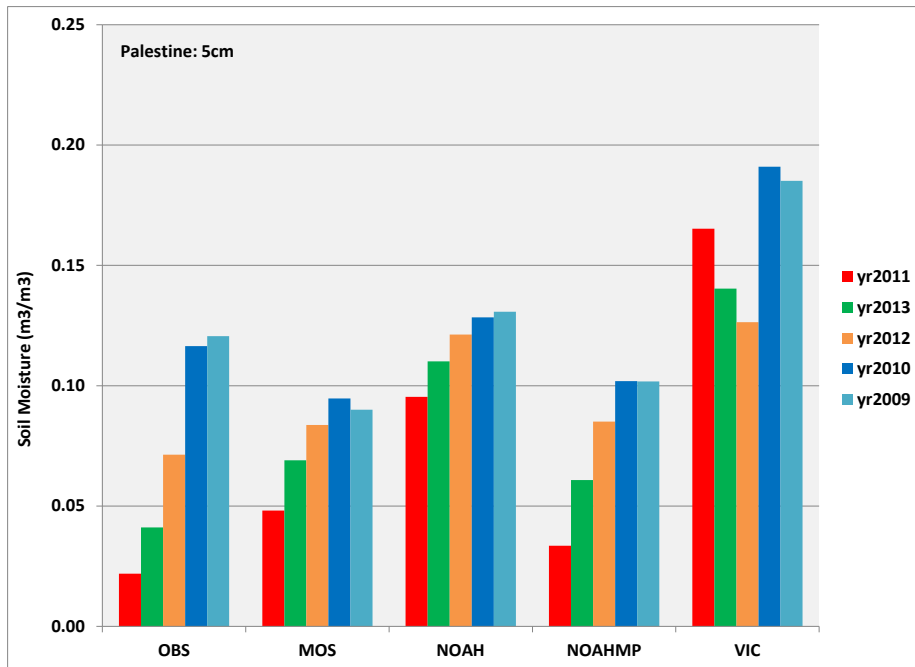
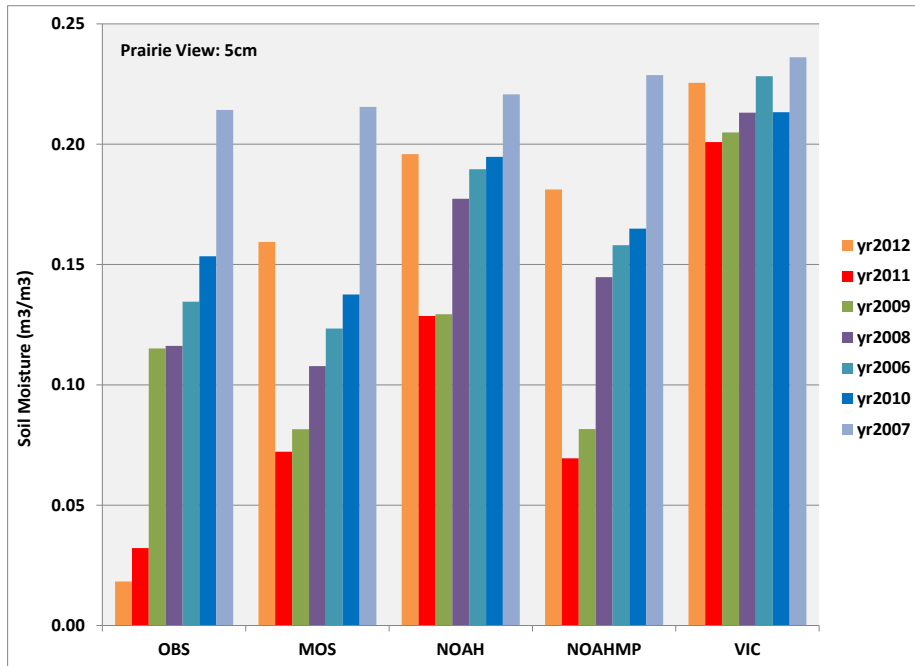
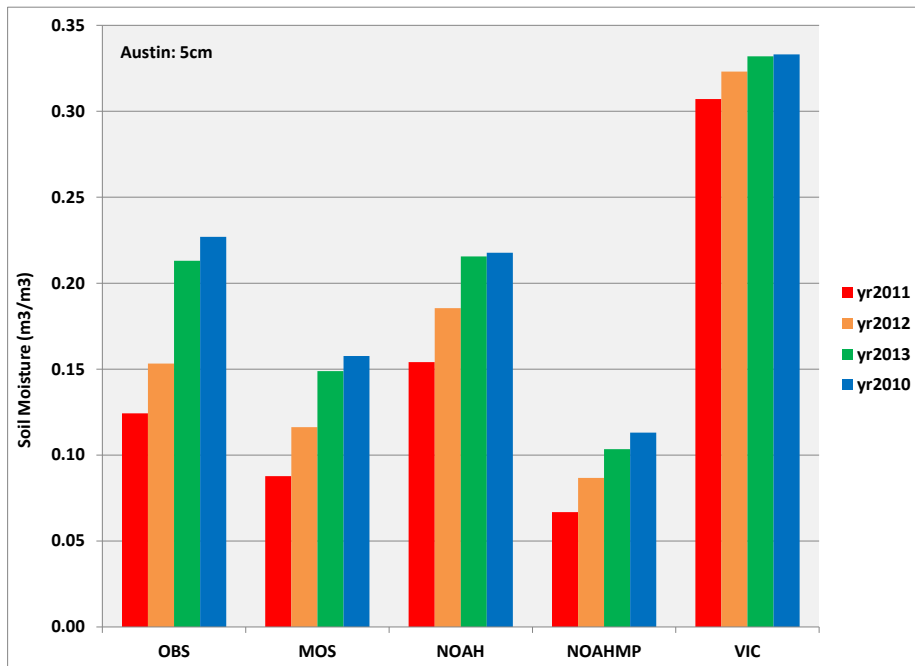


Figure 18 (continued)

(b) Prairie View

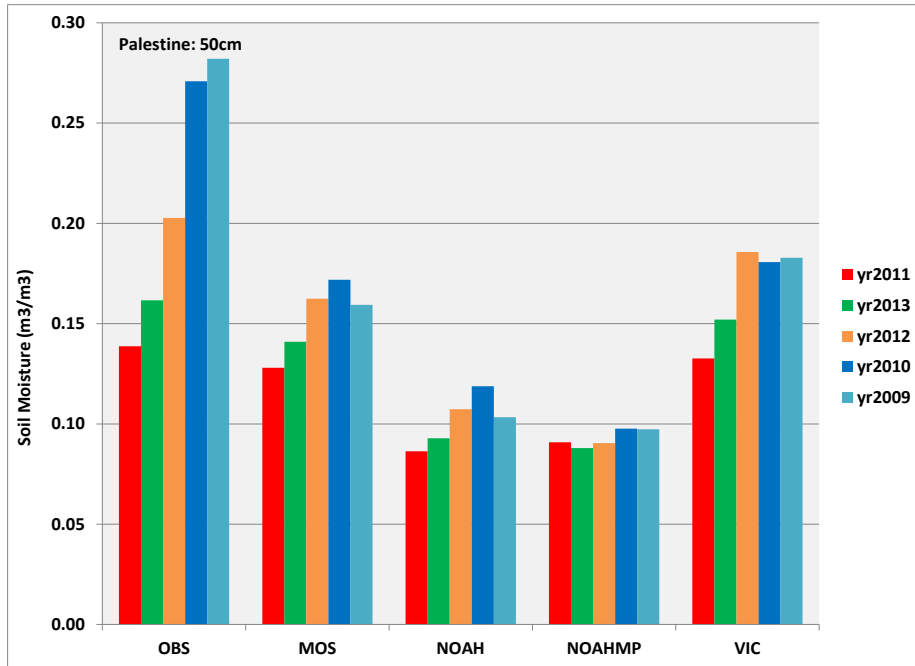


(c) Austin

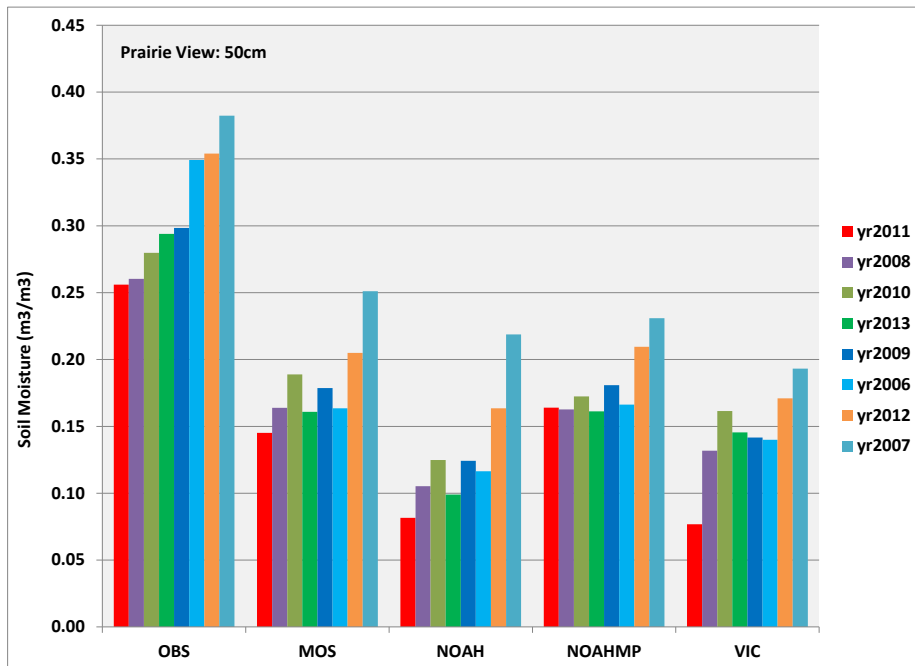


**Figure 19 Summer average 50cm soil moisture during all available years 2006-2013 at (a) Palestine, and (b) Prairie View. Years are ordered by ascending observed values.**

(a) Palestine



(b) Prairie View



### 5.3 Summary

Overall, the comparison between observations and NLDAS-2 predictions at five limited monitoring locations indicates that VIC generally shows the poorest agreement with observations and is consistently too wet in the near-surface layers. Depending on the specific location and season, Noah-MP, Mosaic, or Noah may have the best agreement with observations in the near-surface layers while all models predict substantially drier soil moisture at deeper soil layers compared to observations. The year-to-year directional variability in seasonal average soil moisture values is often captured by the NLDAS-2 models; however, the magnitude of inter-annual differences can be substantially different than observed.

### 5.4 References

- Cai, X., Z.-L. Yang, C. H. David, G.-Y. Niu, and M. Rodell, 2014a. Hydrological evaluation of the Noah-MP land surface model for the Mississippi River Basin, *J. Geophys. Res. Atmos.*, 119, 23–38, doi:10.1002/2013JD020792.
- Xia, Y., J. Sheffield, M. B. Ek, J. Dong, N. Chaney, H. Wei, J. Meng, and E. F. Wood, 2014b. Evaluation of multi-model simulated soil moisture in NLDAS-2, *J. Hydrol.*, 512, 107–125, doi:10.1016/j.jhydrol.2014.02.027.

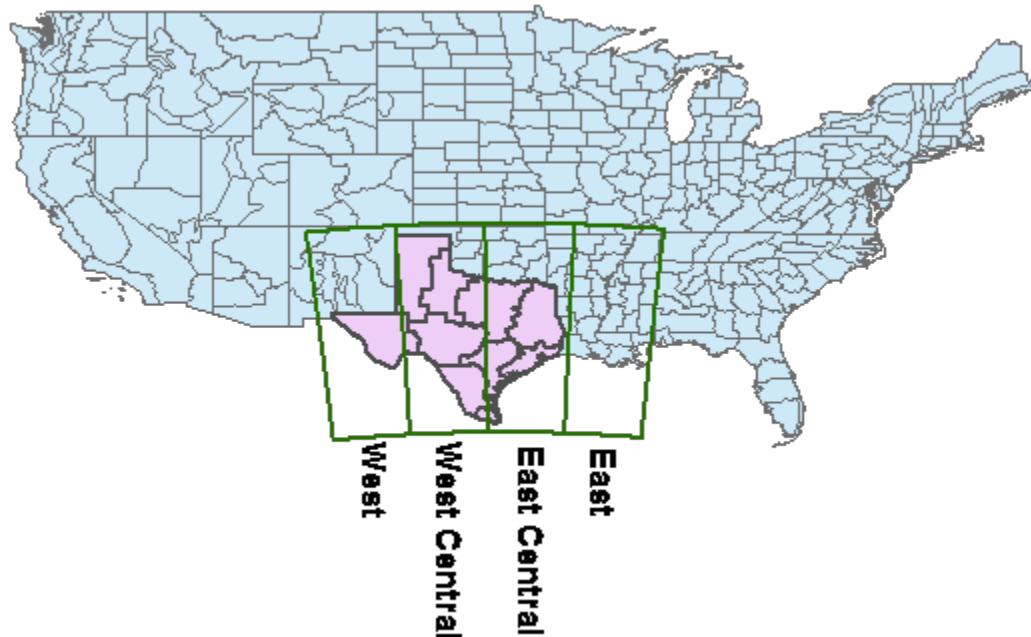
## 6.0 Intercomparison of NLDAS-2 simulated soil moisture datasets during 2006-2013

This section presents an inter-comparison of Noah, Noah-MP, Mosaic, and VIC soil moisture predictions for years 2006-2013. Additionally, results from the NLDAS-2 models are contrasted to GRACE total water storage (TWS).

### 6.1 Methods

The regions of focus include the five eastern Texas climate regions (North Central, South Central, East, Upper Coast, and Edwards Plateau within the 4km grid domain; ref. Figure 2) as well as four subdivisions of the 12km domain: East, East Central, West Central, and West (ref. Figure 20). The longitudes used to define the four 12km sub-regions are roughly along  $-93^{\circ}$ ,  $-98^{\circ}$ , and  $-103^{\circ}$  W to ensure the 4 subdomains have equal spatial area. For the purposes of soil moisture inter-comparisons, predictions from all grid cells within a given target region are averaged; monthly averages are employed instead of daily values to avoid the often dense overlap among model outputs. As discussed previously in Section 4.2, results are analyzed using the Noah vertical soil layer structure, i.e., 0-10, 10-40, 40-100, and 100-200cm.

**Figure 20** The four sub-regions of the 12km grid domain (West, West Central, East Central, East) defined for the NLDAS-2 soil moisture inter-comparison. Analysis regions also include the five eastern Texas regions (North Central, South Central, East, Upper Coast, Edwards Plateau) as shown in Figure 2.



## 6.2 Results

### *12km grid domain*

Figure 21 shows monthly average NLDAS-2 soil moisture contents during 2006-2013 for the four 12km sub-regions. As previously demonstrated with observations (ref. Section 4), NLDAS-2 soil moisture generally decreases moving east to west at all soil depths. For the top two surface layers, the East sub-region, and to a lesser extent East Central, show consistent annual seasonal patterns compared to West Central and West. The VIC predictions are relatively flat and at higher values compared to the other models. Noah predicts the greatest cool season soil moisture values for East and East Central; Mosaic predicts the lowest overall values for the other regions.

For the two deepest soil layers, the West monthly time-series of soil moisture is generally flat across all seasons and years in contrast to the much stronger and regular annual seasonal variability predicted for East. As for the near-surface layers, VIC predicts the highest soil moisture (with the exception of the deeper East layers). The relative agreement between models varies spatially; for example, Noah-MP and Mosaic provide more similar predictions for East at 100-200cm compared to VIC and Noah whereas Mosaic and Noah are more similar for West Central compared to slightly wetter predictions by VIC and Noah-MP. This highlights the tendency for biases between models to vary both horizontally and vertically; that is, the relative directional differences in predictions between models is generally consistent over all years for a given soil depth and location but the directional differences often vary between soil layers and/or regions.

The inter-model differences of simulated soil moisture are caused, in part, by differences in evapotranspiration (ET) because ET controls how much soil water is lost through evaporation and transpiration by vegetation (Xia et al., 2015). Generally, a higher ET would result in drier soils and vice versa. Disparities in soil moisture associated with differences in layer-specific ET are also likely affected by differences in root zone depths between models. Other soil texture related parameters such as total water storage capacity, wilting point, hydraulic conductivity, among others, may also affect soil moisture simulations (Schaafe et al., 2004).

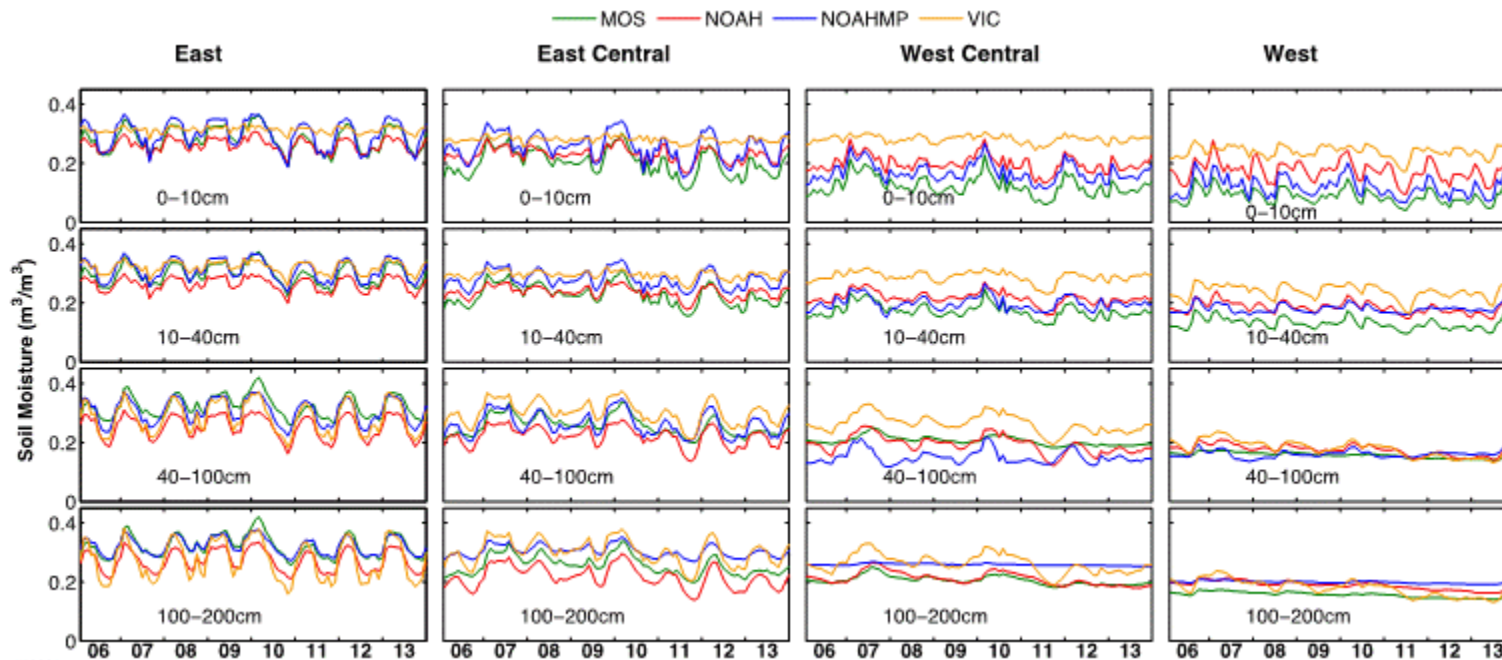
### *Eastern Texas*

Figure 22 presents the monthly average NLDAS-2 results for the five eastern Texas climate divisions. Similar to the results for the 12km sub-regions, the VIC predictions stand out due to a relative lack of temporal variation in the top soil layers and generally provide the wettest predictions. Interestingly, VIC predicts seasonal variability more similar to Noah and Mosaic at 100-200cm contrasted to the flat profile predicted by Noah-MP at this depth. For the top layers, Noah-MP tends to predict the highest soil moisture while Mosaic consistently predicts the lowest values. The Noah and Noah-MP

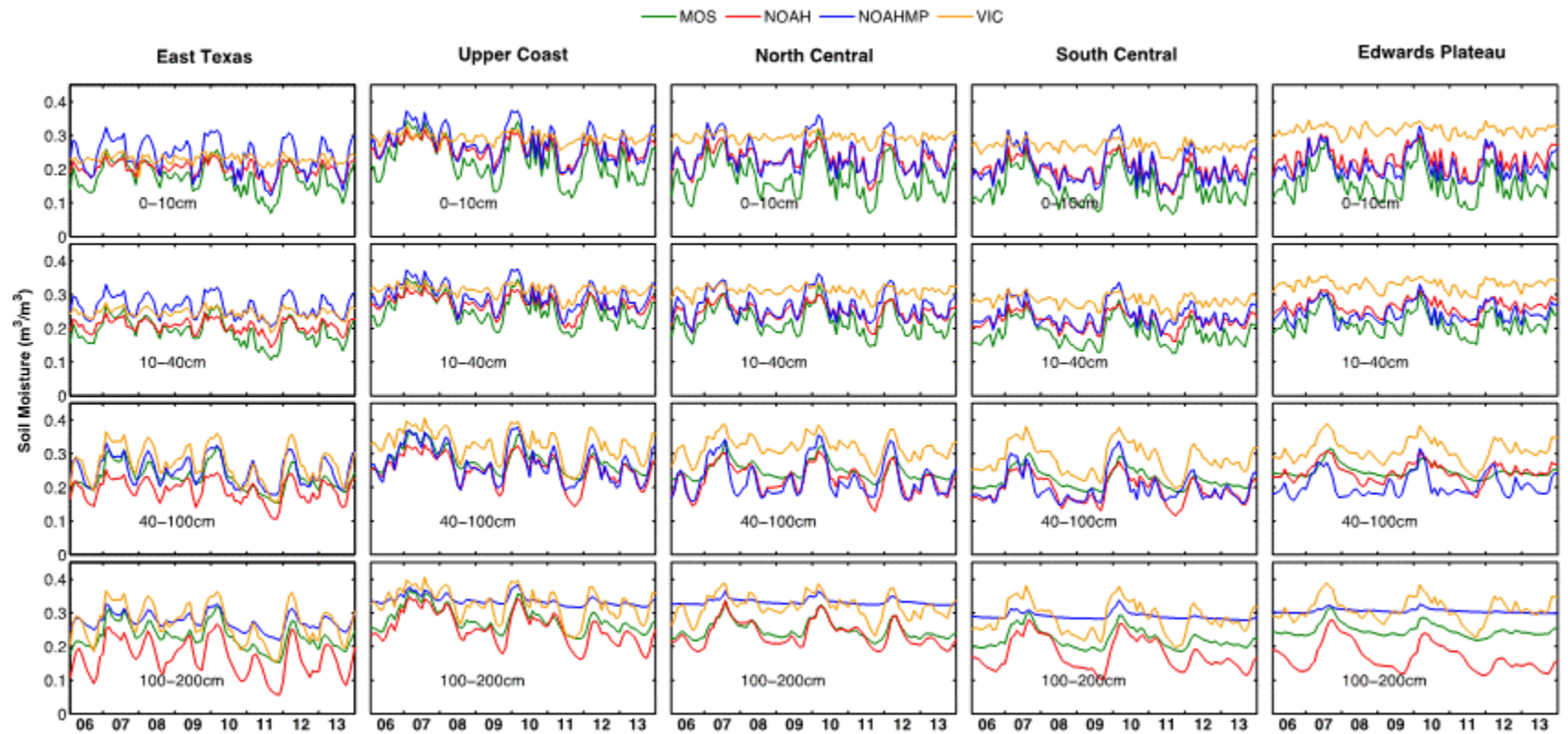
predictions for these layers are similar for all regions except for East Texas. At deeper depths, Noah predicts the driest soil moisture values. While all locations are characterized by variations associated with seasonality, East Texas shows the strongest and most consistent annual patterns; in general, the predictions are more similar among the other regions compared to East Texas.

A visual examination of the soil moisture time series for the eastern Texas climate regions demonstrates that intra-annual (i.e., within a given year) variations often have substantially greater magnitudes than inter-annual variations. With respect to drought, year 2011 is the driest in East Texas for all models and soil layers. For the other climate divisions, all models but VIC simulate relatively low values during mid-2008 to mid-2009 in addition to similar or lower values during 2011. VIC simulates relatively lowest soil moisture during a portion of 2011 at all soil levels and most regions; however, the magnitude of change is small for the near-surface layers compared to the lowest two layers.

**Figure 21 Simulated monthly NLDAS-2 soil moisture ( $\text{m}^3/\text{m}^3$ ) for the four 12km grid domain sub-regions and four soil layers. Each column presents a vertical profile of results for, from left to right: East, East Central, West Central, West; ref. Figure 20). Each row displays a single soil layer; from top to bottom: 0-10cm, 10-40cm, 40-100cm, and 100-200cm.**



**Figure 22 Simulated monthly NLDAS-2 soil moisture ( $\text{m}^3/\text{m}^3$ ) for five eastern Texas climate divisions and four soil layers. Each column presents a vertical profile of results for, from left to right: East Texas, Upper Coast, North Central, South Central, and Edwards Plateau (within the 4km domain; ref. Figure 2). Each row displays a single soil layer; from top to bottom: 0-10cm, 10-40cm, 40-100cm, and 100-200cm.**



### *Spatial distribution of soil moisture anomalies*

Soil moisture anomalies for the growing season were generated by aggregating monthly values over April through October. Partly to reduce the amount of data processing, the analysis was focused on three specific years representative, in Texas, of generally wet conditions (2007), extremely dry conditions (2011) and a special interest year 2012 (TCEQ is currently developing meteorological and air quality modeling for June 2012 that may be expanded to additional months).

For the top soil layer (0-10cm; ref. Figure 23), Noah, Noah-MP, and Mosaic broadly simulate strongly positive soil moisture anomalies in the South Central U.S. and negative anomalies in the southeastern U.S. for 2007, and strongly negative anomalies in the South Central U.S. with positive anomalies over much of the remaining U.S. in 2011. The results for VIC are directionally similar to these patterns but are of lower magnitude and spatial coverage compared to the other NLDAS-2 models. Similarly all models show drought over wide portions of the U.S. centered over the High Plains with weakest dry conditions simulated by VIC. The 2011 dry anomaly is generally of greater magnitude in the east than the west, particularly for Mosaic. Among all models, Mosaic and Noah-MP show highest agreement. The year 2012 was extremely dry in the central Great Plains, but soil water deficits are not simulated in Texas. VIC failed to capture the extreme dry/wet anomalies at 0-10cm for all years, probably because of its low simulation skill in simulating sufficient temporal variability of soil moisture within the top soil layers.

For deep soil layers (100-200cm; ref. Figure 24), Noah-MP predicts directionally similar but much weaker anomalies compared to the other models. Among the remaining three LSMs, VIC has a tendency towards the strongest dry/wet anomalies while Noah and Mosaic predict similar and slightly lower magnitude values compared to VIC. The 2012 dry anomaly over the central Great Plains is not well-simulated by Noah-MP in contrast to the strong dry anomaly predicted by VIC. In contrast to the shallow soil layers, the soil moisture predictions at deep layers by VIC show strong dry/wet spatial and inter-annual differences; this may be caused, in part, by uncertainties in the assumed bare soil fraction leading to an ET enhancement in the top soil layers while moisture at deep levels is less influenced by evaporation.

Figure 23 Comparison of soil moisture anomaly ( $m^3/m^3$ ) for the top soil layer (0-10cm) simulated by NLDAS-2 models. The anomaly is relative to the 2006-2013 average.

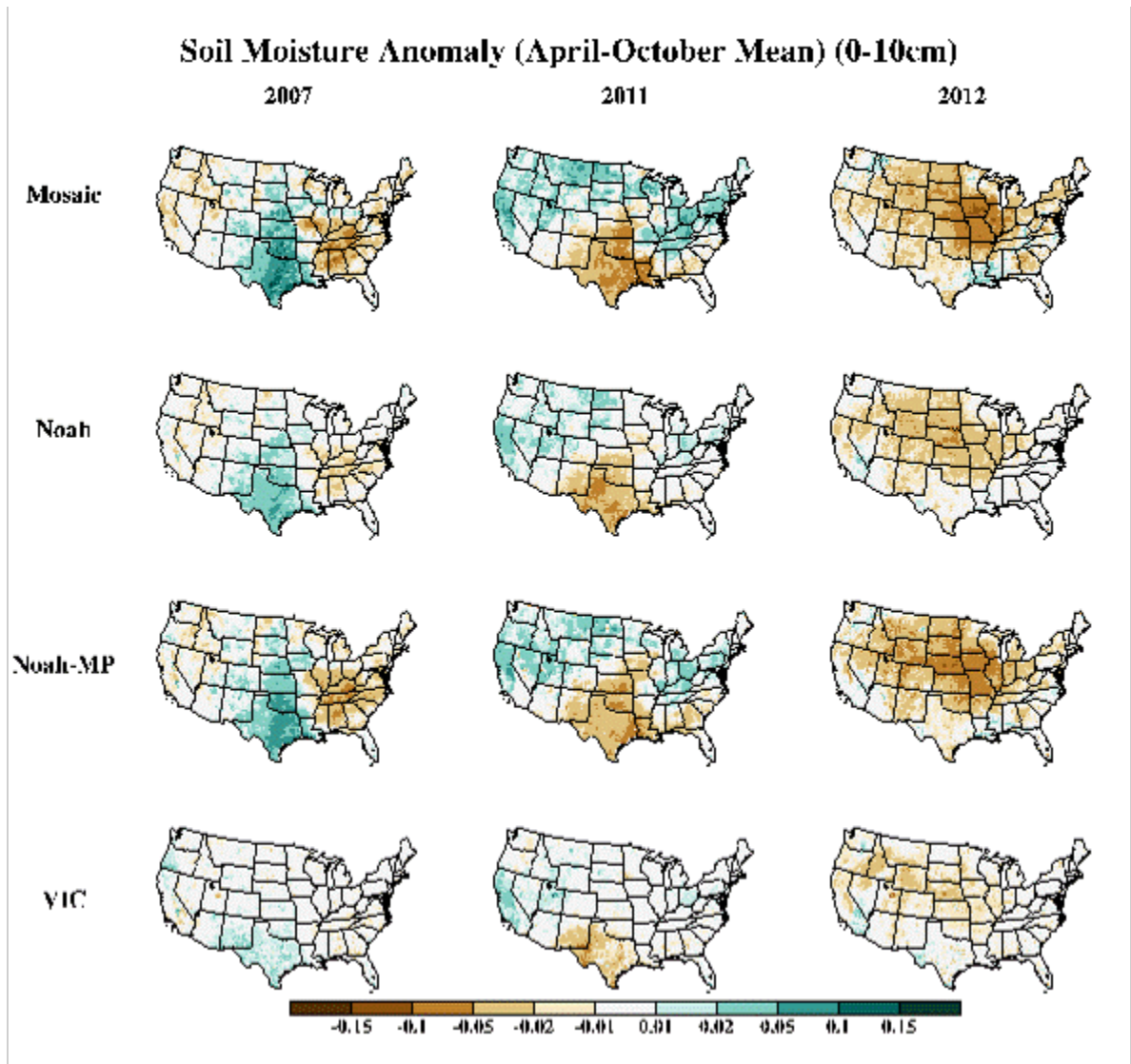
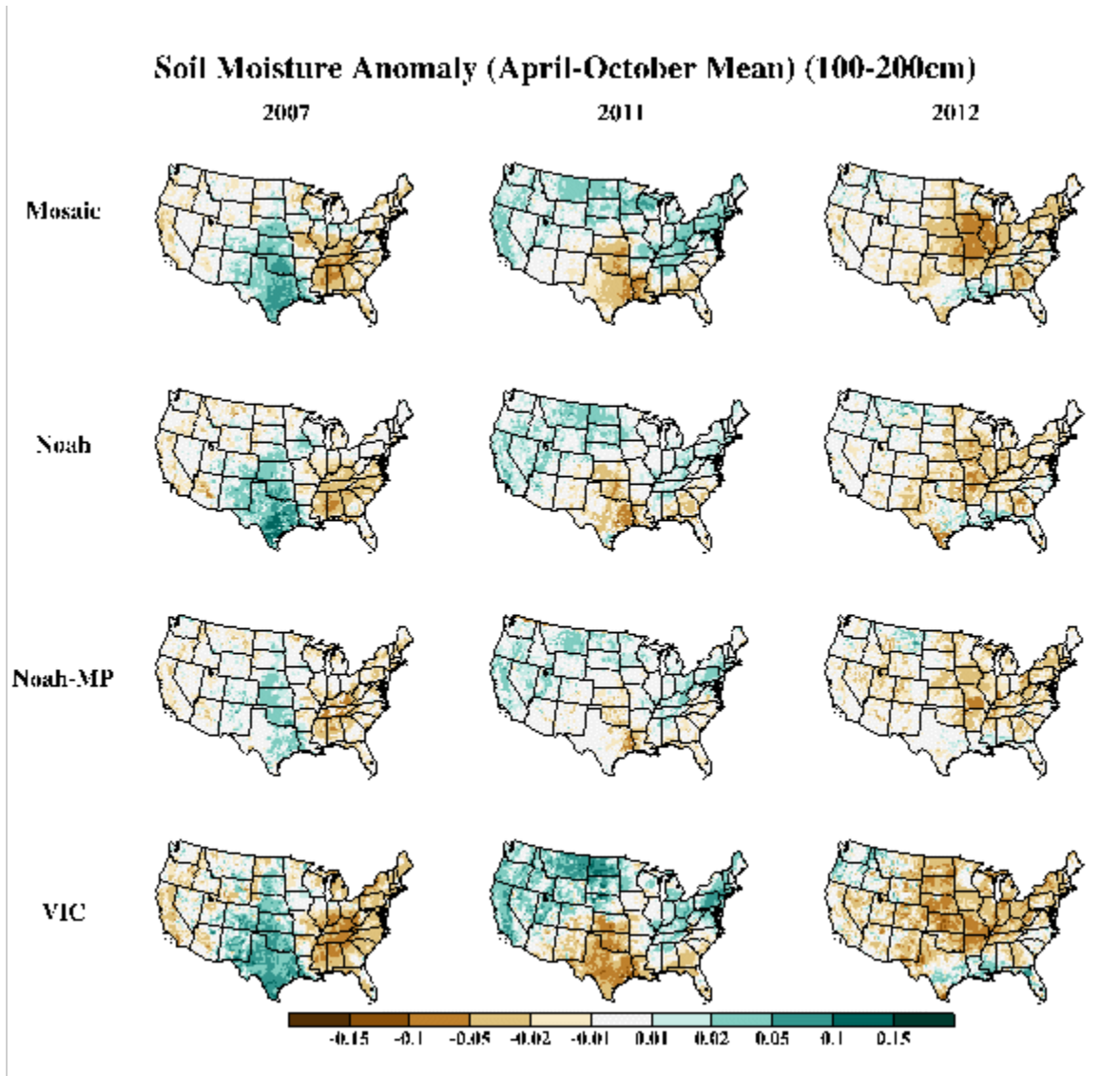


Figure 24 Similar to Figure 23 but for the bottom soil layer, i.e., 100-200cm.



### *Comparison to GRACE*

The Gravity Recovery and Climate Experiment (GRACE) consists of two NASA satellites that use a precise microwave ranging system to measure the distance between themselves due to gravitational acceleration (Tapley, et al., 2004). Changes in Earth's gravity field are directly related to changes in surface mass. The surface mass signal largely reflects total water storage (TWS), which is the sum of groundwater, soil moisture, surface water, snow and ice. The contribution of changes of surface water reservoir to TWS change is typically small compared to soil moisture and groundwater storage. Long et al. (2013) found that the temporal variations of soil moisture and GRACE TWS were in general agreement during the 2011 Texas drought and that the deficit in soil moisture dominated the depletion of TWS.

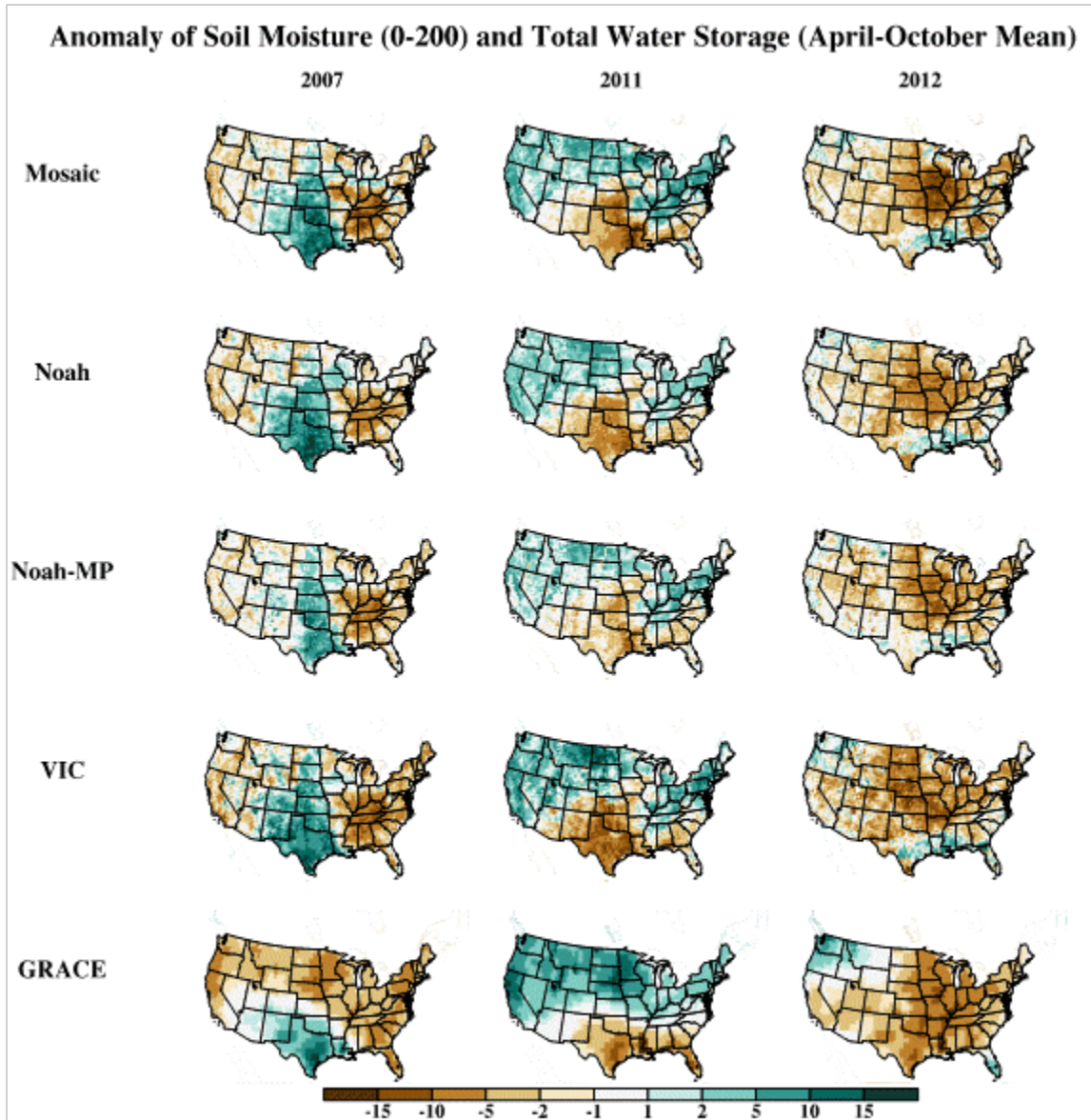
Analyses are performed to contrast GRACE-observed TWS with NLDAS-2 soil moisture predictions. Growing season anomalies for years 2007, 2011, and 2012 (i.e., April-October totals relative to the 2006-2013 averages) for NLDAS-2 soil moisture (integrated over 0-200cm) and GRACE-observed TWS are shown in Figure 25.

As shown in Figure 25, the large-scale gradients between the NLDAS-2 soil moisture and GRACE TWS anomalies have similar spatial patterns. For example, both NLDAS-2 and GRACE indicate relatively wet values in the South Central U.S. during 2007 and very dry conditions in the South Central U.S. for 2011 and Great Plains and Ohio River Valley for 2012. In Texas during 2011, Noah-MP shows the lowest magnitude dry anomalies; this may be due, in part, to the relatively weak response of Noah-MP to interannual variations of deep layer soil moisture shown by our previous investigations.

Although the NLDAS-2 soil moisture and GRACE TWS anomalies are directionally similar, the spatial extents of wet/dry patterns are different. For example, the relatively wet TWS values for 2007 are limited to Texas and portions of surrounding states whereas the NLDAS-2 wet anomalies extend north and northwest into portions of the southwestern U.S. and the Central Plains states of Kansas, Nebraska, and Dakotas. During 2011, GRACE indicates drier than normal conditions throughout Texas and the Gulf Coast states; the magnitudes of predicted NLDAS-2 dry anomalies in the Gulf Coast regions (outside of Texas) are often lower (especially for Florida) and extend farther north into the South Central Plains (i.e., Oklahoma and Nebraska) compared to GRACE.

During 2012, GRACE indicates that most of the U.S. is relatively dry with the exception of the northwestern U.S. and Florida; the spatial extent of predicted NLDAS-2 soil moisture drought covers much of the U.S. but predicts average-to-wet conditions over portions of Texas and the Gulf and Atlantic coastal regions. Combined, the NLDAS-2 and GRACE results might indicate that late 2011/early 2012 rainfall mostly replenished soil moisture throughout Texas but that these rains were insufficient to recharge groundwater storage to pre-drought levels.

**Figure 25 Comparison of April-October anomalies for years 2007, 2011, and 2012 for 0-200cm NLDAS-2 (Mosaic, Noah, Noah-MP, and VIC LSMs) soil moisture and GRACE total water storage. Units are cm.**



### 6.3 Summary

There are large inter-model differences of simulated soil moisture within the five eastern Texas climate divisions and 12km subdivisions studied. This may be primarily caused by the differences in evapotranspiration (ET) because ET controls how much soil water is lost through evaporation and transpiration by vegetation. Different soil layers, root zone depths, and soil-related parameters all contribute to disparities in ET simulation among NLDAS-2 models, which in turn impacts seasonal and interannual variations of soil moisture. In particular, VIC simulates very weak temporal variability at top soil layers and hence cannot well capture the extreme wet/dry events. In contrast, the Noah-MP model exhibits an overly weak temporal variation at deep layers and so fails to reproduce the wet year 2007 and the drought events in 2011.

Overall, soil moisture anomalies simulated by all models can generally capture the broad features of GRACE-observed TWS changes, including the 2007 extreme wet events and 2011 extreme drought, as well as the 2012 central Great Plains drought. This result is consistent with previous studies that showed the soil moisture deficit during 2011 dominated the TWS depletion observed by GRACE. But the spatial pattern of simulated soil moisture differs from the TWS changes, which may be related, in part, to groundwater and/or irrigation processes that are not included in the NLDAS-2 models.

### 6.4 References

Long, D., B. R. Scanlon, L. Longuevergne, A. Y. Sun, D. N. Fernando, and H. Save (2013), GRACE satellite monitoring of large depletion in water storage in response to the 2011 drought in Texas, *Geophys. Res. Lett.*, *40*(13), 3395–3401, doi:10.1002/grl.50655.

Schaake, J.C., Duan, Q., Koren, V., Mitchell, K.E., Houser, P.R., Wood, E.F., Robock, A., Lettenmaier, D.P., Lohmann, D., Cosgrove, B., Sheffield, J., Luo, L., Higgins, R.W., Pinker, R.T., Tarpley, J.D., 2004. An intercomparison of soil moisture fields in the North American Land Data Assimilation System (NLDAS). *J. Geophys. Res.* 109. <http://dx.doi.org/10.1029/2002JD003245>.

Tapley, B. D., S. Bettadpur, J. C. Ries, P. F. Thompson, and M. M. Watkins, 2004: GRACE measurements of mass variability in the Earth system. *Science*, 305, 503-505.

Youlong Xia, Michael B. Ek, Yihua Wu, Trent Ford, and Steven M. Quiring, 2015, Comparison of NLDAS-2 Simulated and NASMD Observed Daily Soil Moisture. Part I: Comparison and Analysis, submitted to *Journal of Hydrometeorology*.

## 7.0 MEGAN simulations

This section presents the MEGAN simulations used to predict the impact of eastern Texas drought on estimates of isoprene emissions. A primary focus of these simulations is to quantify the emissions differences associated with differences between the NLDAS-2 soil moisture databases.

### 7.1 MEGAN methodology

The latest version of MEGAN (MEGANv2.1) is described in detail by Guenther et al. (2012). The emissions rate ( $F$ ) of isoprene from terrestrial landscapes in units of flux ( $\mu\text{g m}^{-2}$  ground area  $\text{h}^{-1}$ ) is calculated as:

$$F = \gamma \sum \varepsilon_j \chi_j \quad \text{Eq. 1}$$

where  $\varepsilon$  is the basal emission factor for vegetation type  $j$  with fractional coverage  $\chi_j$ ; it represents the emission rate under standard environmental conditions defined in Guenther et al. (2006, 2012) including an air temperature of 303 K, solar angle of 60 degrees, photosynthetic photon flux density (PPFD) transmission of 0.6, LAI of  $5 \text{ m}^2/\text{m}^2$  consisting of 80% mature, 10% growing and 10% old foliage, and volumetric soil moisture of  $0.3 \text{ m}^3/\text{m}^3$ .  $\gamma$  is the overall emissions activity factor that multiplicatively accounts for the effects of environmental variations on leaf age, canopy environment, and soil moisture such that:

$$\gamma = \gamma_{age} \cdot \gamma_{SM} \cdot \gamma_{CE} \quad \text{Eq. 2}$$

with each of the individual gammas calculated as below:

$$\text{leaf age: } \gamma_{age} = A_{new} F_{new} + A_{gro} F_{gro} + A_{mat} F_{mat} + A_{old} F_{old} \quad \text{Eq. 3}$$

$$\text{soil moisture: } \gamma_{SM} = \sum_{i=1}^4 f_{root}^i \max(0, \min(1, (\theta^i - \theta_{wilt}) / 0.04)) \quad \text{Eq. 4}$$

canopy environment:

$$\gamma_{CE} = 0.56 \cdot \sum_{i=1}^5 [(\gamma_T^i)_{sun} (\gamma_P^i)_{sun} f_{sun}^i + (\gamma_T^i)_{shade} (\gamma_P^i)_{shade} f_{shade}^i] \cdot LAI^i \quad \text{Eq. 5}$$

The default MEGAN configuration sets the relative emission rates based on mature leaves.  $\gamma_{age}$  accounts for differences in basal emission rates among four leaf stages – new, growing, mature and old foliage. The distribution of leaf ages is determined by changes in LAI between the current and previous time steps; a positive difference increases the amount of new and growing leaves and vice versa.

The canopy environment model within MEGAN consists of five canopy layers. For each layer, temperature ( $\gamma_T, \gamma_{T\_LIF}$ ) and light ( $\gamma_P$ ) activity factors are calculated for both sun and shaded leaves based on layer-specific temperature and PPFD, and then summed

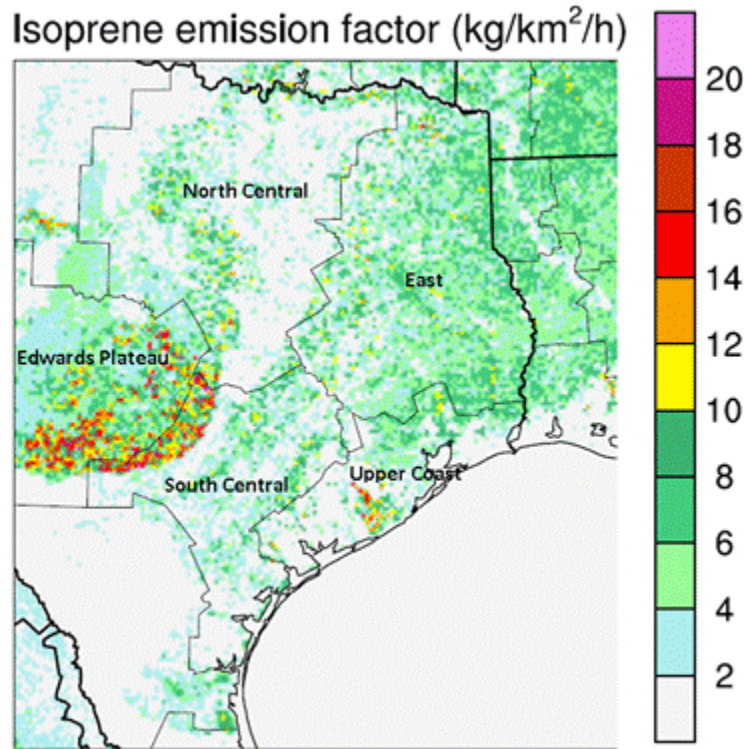
based on the sun/shaded fractions ( $f$ ) for each layer. LAI is distributed between the layers using a Gaussian distribution. The sum of the product of  $\gamma_T$ ,  $\gamma_P$  and LAI over the five layers provides the canopy environment activity factor ( $\gamma_{CE}$ ).

MEGAN sets the default soil moisture activity factor to a value of one; for this work, source codes were modified to include the direct impact of soil moisture on isoprene emissions following Guenther et al. (2012). The impact of drought on a plant's physiology can lead to an initial increase in emissions followed by substantial reduction and eventual termination of emissions (Potosnak et al., 2014; Beckett et al., 2012; Pegoraro et al., 2004). Based on the observations of Pegoraro et al., 2004, MEGAN simulates the impact of soil moisture on isoprene emissions using a simple algorithm that relates emission activity to soil moisture and wilting point (the soil moisture below which water is unavailable to plants). The calculation of  $\gamma_{SM}$  is shown in Eq. 4;  $\theta$  is the soil moisture content,  $\theta_{wilt}$  is the wilting point, 0.04 is an empirical coefficient, and  $f_{root}$  is the fraction of root mass within each soil layer.  $\gamma_{SM}$  decreases linearly from a value of one at 0.04 above the wilting point to zero at and below the wilting point.

#### *MEGAN configuration*

MEGAN was run at a 1-km horizontal spatial resolution and configured according to the approach of Huang et al. (2014). MEGAN requires meteorological fields for air temperature, solar radiation, relative humidity, wind speed and soil moisture, and vegetation parameters including Plant Functional Type (PFT) fractions, LAI, and base emission rates (Guenther et al., 2012). Emission factors for isoprene (ref. Figure 26) were those specified by the default MEGAN gridded maps. In eastern Texas, the highest isoprene emission rates are found in eastern portions of Edwards Plateau and far northwestern South Central Texas likely associated with dense concentrations of live oak trees.

**Figure 26 Isoprene emission factors (kg/km<sup>2</sup>/hr). The boundaries of five Texas climate divisions are also shown.**



MEGAN was modified to accept a recently available 4-day LAI product as an alternative to the 8-day LAI product. LAI values for urban areas were not reported in the MODIS product but were estimated for this work as an average LAI from surrounding 5-km buffer regions. Assigning suburban LAI values to urban areas may cause an overestimation in LAI values and subsequent estimations of biogenic emissions in urban regions. The TCEQ land cover data had a spatial resolution of 30-m with 36 Texas Land Classification System classes that were mapped to MEGAN's 16 PFTs. For each MEGAN 1-km grid cell, the fractional coverage of each PFT was determined by summing the number of 30-m resolution cells whose centroid fell within a given grid cell.

Meteorological variables, except Photosynthetically Active Radiation (PAR), were obtained from the National Centers for Environmental Prediction (NCEP) North American Regional Reanalysis (NARR) products. NARR data with a 3-hour temporal and 32-km (nominal) spatial resolution were interpolated to a 1-km grid and a 1-hour resolution. Hourly surface insolation from the Geostationary Operational Environmental Satellite (GOES, generated by University of Alabama in Huntsville) with a spatial resolution of 4-km were re-gridded into a 1-km grid and converted to PAR based on a conversion factor of 0.45 (McNider, 2013; ENVIRON, 2011).

*Soil moisture databases*

MEGAN simulations utilized hourly NLDAS-2 soil moisture predictions for four layers (0-10cm, 10-40cm, 40-100cm, 100-200cm; ref. Sections 4 and 6); these soil layers are the depth definitions used by Noah and Noah-MP. (The deepest Mosaic layer spans 40-200cm; therefore, the Mosaic soil moisture predictions for 40-100cm and 100-200cm are identical). Because VIC employs soil layer definitions that vary in time and space, VIC soil moisture values were interpolated to the four soil depths used by the NLDAS-2 LSMs.

In addition to uncertainties in the accurate simulation of soil moisture within LSMs, substantial errors can also be introduced when sharing data between environmental applications because the LSM predictions are often highly model-dependent (e.g., Koster et al., 2009). As stressed by Müller et al. (2008) and Guenther et al. (2012), wilting point values for a given MEGAN simulation should be consistent with the specific LSM database employed. The Noah, Noah-MP, and Mosaic LSMs employ a single wilting point value at each grid node representative of average conditions throughout the soil layers so that a two-dimensional wilting point field interpolated from the NLDAS-2 wilting point databases was used.

#### *Analysis regions and study period*

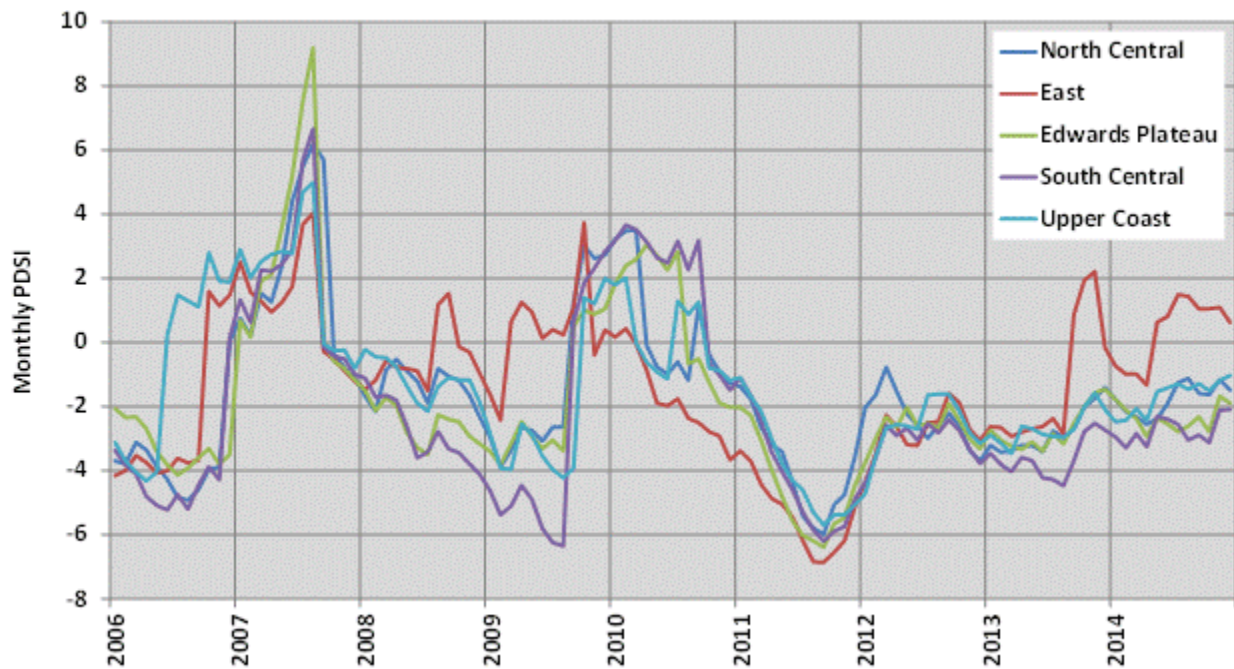
MEGAN runs were performed for a basecase (impact of soil moisture not considered) in addition to the simulations that utilized the NLDAS-2 soil moisture databases: Noah, Noah-MP, Mosaic, and VIC. An emphasis is placed on area-averaged and seasonal isoprene emissions for the four eastern Texas climate divisions: North Central, East, Upper Coast, and South Central. Additionally, in order to more fully investigate the relatively high emissions regions located inland from the northwestern boundary of South Central Texas (ref. Figure 26), emissions were summarized for portions of Edwards Plateau wholly contained within the 4km grid domain.

MEGAN simulations were conducted for March-October for years 2006, 2007 and 2011. As shown by the monthly Palmer Drought Severity Index (PDSI) values in Figure 27, year 2007 had mostly positive values during the March-October growing season suggesting wet conditions. In contrast, year 2006 (with the exception of Upper Coast) and 2011 (for all regions) had negative values indicative of drought.

Hourly isoprene emissions were predicted for each 1-km grid cell in the 4km grid domain. The daily total emissions at each grid cell were then averaged by season (spring: March-April-May or MAM; summer: June-July-August or JJA; fall: September-October or SO), eastern Texas climate region (North Central, South Central, East, Upper Coast, Edwards Plateau) and year to generate area- and season- averaged values. Grid cells designated as water by the land cover database were ignored.

**Figure 27 Monthly PDSI for 2006-2014 for five Texas climate divisions: North Central, South Central, East, Upper Coast and Edwards Plateau. (Source: National**

Climatic Data Center; <http://www.ncdc.noaa.gov/temp-and-precip/drought/historical-palmers/>)



## 7.2 Results

*Basecase (impact of soil moisture not considered)*

Area-averaged daily total isoprene emissions ( $\text{kg}/\text{km}^2/\text{day}$ ) for each of the five Texas regions are summarized in Table 6 and presented graphically in Figure 28. Results shown in Table 6 are sorted by ascending regional emissions during the non-drought year 2007; emissions are lowest for North Central and Upper Coast and greatest for Edwards Plateau and East Texas. Consistent with other studies for the South Central U.S. (e.g., Lamb et al., 1993; Kleindienst et al., 2007; Huang et al., 2014), isoprene emissions peak during summer; by region, summer emissions can be more than three times greater compared to spring/fall. East Texas and Edwards Plateau exhibit the highest emissions among the five climate regions, presumably due to regions of dense forest.

**Table 6 Area-averaged isoprene emissions (kg/km<sup>2</sup>/day) predicted for five Texas climate regions during 2006, 2007, and 2011.**

Year	Season*	North Central	Upper Coast	South Central	Edwards Plateau**	East
2006	Spring	10.87	11.29	15.97	25.55	22.41
	Summer	31.96	24.21	36.59	59.50	64.92
	Fall	7.90	12.84	14.64	18.42	23.88
2007	Spring	4.87	7.04	8.23	12.03	12.97
	Summer	21.43	21.34	29.53	41.96	44.64
	Fall	9.37	12.26	15.79	20.76	21.47
2011	Spring	11.05	12.29	17.83	25.10	26.70
	Summer	43.94	38.26	50.74	72.82	104.14
	Fall	8.53	14.15	16.38	21.03	26.89

\*Spring=Mar/Apr/May or MAM; Summer=Jun/Jul/Aug or JJA; Fall=Sep/Oct or SO

\*\*Limited to portions within the 4km grid domain (ref. Figure 1).

**Figure 28 As presented in Table 6 but in graphical format.**

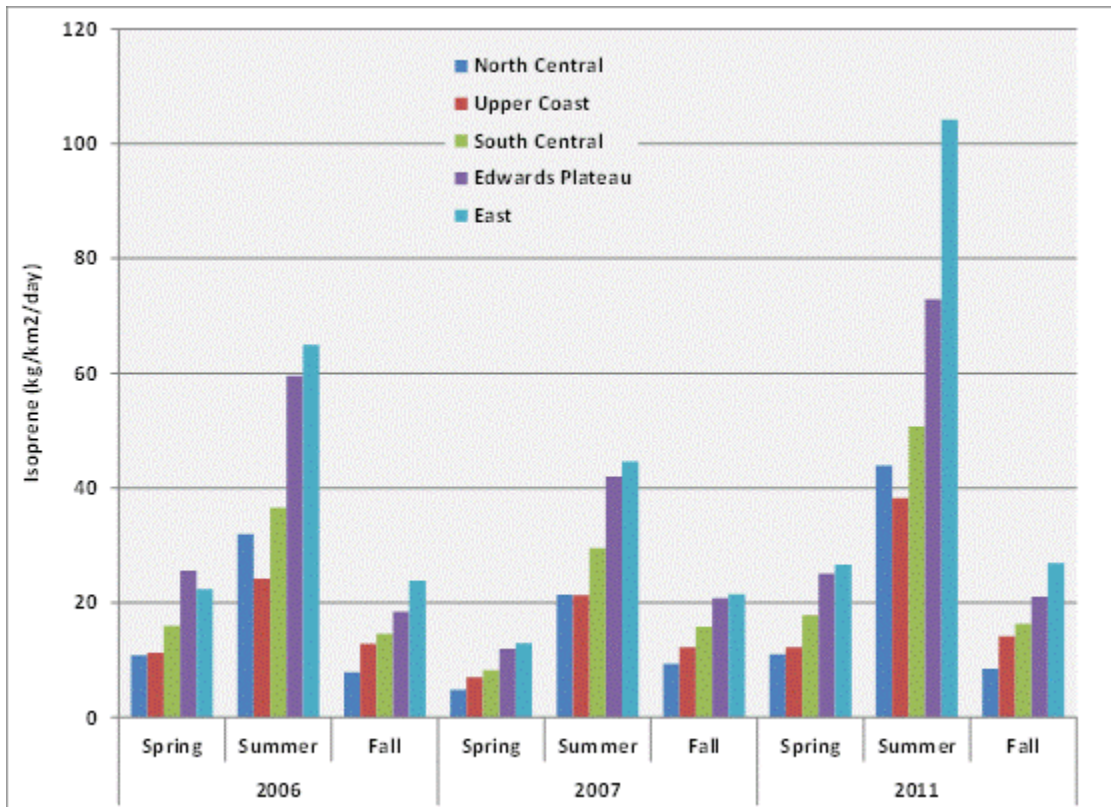


Table 7 presents the seasonal emissions ratios between 2006 and 2011 versus 2007. Spring emissions for 2006 and 2011 are approximately twice those for 2007; in contrast, fall emissions are similar among the three years. These results are directionally consistent with the interannual trends in seasonal temperatures; spring 2006/2011 had relatively higher temperatures compared to 2007 while fall temperatures among the three years were more similar (Huang et al., 2015). The results in Table 7 indicate substantially greater emissions during the drought year summers compared to 2007. On average across all regions, summer emissions were factors of 1.4 and 1.9 greater during 2006 and 2011, respectively, compared to 2007.

**Table 7 Ratio of seasonal area-averaged isoprene emissions during 2006 and 2011 relative to 2007.**

Region	2006			2011		
	Spring	Summer	Fall	Spring	Summer	Fall
North Central	2.23	1.49	0.84	2.27	2.05	0.91
Upper Coast	1.60	1.13	1.05	1.75	1.79	1.15
South Central	1.94	1.24	0.93	2.17	1.72	1.04
Edwards Plateau*	2.12	1.42	0.89	2.09	1.74	1.01
East	1.73	1.45	1.11	2.06	2.33	1.25
Average	1.93	1.35	0.96	2.07	1.93	1.07

\*Limited to portions within the 4km grid domain (ref. Figure 1).

### *Soil Moisture Scenarios*

In order to test the sensitivity of isoprene predictions to reduced soil moisture availability during periods of drought, MEGAN simulations were performed using each NLDAS-2 soil moisture database: Noah, Noah-MP, Mosaic, and VIC. Season- and area-averaged isoprene emissions by eastern Texas climate region are summarized in Table 8 (and graphically in Figure 29) for years (a) 2006, (b) 2007, and (c) 2011. The percentage changes in emissions relative to the basecase are also shown. The by-region seasonal emissions for all years are presented graphically in Figure 29 for (a) North Central, (b) Upper Coast, (c) South Central, (d) Edwards Plateau, and (e) East Texas.

**Table 8 Predicted area-averaged isoprene emissions by season for five Texas climate regions during (a) 2006, (b) 2007, and (c) 2011. Results are shown for the basecase and each of the four soil moisture scenarios. The last four columns in Table 8 show the percentage changes in emissions relative to the basecase.**

(a) Year 2006

Spring (MAM) 2006									
Region	Basecase	Noah	NoahMP	Mosaic	VIC	Noah	NoahMP	Mosaic	VIC
	Isoprene emissions (kg/km <sup>2</sup> /day)					Percentage change relative to basecase			
North Central	10.9	10.9	10.5	6.1	10.70	-0.1%	-3.8%	-44.2%	-1.6%
Upper Coast	11.3	11.2	11.3	5.9	10.88	-0.6%	-0.3%	-47.7%	-3.6%
South Central	16.0	15.6	15.2	7.0	15.14	-2.4%	-4.5%	-55.9%	-5.2%
Edwards Plateau*	25.6	25.0	24.3	7.8	23.95	-2.2%	-4.8%	-69.4%	-6.3%
East	22.4	22.4	22.4	20.3	22.11	0.0%	-0.3%	-9.5%	-1.4%
AVG	17.2	17.0	16.7	9.4	16.6	-1.1%	-2.7%	-45.3%	-3.6%
Summer (JJA) 2006									
Region	Basecase	Noah	NoahMP	Mosaic	VIC	Noah	NoahMP	Mosaic	VIC
	Isoprene emissions (kg/km <sup>2</sup> /day)					Percentage change relative to basecase			
North Central	31.96	30.84	28.24	11.58	31.27	-3.5%	-11.6%	-63.7%	-2.1%
Upper Coast	24.21	24.08	24.18	20.06	23.91	-0.5%	-0.1%	-17.1%	-1.2%
South Central	36.59	34.89	33.60	15.65	35.52	-4.6%	-8.2%	-57.2%	-2.9%
Edwards Plateau*	59.50	56.70	53.19	11.66	55.96	-4.7%	-10.6%	-80.4%	-6.0%
East	64.92	63.81	62.99	52.18	64.69	-1.7%	-3.0%	-19.6%	-0.4%
AVG	43.4	42.1	40.4	22.2	42.3	-3.0%	-6.7%	-47.6%	-2.5%
Fall (SO) 2006									
Region	Basecase	Noah	NoahMP	Mosaic	VIC	Noah	NoahMP	Mosaic	VIC
	Isoprene emissions (kg/km <sup>2</sup> /day)					Percentage change relative to basecase			
North Central	7.90	7.17	7.34	3.90	7.80	-9.3%	-7.2%	-50.7%	-1.3%
Upper Coast	12.84	12.12	12.82	10.27	12.63	-5.6%	-0.1%	-20.0%	-1.6%
South Central	14.64	13.02	14.11	7.60	14.23	-11.1%	-3.6%	-48.1%	-2.8%
Edwards Plateau*	18.42	16.20	17.43	5.60	17.58	-12.1%	-5.4%	-69.6%	-4.6%
East	23.88	21.80	23.47	19.46	23.47	-8.7%	-1.7%	-18.5%	-1.7%
AVG	15.5	14.1	15.0	9.4	15.1	-9.4%	-3.6%	-41.4%	-2.4%

\*portion within the 4km grid domain.

Table 8 (continued)

(b) Year 2007

Spring (MAM) 2007									
Region	Basecase	Noah	NoahMP	Mosaic	VIC	Noah	NoahMP	Mosaic	VIC
	Isoprene emissions (kg/km <sup>2</sup> /day)					Percentage change relative to basecase			
North Central	4.87	4.86	4.86	4.28	4.84	-0.1%	-0.1%	-12.1%	-0.6%
Upper Coast	7.04	7.04	7.04	6.91	6.92	0.0%	0.0%	-1.7%	-1.7%
South Central	8.23	8.21	8.22	7.15	8.09	-0.3%	-0.2%	-13.2%	-1.8%
Edwards Plateau*	12.03	11.76	11.90	8.09	11.90	-2.3%	-1.1%	-32.7%	-1.1%
East	12.97	12.97	12.97	12.96	12.91	0.0%	0.0%	-0.1%	-0.5%
AVG	9.0	9.0	9.0	7.9	8.9	-0.5%	-0.3%	-12.0%	-1.1%
Summer (JJA) 2007									
Region	Basecase	Noah	NoahMP	Mosaic	VIC	Noah	NoahMP	Mosaic	VIC
	Isoprene emissions (kg/km <sup>2</sup> /day)					Percentage change relative to basecase			
North Central	21.43	21.42	21.25	19.41	21.23	-0.1%	-0.8%	-9.4%	-1.0%
Upper Coast	21.34	21.34	21.34	20.92	21.16	0.0%	0.0%	-2.0%	-0.8%
South Central	29.53	29.52	29.48	27.47	29.36	0.0%	-0.2%	-7.0%	-0.6%
Edwards Plateau*	41.96	41.67	41.25	32.97	41.65	-0.7%	-1.7%	-21.4%	-0.7%
East	44.64	44.64	44.54	44.49	44.40	0.0%	-0.2%	-0.3%	-0.5%
AVG	31.8	31.7	31.6	29.1	31.6	-0.2%	-0.6%	-8.0%	-0.7%
Fall (SO) 2007									
Region	Basecase	Noah	NoahMP	Mosaic	VIC	Noah	NoahMP	Mosaic	VIC
	Isoprene emissions (kg/km <sup>2</sup> /day)					Percentage change relative to basecase			
North Central	9.37	9.36	9.07	7.58	9.30	0.0%	-3.1%	-19.1%	-0.7%
Upper Coast	12.26	12.26	12.25	11.93	12.13	0.0%	-0.1%	-2.7%	-1.1%
South Central	15.79	15.79	15.50	13.99	15.67	0.0%	-1.9%	-11.4%	-0.8%
Edwards Plateau*	20.76	20.75	19.73	14.74	20.68	0.0%	-5.0%	-29.0%	-0.4%
East	21.47	21.47	21.37	21.17	21.44	0.0%	-0.4%	-1.4%	-0.1%
AVG	15.9	15.9	15.6	13.9	15.8	0.0%	-2.1%	-12.7%	-0.6%

\*portion within the 4km grid domain.

Table 8 (continued)

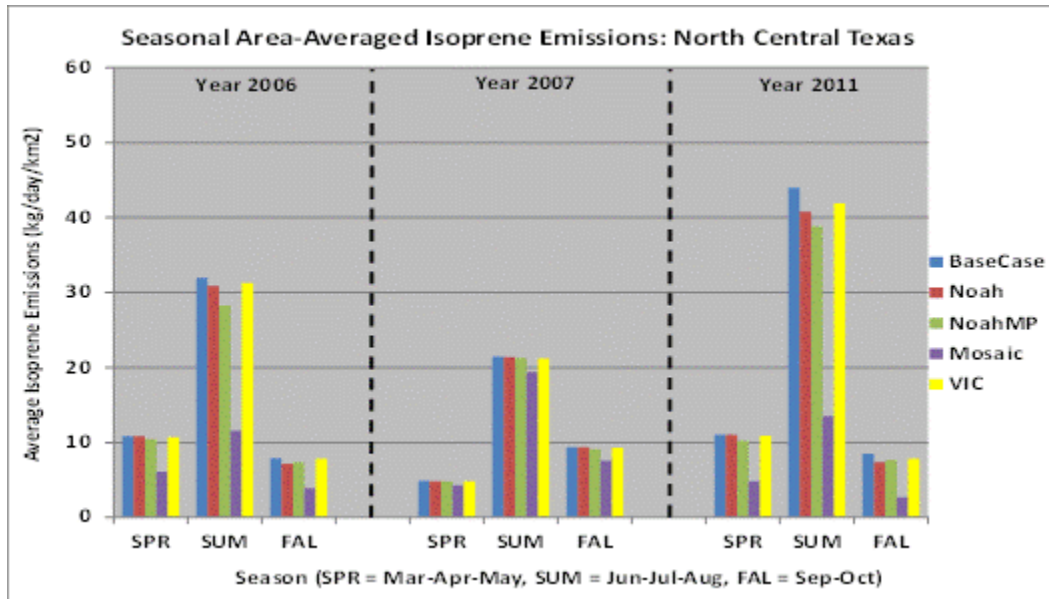
## (c) Year 2011

Spring (MAM) 2011									
Region	Basecase	Noah	NoahMP	Mosaic	VIC	Noah	NoahMP	Mosaic	VIC
	Isoprene emissions (kg/km <sup>2</sup> /day)					Percentage change relative to basecase			
North Central	11.05	11.02	10.22	4.80	10.91	-0.3%	-7.5%	-56.6%	-1.3%
Upper Coast	12.29	12.07	11.97	4.60	11.12	-1.7%	-2.6%	-62.5%	-9.5%
South Central	17.83	17.12	16.11	6.59	16.73	-4.0%	-9.7%	-63.1%	-6.2%
Edwards Plateau*	25.10	24.20	22.68	3.95	21.14	-3.6%	-9.6%	-84.3%	-15.8%
East	26.70	26.56	26.40	18.62	26.16	-0.5%	-1.1%	-30.2%	-2.0%
AVG	18.6	18.2	17.5	7.7	17.2	-2.0%	-6.1%	-59.3%	-7.0%
Summer (JJA) 2011									
Region	Basecase	Noah	NoahMP	Mosaic	VIC	Noah	NoahMP	Mosaic	VIC
	Isoprene emissions (kg/km <sup>2</sup> /day)					Percentage change relative to basecase			
North Central	43.94	40.77	38.84	13.54	41.92	-7.2%	-11.6%	-69.2%	-4.6%
Upper Coast	38.26	36.84	36.97	11.33	32.80	-3.7%	-3.4%	-70.4%	-14.3%
South Central	50.74	47.40	44.59	15.08	44.46	-6.6%	-12.1%	-70.3%	-12.4%
Edwards Plateau*	72.82	67.09	64.77	9.56	57.48	-7.9%	-11.1%	-86.9%	-21.1%
East	104.14	100.25	96.47	59.57	100.30	-3.7%	-7.4%	-42.8%	-3.7%
AVG	62.0	58.5	56.3	21.8	55.4	-5.8%	-9.1%	-67.9%	-11.2%
Fall (SO) 2011									
Region	Basecase	Noah	NoahMP	Mosaic	VIC	Noah	NoahMP	Mosaic	VIC
	Isoprene emissions (kg/km <sup>2</sup> /day)					Percentage change relative to basecase			
North Central	8.53	7.39	7.65	2.69	7.80	-13.4%	-10.3%	-68.4%	-8.5%
Upper Coast	14.15	12.21	13.72	4.16	12.22	-13.7%	-3.0%	-70.6%	-13.6%
South Central	16.38	13.43	14.76	4.84	13.85	-18.0%	-9.9%	-70.5%	-15.5%
Edwards Plateau*	21.03	17.41	19.10	2.86	16.26	-17.2%	-9.2%	-86.4%	-22.7%
East	26.89	23.58	25.28	16.21	25.18	-12.3%	-6.0%	-39.7%	-6.3%
AVG	17.4	14.8	16.1	6.2	15.1	-14.9%	-7.7%	-67.1%	-13.3%

\*portion within the 4km grid domain.

**Figure 29** Isoprene emissions as reported in Table 8 but in graphical format for (a) North Central, (b) Upper Coast, (c) South Central, (d) Edwards Plateau and (e) East. Note difference in y-axis scales between figures.

(a) North Central



(b) Upper Coast

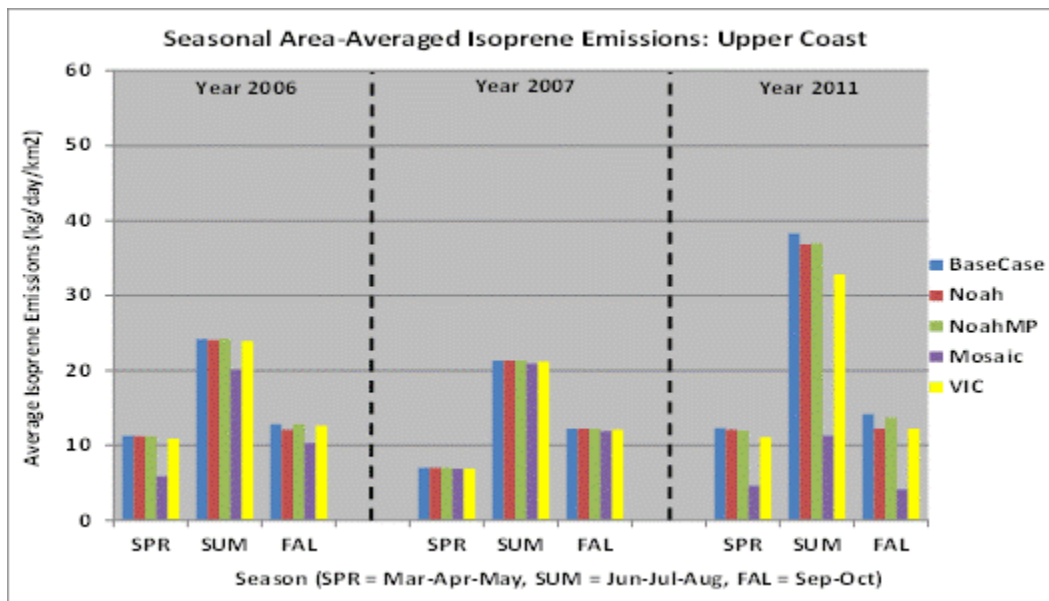
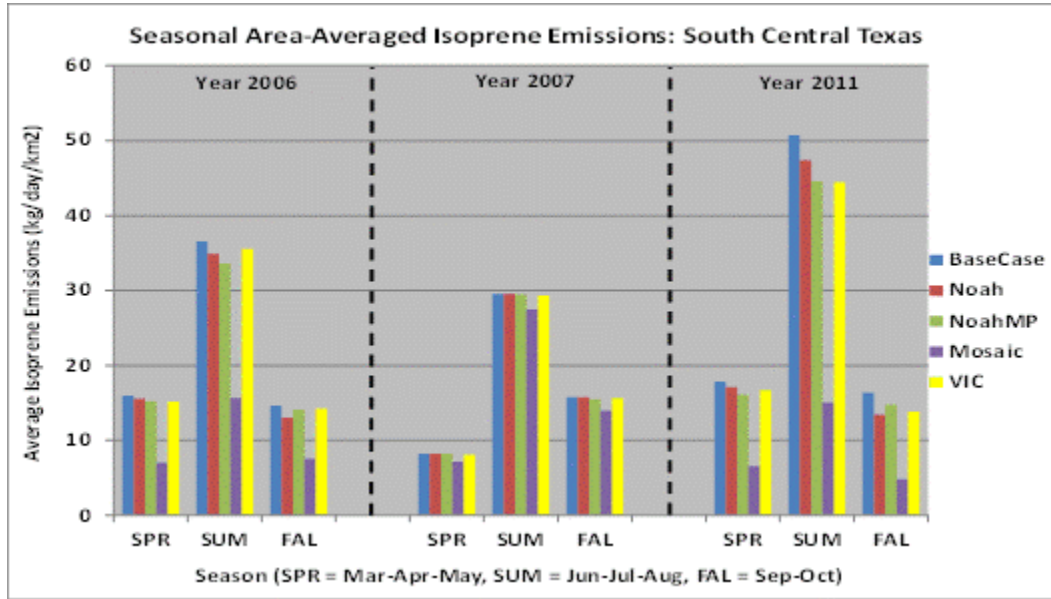


Figure 29 (continued)

(c) South Central



(d) Edwards Plateau

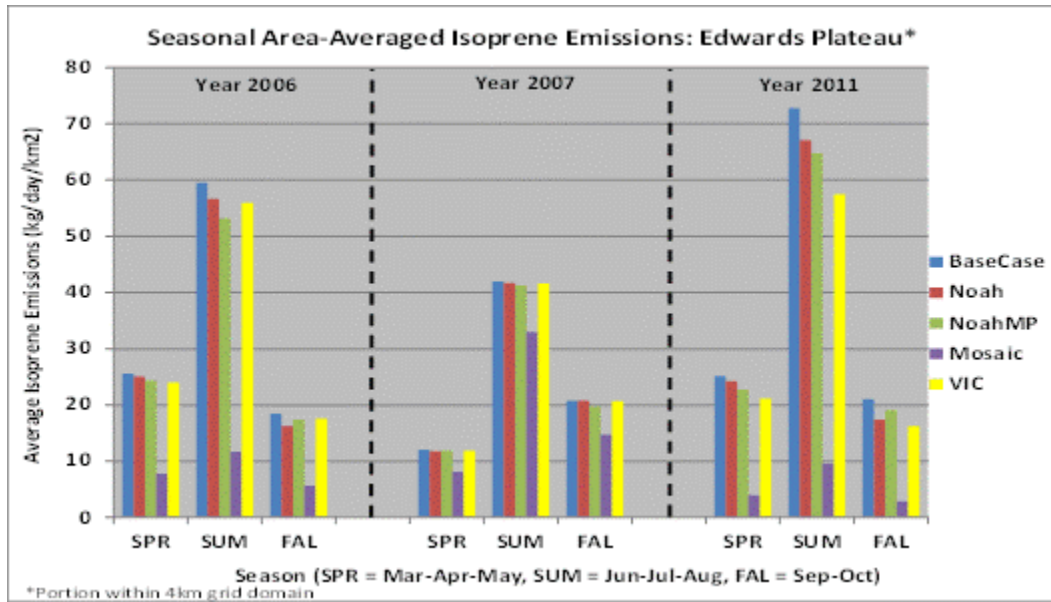
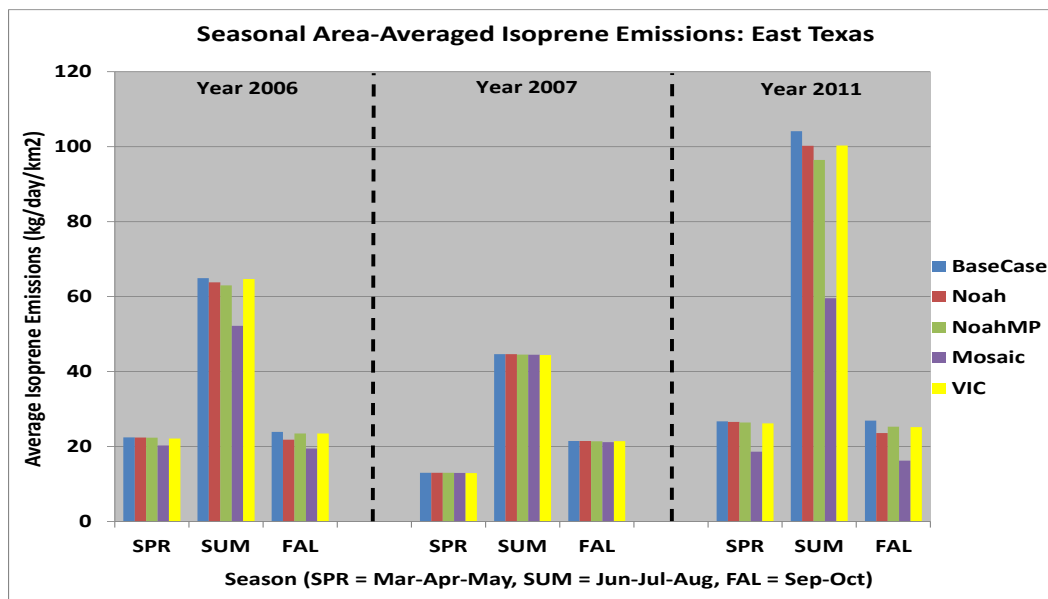


Figure 29 (continued)

(e) East



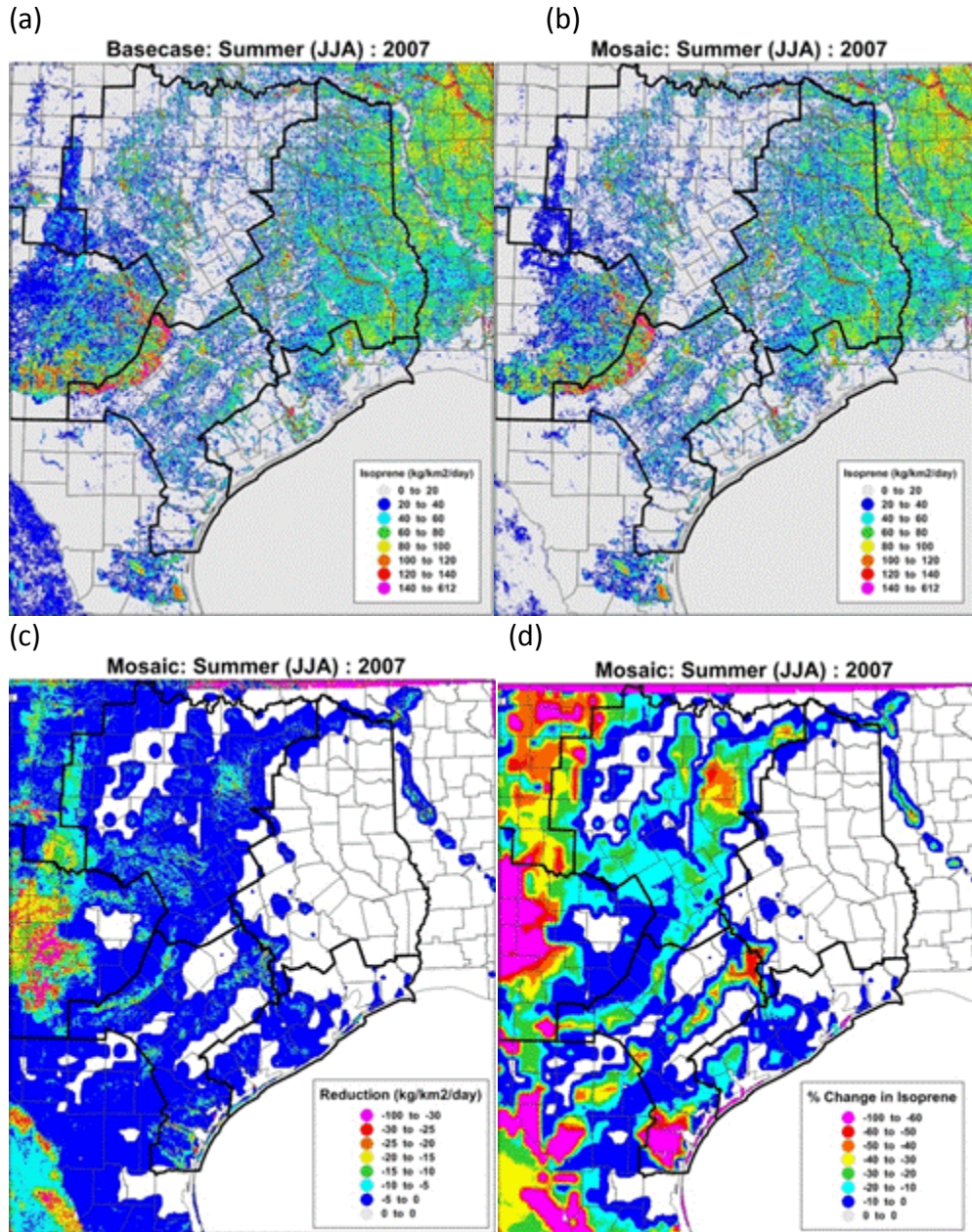
The NLDAS-2 MEGAN simulations demonstrate that the soil moisture impacts on predicted isoprene emissions are generally similar between Noah, Noah-MP, and VIC; for these latter three soil moisture databases, reductions in isoprene (relative to the basecase) during periods of drought are lower compared to those for the Mosaic simulation. For example, changes in summer 2006 emissions, averaged across all regions, are -2.5%, -3.0% and -6.7% for VIC, Noah and Noah-MP compared to -47.6% for Mosaic. Similar variability in predictions occurs for 2011; by region, maximum isoprene reductions are -12.1% for Noah MP (South Central during summer), -18.0% for Noah (South Central during fall), -22.7% for VIC (Edwards Plateau during fall), compared to -86.9% for Mosaic (Edwards Plateau during summer).

Year 2007 was not characterized by drought in eastern Texas (ref. Figure 27); however, changes in summer 2007 emissions relative to the basecase, averaged across all regions, are -0.2%, -0.6%, and -0.7% for Noah, Noah-MP and VIC compared to -8.0% for Mosaic. Maximum Mosaic reductions are -21.4% for Edwards Plateau during summer compared to reductions less than -2.0% for the other LSMs. Because all five eastern Texas regions had wet conditions during 2007, the substantially lower predicted isoprene emissions for Mosaic might not be reasonable.

In order to investigate the spatial distributions of emissions reductions for year 2007 for the Mosaic scenario, Figure 30 shows maps of predicted 1km isoprene emissions over

the entire 4km grid domain for the basecase and Mosaic simulations. Maps showing the absolute difference as well as the percentage change relative to the basecase are included. The magnitude and spatial patterns of predicted emissions for Mosaic are similar to the basecase predictions in most of East Texas. Regions of significant differences exist over substantial portions of other eastern Texas climate regions with substantially lower emissions predicted over interior portions of Edwards Plateau. This inferred deficit in soil moisture availability throughout much of eastern Texas is inconsistent with the available drought and precipitation observational data (e.g., refer to PDSI values in Figure 27 as well as radar estimates of monthly rainfall available from <http://water.weather.gov/precip/>) and, as discussed in subsequent sections, may instead be primarily associated with differences in the wilting point values employed by the Mosaic LSM compared to the other models.

Figure 30 Isoprene emissions for summer 2007 predicted by MEGAN on the 4km grid domain (1km horizontal resolution) for the (a) basecase and (b) Mosaic simulations. Differences and percentage changes are shown in (c) and (d); refer to legend for changes in units and scale.



### *Sensitivity of isoprene predictions to wilting point values*

As demonstrated in Equation 4, differences in wilting points between the NLDAS-2 databases can be crucially important because the wilting point is the threshold value below which isoprene emissions are set to zero. Figure 31 compares the by-region area-averaged wilting point values among the four NLDAS-2 datasets. The wilting points for Noah and Noah-MP vary from 0.05 m<sup>3</sup>/m<sup>3</sup> for East Texas to 0.11 m<sup>3</sup>/m<sup>3</sup> for Edwards Plateau. Compared to Noah/Noah-MP, the Mosaic and VIC wilting points are greater by a factor of approximately two. As discussed previously (ref. Sections 4 and 6), VIC has a wet bias in the near-surface layers compared to the other NLDAS-2 LSMs that appears to compensate for the impact of relatively higher wilting point values on predicted isoprene; in contrast, the higher wilting points for Mosaic, which has a slightly dry bias compared to the other models in the 0-10cm and 10-40cm layers (e.g., ref. Table 9), likely plays an important role in the estimation of often substantial isoprene reductions compared to the basecase and other NLDAS-2 simulations.

In order to investigate the potential influence of differences in wilting points on predicted emissions, a MEGAN simulation was performed for the summers of 2006, 2007, and 2011 that used Mosaic soil moisture availabilities and Noah wilting points. The by-region summer results are shown in Table 9. For all years and regions, the emissions predicted by this sensitivity simulation are closer in magnitude to those predicted by Noah-MP compared to the original Mosaic simulation (i.e., Mosaic soil moisture availabilities and Mosaic wilting points). The emissions estimated by the sensitivity run for summer 2007 are the same or greater as those predicted by the Noah-MP simulation. The reductions during drought years are substantially lower than those predicted by the original Mosaic simulation.

Figure 31 Area-averaged NLDAS-2 wilting point values by region.

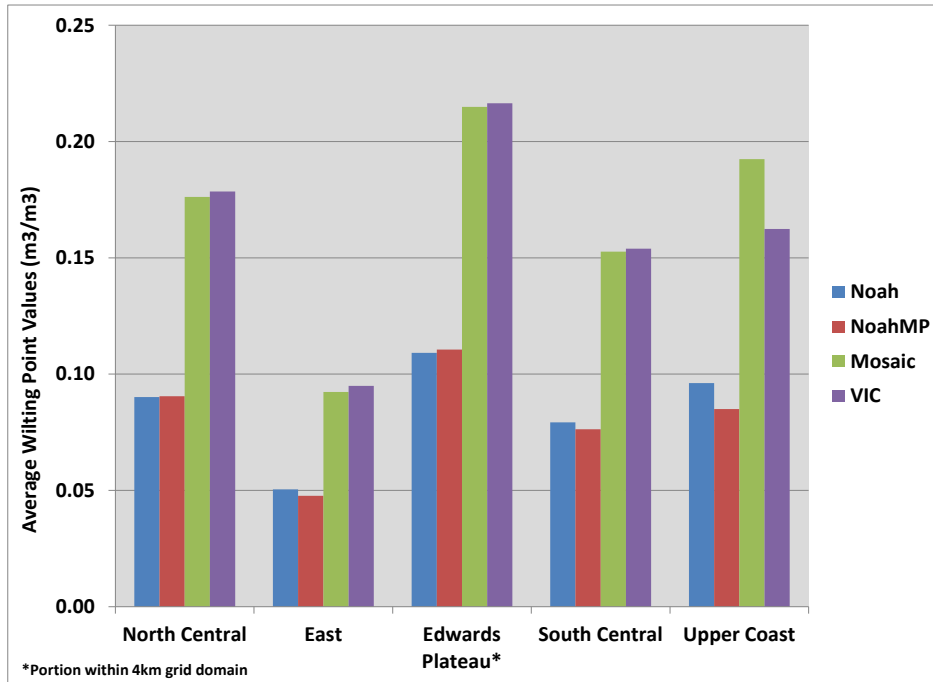


**Table 9 Predicted area-averaged summer isoprene emissions during 2006, 2007, and 2011 for three simulations: Noah-MP, Mosaic, and the Mosaic sensitivity run that used Mosaic soil moisture values and Noah-MP wilting points. The final two columns show the ratio of Mosaic predictions to the Noah-MP values.**

Year	Region	Noah-MP	Mosaic with Noah-MP wilting points	Mosaic	Mosaic with Noah-MP wilting points	Mosaic
		Emissions (kg/km <sup>2</sup> /day)			Ratio relative to Noah-MP	
2006	North Central	28.24	24.35	11.58	0.86	0.41
	Upper Coast	24.18	24.06	20.06	0.99	0.83
	South Central	33.60	30.83	15.65	0.92	0.47
	Edwards Plateau*	53.19	44.32	11.66	0.83	0.22
	East	62.99	62.31	52.18	0.99	0.83
	Average	40.40	37.20	22.20	0.92	0.55
2007	North Central	21.25	21.36	19.41	1.01	0.91
	Upper Coast	21.34	21.34	20.92	1.00	0.98
	South Central	29.48	29.48	27.47	1.00	0.93
	Edwards Plateau*	41.25	41.65	32.97	1.01	0.80
	East	44.54	44.64	44.49	1.00	1.00
	Average	31.60	31.70	29.10	1.00	0.92
2011	North Central	38.84	30.80	13.54	0.79	0.35
	Upper Coast	36.97	31.91	11.33	0.86	0.31
	South Central	44.59	36.09	15.08	0.81	0.34
	Edwards Plateau*	64.77	46.77	9.56	0.72	0.15
	East	96.47	91.66	59.57	0.95	0.62
	Average	56.30	47.40	21.80	0.84	0.39

In order to understand why there can be substantial differences in wilting points between the NLDAS-2 LSMs it is useful to provide an overview of the relevant soil properties and their potential treatment with respect to field measurements and modeled simulations. Soil moisture at any particular location and depth is described and controlled by a number of factors including field capacity and wilting point. Field capacity is the amount of water in the soil after it has been saturated and allowed to drain freely. Wilting point, which in the soil sciences is typically referred to as permanent wilting point, is the water content at which plants wilt and fail to recover when re-supplied with sufficient moisture. Soil water available to plants (available water capacity) is the difference between field capacity and wilting point and is affected by soil characteristics (e.g., texture and particle size distribution as a function of depth, organic/salt content, compaction, etc.) as well as overlying land cover such as vegetation in addition to atmospheric conditions.

According to NRCS (2008), the available water capacity generally increases as soil texture becomes finer (i.e., from sand to loams to silt). Coarse textured soils have lower capacity due to large pore spaces that assist free drainage. Fine textured soils have smaller pores with enhanced water storage properties (via lower hydraulic conductivity). The finest soil type is clay, which tends to have relatively lower available water capacity because of increased permanent wilting points.

With regard to vegetation type, wilting points vary dependent on the specific plant species as well as their season of growth, maturity, rooting pattern and depth, and numerous other environmental conditions (Tolk, 2003). Historically, wilting point was determined visually via “the sunflower method”. Representative plants are grown in containers of uniform soil sealed to limit evaporative loss. Plants are allowed to approach a specific stage of maturity in a low transpiration environment until wilting is observed. This methodology may also be applied in the field, where the soil water content or potential is directly measured after plant dormancy or premature death occurs. Operationally, wilting point is estimated as the soil water content at 1.5 MPa matric potential, which mostly represents the lower limit provided by the sunflower or field methods.

Observed soil texture has substantial spatial variability (both horizontally and vertically) on scales as small as a few meters. The soil type properties such as porosity, field capacity, and hydraulic conductivity are expressed numerically in the NLDAS-2 LSMs based on 16 soil type categories (<http://ldas.gsfc.nasa.gov/nldas/NLDASsoils.php>). The LSMs employ their own calibrations using model-specific vegetation and/or soil definitions that result in different simulations of soil parameters including wilting points. For example, an investigation of differences in predicted soil moisture between NLDAS models by Robock et al. (2003) noted that observed (and modeled) values for porosity were similar between soil types; however, water availabilities often differed significantly because of large differences in field capacity and calculated wilting point for the same location. Saturated hydraulic conductivity and  $b$  parameter (Clapp and Hornberger, 1978) determine the complicated relationship between soil water content and soil water flow inside the soil; different values cause models to perform differently in soil moisture, runoff, and evaporation simulations.

Maps showing the gridded 0-200cm average wilting points on the 4km MEGAN grid domain for the Noah, Noah-MP, Mosaic, and VIC datasets are shown in Figure 32. The magnitude and spatial gradients of wilting point values are basically similar between Noah and Noah-MP and range up to  $0.14 \text{ m}^3/\text{m}^3$ ; the Mosaic and VIC maximum values are just over  $0.27 \text{ m}^3/\text{m}^3$ . As discussed previously, the VIC near-surface soil moisture predictions are typically greater than those predicted by Noah, Noah-MP, and Mosaic. This VIC wet bias likely accounts for the more similar isoprene predictions for VIC to those for Noah/Noah-MP in contrast to the sometimes substantial reductions predicted by the Mosaic MEGAN simulations.

The NLDAS-2 LSMs rely on identical  $1/8^\circ$  NLDAS soil type information (ref. Figure 33a) that is derived from a 1km STATSGO database (Miller and White, 1998). The spatial variations of the NLDAS-2 wilting points (ref. Figure 32) clearly mimic the NRCS soil textures. Furthermore, the biases between models may also be related to differences in LSM treatments between soil types. For example, the Mosaic model predicted significant reductions in isoprene (related to differences in wilting point values) over various portions of the 4km grid domain as summarized in Figure 33b. The spatial pattern of significant reductions in isoprene emissions is clearly correlated to regions of clay and/or clay loam soils suggesting that the Mosaic-specific treatment (that impacts both wilting points and simulated soil water contents) for clay soils results in substantial differences compared to the other LSM models.

Figure 32 NLDAS-2 wilting point values on the 4km grid domain for (a) Noah, (b) Noah-MP, (c) Mosaic and (d) VIC.

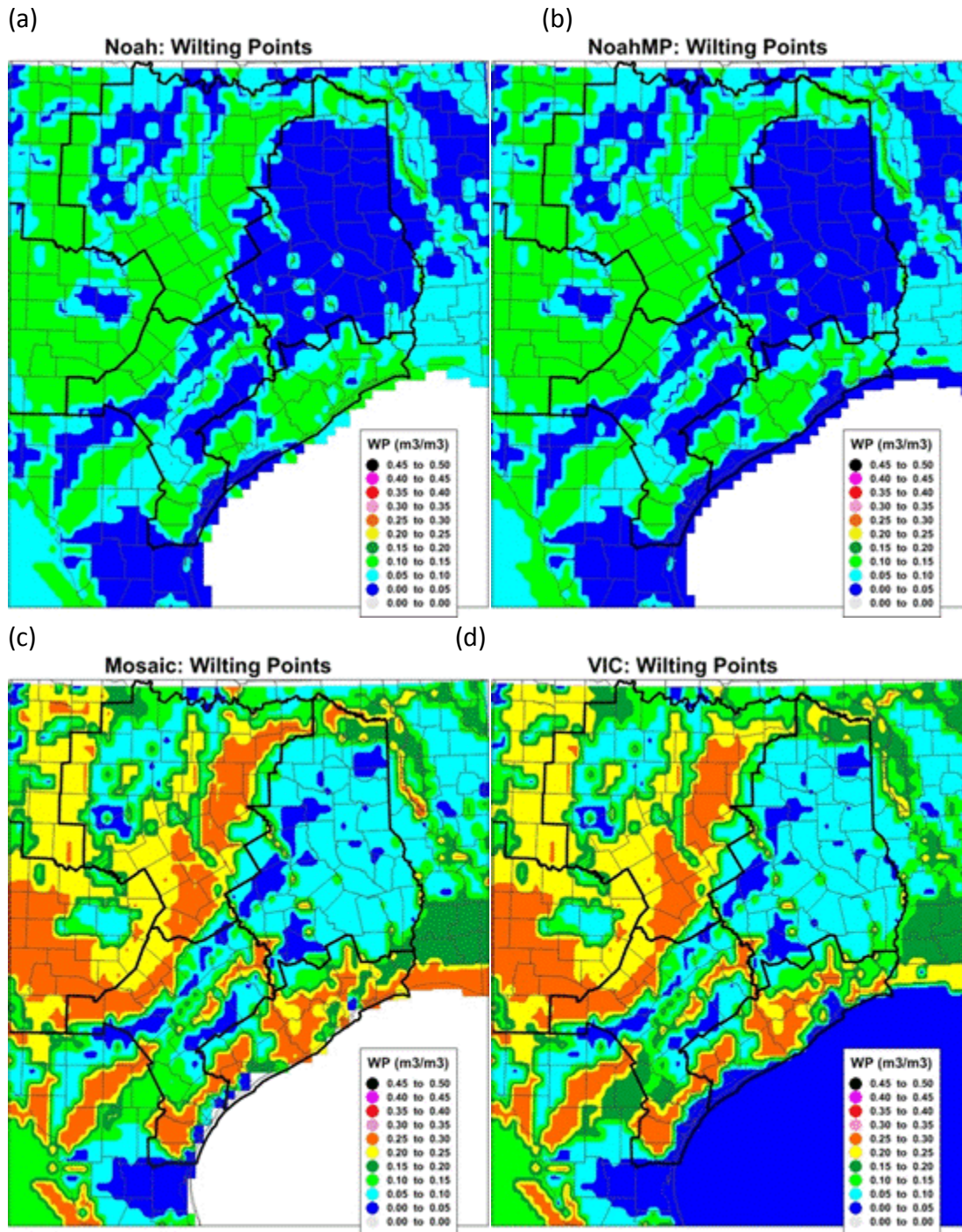
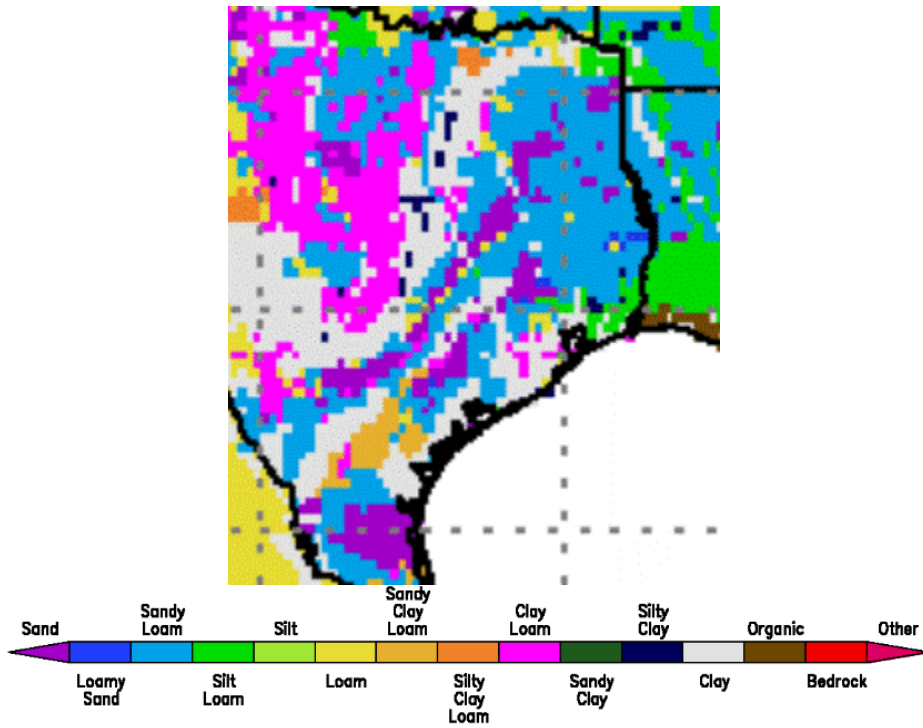
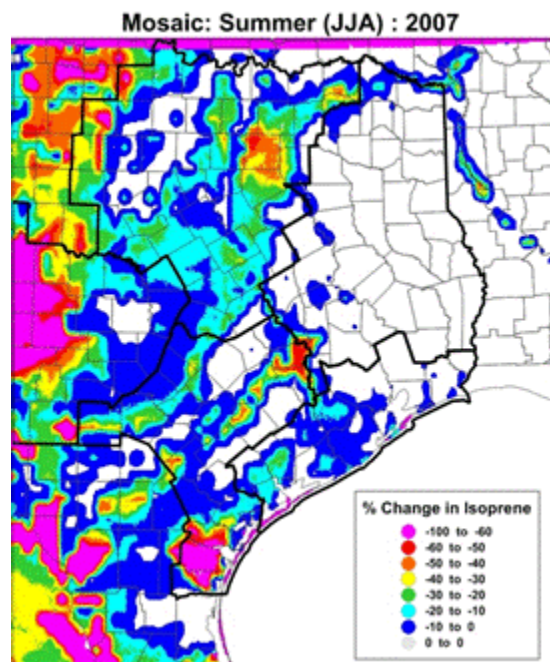


Figure 33 A comparison of (a) STATSGO soil texture employed by NLDAS-2 and (b) percentage changes in predicted isoprene for the Mosaic simulation relative to the basecase for summer 2007.

(a)



(b)



### Isoprene predictions at monitoring locations

MEGAN simulations were developed to investigate the impact of observed and (representative) NLDAS-2 soil moisture databases on predicted isoprene emissions during 2011 at three eastern Texas in-situ monitoring locations: Palestine, Port Aransas, and Prairie View. As previously summarized in Figure 15 for Palestine, Mosaic had relatively good agreement with in-situ observations during 2011 while Noah predicted higher soil moisture availabilities than observed for the near-surface layers. Figure 34 compares observed, Noah, and Mosaic average growing season (March-October) soil moisture at the Port Aransas and Prairie View locations. Noah shows little sensitivity with respect to depth at both locations and is mostly too wet compared to observations except at 100 cm. Mosaic shows better directional changes with depth compared to observations and has generally good agreement at Port Aransas (except at 100cm) but for Prairie View is too wet at 5cm and too dry at deeper depths.

The observed soil moisture dataset for input to MEGAN consisted of the hourly in-situ soil moisture values in addition to STATSGO (e.g., survey-based; <http://water.usgs.gov/GIS/metadata/usgswrd/XML/ussoils.xml>) wilting points. Table 10 compares the NLDAS-2 and STATSGO wilting points (averaged over 0-200cm) at each of the three Texas locations. The STATSGO values are consistently greater than the NLDAS-2 values with maximum differences at Palestine.

**Figure 34 Average growing season (March-October) soil moisture during 2011 at Port Aransas and Prairie View for in-situ observations (Measured) and as simulated by Mosaic and Noah.**

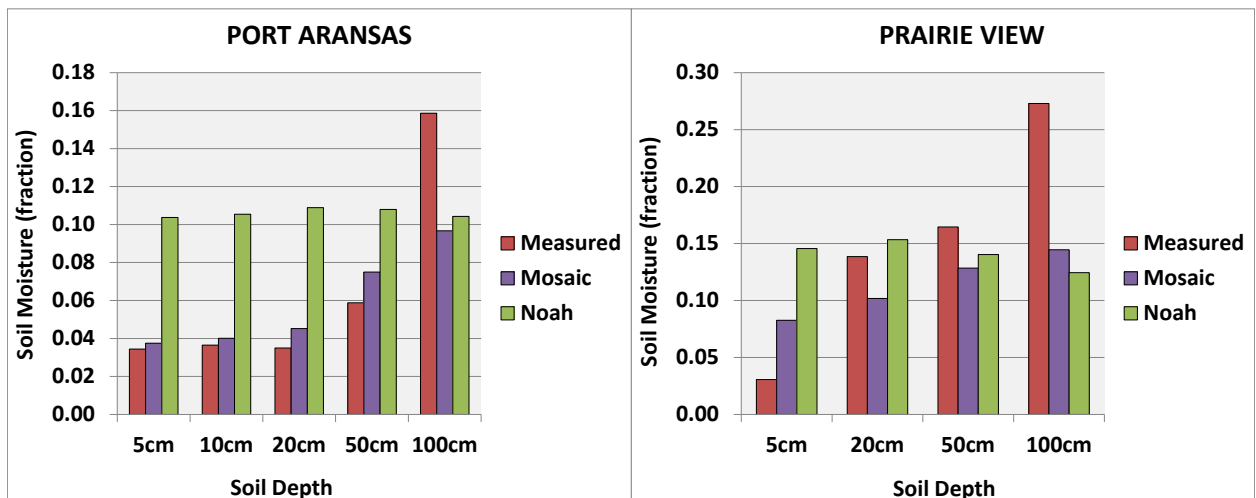
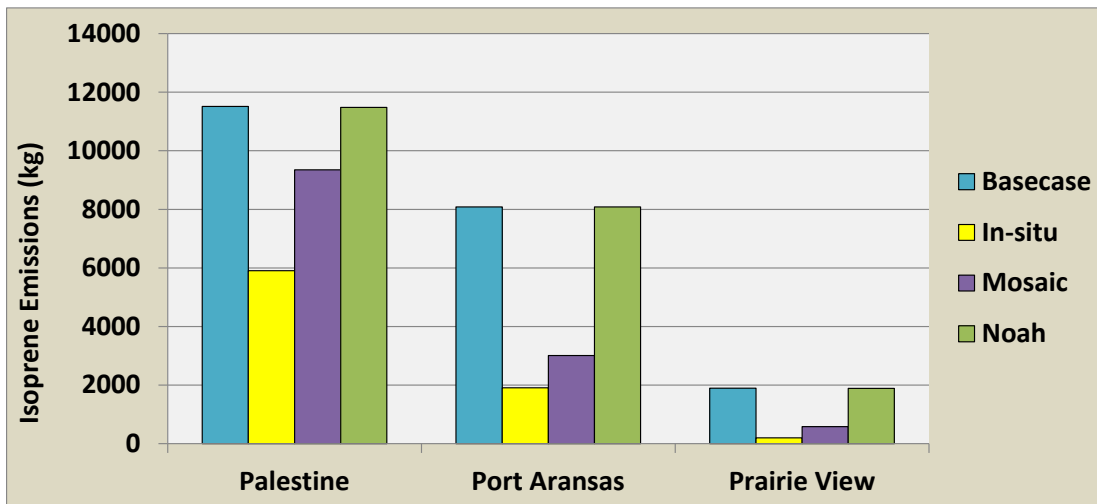


**Table 10 Average wilting points (0-200cm) at Palestine, Port Aransas, and Prairie View.**

Location	SSURGO	Noah	Mosaic
Palestine	0.107	0.023	0.018
Port Aransas	0.040	0.023	0.018
Prairie View	0.162	0.047	0.091

MEGAN simulations were run for four scenarios at each monitoring location: (1) basecase (i.e., soil moisture not considered) in addition to runs that employed (2) observed, (3) Noah, and (4) Mosaic soil moisture databases. The predicted total isoprene emissions for Mar-Oct between the scenarios are compared in Figure 35. Differences in the magnitude of emissions between locations reflect MEGAN vegetation types; Prairie View is dominated by grasses, Port Aransas by broadleaf deciduous trees, Palestine has significant contributions from needleleaf evergreen trees. Isoprene emissions estimates had substantial sensitivity to differences in the input soil moisture datasets; predictions for Noah were similar to the basecase while the observation-based isoprene predictions were lower by at least 50%. The Mosaic emissions were predicted at values between the observed and Noah values.

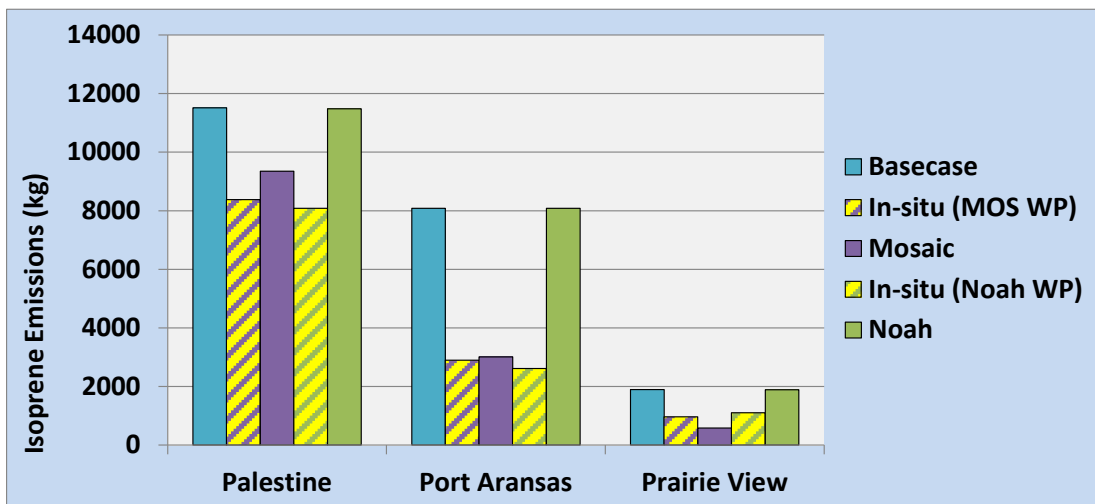
**Figure 35 Total isoprene predicted for Mar-Oct 2011 at three Texas locations using observed, Noah, and Mosaic soil moisture databases.**



In order to determine the relative importance of wilting points and soil moisture availabilities to isoprene predictions, additional MEGAN runs were performed that used in-situ soil moisture availabilities and NLDAS-2 wilting points. Predictions that used observed soil moisture and Mosaic wilting points were generally similar to predictions for the Mosaic simulations at all locations (ref. Figure 36); the run that used in-situ soil

moisture availabilities with Noah wilting points provided emissions estimates that remained substantially lower than those estimated by the Noah simulation. Overall, results from these MEGAN runs re-emphasize the large sensitivity of predicted emissions to the specific soil moisture database (both absolute soil water contents and especially wilting points) employed.

**Figure 36** As in Figure 35 but adding MEGAN simulations that utilized observed soil moisture and NLDAS-2 wilting points.



### 7.3 Summary

Utilization of the Noah, Noah-MP, and VIC soil moisture databases within MEGAN to predict isoprene emissions during drought often showed wide variability among models dependent on the location, season, and year but emissions reductions compared to the basecase (i.e., impact of soil moisture not considered) were mostly less than 15%. In contrast, the simulations that employed the Mosaic database often predicted substantial emissions reductions in response to drought. Analysis of results for Mosaic demonstrated that emissions reductions were sometimes predicted even during non-drought conditions especially in regions dominated by clay soils. The substantial differences in Mosaic predictions from the other models are due, in part, to the relatively high wilting point database employed by Mosaic. Overall the results of the MEGAN simulations indicate high sensitivity to the input soil moisture databases (absolute water contents as well as wilting points).

## 7.4 References

Beckett M, Loreto F, Velikova V, Brunetti C, Di Ferdinando M, Tattini M, Calafapietra C, Farrant JM, 2012. Photosynthetic limitations and volatile and non-volatile isoprenoids in the poikilochlorophyllous resurrection plant *Xerophyta humilis* during dehydration and rehydration. *Plant, Cell & Environment* 35: 2061–2074.

Clapp, R. B., and G. M. Hornberger, 1978. Empirical equations for some soil hydraulic properties, *Water Resour. Res.*, 14(4), 601–604, doi:10.1029/WR014i004p00601.

ENVIRON International Corporation, 2011. Project status updates and isoprene comparisons from using different sources of PAR [PowerPoint Slides]. Retrieved February 19, 2014, from [http://www.wrapair2.org/pdf/MGN210\\_sat\\_vs\\_wrf\\_DecCall14.Final2.ppt](http://www.wrapair2.org/pdf/MGN210_sat_vs_wrf_DecCall14.Final2.ppt)

Guenther, A. B., Jiang, X., Heald, C. L., Sakulyanontvittaya, T., Duhl, T., Emmons, L. K., & Wang, X., 2012. The Model of Emissions of Gases and Aerosols from Nature version 2.1 (MEGAN2.1): an extended and updated framework for modeling biogenic emissions. *Geoscientific Model Development*, 5(6), 1471–1492. doi:10.5194/gmd-5-1471-2012

Guenther, A., Karl, T., Harley, P., Wiedinmyer, C., Palmer, P. I., & Geron, C., 2006. Estimates of global terrestrial isoprene emissions using MEGAN (Model of Emissions of Gases and Aerosols from Nature). *Atmospheric Chemistry and Physics*, 6(1), 107–173. doi:10.5194/acpd-6-107-2006.

Huang, L., McGaughey, G., McDonald-Buller, E., Kimura, Y., & Allen, D. T., 2015. Quantifying regional, seasonal and interannual contributions of environmental factors on isoprene and monoterpene emissions estimates over eastern Texas. *Atmospheric Environment*, 106, 120-128. 10.1016/j.atmosenv.2015.01.072

Huang, L., McDonald-Buller, E. C., McGaughey, G., Kimura, Y., & Allen, D. T., 2014. Annual variability in leaf area index and isoprene and monoterpene emissions during drought years in Texas. *Atmospheric Environment*, 92, 240-249.

Kleindienst, T. E., Jaoui, M., Lewandowski, M., Offenberg, J. H., Lewis, C. W., Bhave, P. V., & Edney, E. O., 2007. Estimates of the contributions of biogenic and anthropogenic hydrocarbons to secondary organic aerosol at a southeastern US location. *Atmospheric Environment*, 41(37), 8288-8300.

Koster, R. D., Guo, Z., Yang, R., Dirmeyer, P. A., Mitchell, K. & Puma, M. J., 2009. On the nature of soil moisture in land surface models. *Journal of Climate*, 22, 4322–4335.

Lamb, B., Gay, D., Westberg, H., & Pierce, T., 1993. A biogenic hydrocarbon emission inventory for the USA using a simple forest canopy model. *Atmospheric Environment. Part A. General Topics*, 27(11), 1673-1690.

McNider, R., personal communication, July 31, 2013.

Miller, D. A., and R. A. White, 1998. A conterminous United States multi-layer soil characteristics data set for regional climate and hydrology modeling, *Earth Inter.*, 2, Paper No. 2.

Müller, J. F., Stavrou, T., Wallens, S., Smedt, I. D., Roozendaal, M. V., Potosnak, M. J., Rinne, J., Munger, B., Goldstein, A., & Guenther, A. B., 2008. Global isoprene emissions estimated using MEGAN, ECMWF analyses and a detailed canopy environment model. *Atmospheric Chemistry and Physics*, 8(5), 1329-1341.

NRCS, 2009. Soil Quality Indicators.

[http://www.nrcs.usda.gov/Internet/FSE\\_DOCUMENTS/nrcs142p2\\_053288.pdf](http://www.nrcs.usda.gov/Internet/FSE_DOCUMENTS/nrcs142p2_053288.pdf)

Pegoraro, E., Rey, A., Greenberg, J., Harley, P., Grace, J., Malhi, Y., & Guenther, A., 2004. Effect of drought on isoprene emission rates from leaves of *Quercus virginiana* Mill. *Atmospheric Environment*, 38(36), 6149-6156.

Potosnak, M. J., LeSturgeon, L., Pallardy, S. G., Hosman, K. P., Gu, L., Karl, T., Geron, C., & Guenther, A. B., 2014. Observed and modeled ecosystem isoprene fluxes from an oak-dominated temperate forest and the influence of drought stress. *Atmospheric Environment*, 84, 314-322.

Robock, A., Luo, L., Wood, E. F., Wen, F., Mitchell, K. E., Houser, P. R., Schaake, J. C., Lohmann, D., Cosgrove, B., Sheffield, J., Duan, Q., Higgins, R. W., Pinker, R. T., Tarpley, J. D., Basara, J. B., Crawford, K. C., 2003. Evaluation of the North American Land Data Assimilation System over the southern Great Plains during the warm season, *J. Geophys. Res.*, 108, 8846, doi:10.1029/2002JD003245, D22.

TOLK, J.A., 2003. SOILS, PERMANENT WILTING POINTS. STEWART, B.A., HOWELL, T.A., EDITORS. MARCEL-DEKKER, INC., NEW YORK, NY. ENCYCLOPEDIA OF WATER SCIENCE. P. 927-929

## 8.0 Discussion

Drought evolves through a complex interaction of land/atmosphere processes; typical components of drought include reductions in volumetric soil moisture and increases in land/atmospheric temperatures. The impact of drought conditions on isoprene emissions remains somewhat controversial; a review by Penuelas and Staudt (2010) indicated that ~50% of studies relating isoprene emissions and drought identified emissions decreases compared to ~25% reporting increased emissions and the remaining reporting no change (Zielinski et al., 2014). Limited ecosystem-level observations during natural drought conditions have shown increases (e.g., within a northern Michigan mixed hard wood forest during 2000-2002; Pressley et al., 2006) as well as short-term increases followed by long-term decreases (e.g., Potosnak et al., 2014). Overall, leaf-level isoprene emissions have been found to respond inconsistently to mild water stress but generally decreased substantially under conditions of severe water stress (Pegoraro et al., 2004; Brill et al., 2007; Staudt et al., 2008; Lavoie et al., 2009; etc.). Although photosynthesis may be greatly reduced (due to stomata closure), emissions may be uncoupled from photosynthesis during induced water stress; however, with continued reductions in water availability, emissions are eventually fully inhibited with the timing dependent on the species being studied (Zielinski et al., 2014).

The impacts of drought as currently captured by MEGANv2.1 may have substantial uncertainty; however, soil moisture represents a primary mechanism by which drought effects are manifested in isoprene estimates. Previous MEGAN studies have typically employed a single soil moisture database; predicted impacts on isoprene emissions have ranged from minimal (e.g., Guenther, et al, 2006; Potosnak et al., 2014) to substantial (e.g., global isoprene reductions of 20-50% for Müller et al., 2008; Tawfik et al., 2012; Sindelarova et al., 2014) suggesting that the emissions impact associated with reduced soil water availabilities are characterized by substantial uncertainty.

Based on the MEGAN simulations performed in our work, Table 11 presents the percentage change in summer emissions for the Noah-MP and Mosaic scenarios between 2007, which had average-to-wet conditions, and 2011, a year characterized by all-time record drought and heat throughout Texas. The ratio of emissions between 2007 and 2011 is also shown.

As discussed in Huang et al. (2015) higher temperatures between 2007 and 2011 drive a nonlinear increase in predicted isoprene emissions while drought-induced summer LAI reductions (especially for the central regions) suggest a strong negative effect of drought on emissions. For the isoprene simulation with Noah-MP, the combined negative impacts of LAI and reduced soil moisture are dominated by emissions increases associated with temperature; emissions increases range from a factor of 1.5 for South Central to 2.2 for East Texas. In contrast, if the Mosaic soil moisture database better represents actual conditions compared to Noah-MP, relatively larger decreases in isoprene emissions associated with reduced soil moisture availability often overwhelm

increases in emissions caused by warmer temperatures. The negative impacts on emissions cause reductions between 2007 and 2011 of -30% for North Central increasing to -71% for Edwards Plateau. In East Texas, relatively lower impacts associated with smaller magnitude differences in soil moisture (and LAI; Huang et al., 2015) between 2007 and 2011 result in an emissions increase in 34% that is well below the increase of more than 100% predicted by the Noah-MP simulation.

**Table 11 Predicted isoprene (kg/m<sup>2</sup>/day) for summer 2007 and summer 2011 by region for the Noah-MP and Mosaic simulations.**

Region	Noah-MP			Mosaic		
	Summer 2007	Summer 2011	Ratio (Summer 2011/Summer 2007)	Summer 2007	Summer 2011	Ratio (Summer 2011/Summer 2007)
North Central	21.25	38.84	1.83	19.41	13.54	0.70
Upper Coast	21.34	36.97	1.73	20.92	11.33	0.54
South Central	29.48	44.59	1.51	27.47	15.08	0.55
Edwards Plateau	41.25	64.77	1.57	32.97	9.56	0.29
East	44.54	96.47	2.17	44.49	59.57	1.34

The current soil moisture algorithm is based on results from a single laboratory leaf-level study of *Quercus virginiana* Mill. (species of live oak) by Pegoraro et al. (2004). The MEGAN approach used to calculate the soil activity factor is linked directly to the difference between soil moisture and wilting point (ref. Eqn. 4); Guenther et al. (2006) employed the Chen and Dudhia (2001) global wilting point dataset as input (Guenther et al., 2012). The MEGAN studies performed in our work (and others) highlight the potential uncertainty associated with the specific soil moisture database, especially wilting points, utilized. This suggests a continued need for investigations to evaluate and improve the drought stress parameterizations and/or representations in models such as MEGAN (e.g., Potosnak, et al., 2014). Additionally, the evaluation and validation of simulated soil moisture datasets is important; however, the current spatial coverage of in-situ root-zone measurements is sparse for most of the U.S. (e.g., Ochsner, et al., 2013). Future work that generates inputs and/or evaluates outputs from LSMs such as NLDAS-2 with additional in-situ monitors as well as comparisons to satellite-derived soil moisture estimates would likely be beneficial.

The current MEGAN algorithm can only reduce emissions in response to long-term drought and assumes a consistent response regardless of the magnitude and timing of soil water stress and vegetation type. However, drought response is species specific; for example, a recent leaf-level study by Zielinski et al. (2014) of a drought-adapted species of Downy oak (*Quercus pubescens* Willd.) found that mild water stress was associated with increased isoprene emissions compared to the control and that conditions of severe water stress had emission rates similar to the control despite a 47% reduction in

photosynthesis. Another recent study by Potosnak et al. (2014) of an oak-dominated temperate forest observed a time-dependent response of field isoprene emissions to drought where an initial increase of emissions (about a week) was followed by a subsequent decrease that could not be simulated using the MEGAN time-independent soil moisture algorithm. Additional ecosystem-level studies under a range of natural drought conditions would likely provide valuable insights toward improved predictions of regional biogenic emissions.

It should also be mentioned that the direct impact of reduced soil moisture availability within MEGAN is currently limited to isoprene. Recent leaf-level observations by Wu et al. (2015) suggest that the long-term drought effects on monoterpenes are similar to those found for isoprene so that it may be appropriate to extend the soil moisture algorithm to incorporate additional BVOCs.

## References

Brilli, F., Barta, C., Fortunati, A., Lerdau, M., Loreto, F., & Centritto, M., 2007. Response of isoprene emission and carbon metabolism to drought in white poplar (*Populus alba*) saplings. *The New Phytologist*, 175(2), 244–54. doi:10.1111/j.1469-8137.2007.02094.x

Fei Chen and Jimy Dudhia, 2001. Coupling an Advanced Land Surface–Hydrology Model with the Penn State–NCAR MM5 Modeling System. Part I: Model Implementation and Sensitivity. *Mon. Wea. Rev.*, 129, 569–585.

Guenther, A., Karl, T., Harley, P., Wiedinmyer, C., Palmer, P. I., & Geron, C., 2006. Estimates of global terrestrial isoprene emissions using MEGAN (Model of Emissions of Gases and Aerosols from Nature). *Atmospheric Chemistry and Physics*, 6(1), 107–173. doi:10.5194/acpd-6-107-2006

Guenther, A. B., Jiang, X., Heald, C. L., Sakulyanontvittaya, T., Duhl, T., Emmons, L. K., & Wang, X., 2012. The Model of Emissions of Gases and Aerosols from Nature version 2.1 (MEGAN2.1): an extended and updated framework for modeling biogenic emissions. *Geoscientific Model Development*, 5(6), 1471–1492. doi:10.5194/gmd-5-1471-2012

Huang, L., McGaughey, G., McDonald-Buller, E., Kimura, Y., & Allen, D. T., 2015. Quantifying regional, seasonal and interannual contributions of environmental factors on isoprene and monoterpene emissions estimates over eastern Texas. *Atmospheric Environment*, 106, 120-128. 10.1016/j.atmosenv.2015.01.072

Huang, L., McDonald-Buller, E. C., McGaughey, G., Kimura, Y., & Allen, D. T., 2014. Annual variability in leaf area index and isoprene and monoterpene emissions during drought years in Texas. *Atmospheric Environment*, 92, 240-249.

Lavoir, A.-V., Staudt, M., Schnitzler, J. P., Landais, D., Massol, F., Rocheteau, A., et al., 2009. Drought reduced monoterpene emissions from the evergreen Mediterranean oak *Quercus ilex*: results from a throughfall displacement experiment. *Biogeosciences*, 6(7), 1167–1180. doi:10.5194/bg-6-1167-2009

Müller, J. F., Stavrakou, T., Wallens, S., Smedt, I. D., Roozendaal, M. V., Potosnak, M. J., Rinne, J., Munger, B., Goldstein, A., & Guenther, A. B., 2008. Global isoprene emissions estimated using MEGAN, ECMWF analyses and a detailed canopy environment model. *Atmospheric Chemistry and Physics*, 8(5), 1329-1341.

Pegoraro, E., Rey, A., Greenberg, J., Harley, P., Grace, J., Malhi, Y., & Guenther, A., 2004. Effect of drought on isoprene emission rates from leaves of *Quercus virginiana* Mill. *Atmospheric Environment*, 38(36), 6149–6156. doi:10.1016/j.atmosenv.2004.07.028

Ochsner, Tyson E.; Cosh, Michael H.; Cuenca, Richard H.; Dorigo, Wouter A.; Draper, Clara S.; Hagimoto, Yutaka; Kerr, Yann H.; Njoku, Eni G.; Small, Eric E.; Zreda, Marek, 2013. State of the art in large-scale soil moisture monitoring. *Soil Science Society of America Journal*, 77(6), 1888-1919. doi:10.2136/sssaj2013.03.0093  
Peñuelas, J, Staudt, M (2010) Biogenic volatile organic compounds and global change. *Trends in Plant Science*, 15, 133-144.

Potosnak, M. J., LeSturgeon, L., Pallardy, S. G., Hosman, K. P., Gu, L., Karl, T., Geron, C., & Guenther, A. B., 2014. Observed and modeled ecosystem isoprene fluxes from an oak-dominated temperate forest and the influence of drought stress. *Atmospheric Environment*, 84, 314-322.

Pressley, S., Lamb, B., Westberg, H., Flaherty, J., & Chen, J., 2005. Long-term isoprene flux measurements above a northern hardwood forest. *Journal of Geophysical Research*, 110(D7), D07301. doi:10.1029/2004JD005523

Sindelarova, K., Granier, C., Bouarar, I., Guenther, A., Tilmes, S., Stavrakou, T., Müller, J. F., Kuhn, U., Stefani, P., & Knorr, W., 2014. Global dataset of biogenic VOC emissions calculated by the MEGAN model over the last 30 years. *Atmospheric Chemistry and Physics Discussions*, 14, 10725-10788.

Tawfik, A. B., Stöckli, R., Goldstein, A., Pressley, S., & Steiner, A. L., 2012. Quantifying the contribution of environmental factors to isoprene flux interannual variability. *Atmospheric Environment*, 54, 216-224.

Wu, C., Pullinen, I., Andres, S., Carriero, G., Fares, S., Goldbach, H., Hacker, L., Kasal, T., Kiendler-Scharr, A., Kleist, E., Paoletti, E., Wahner, A., Wildt, J., and Mentel, Th. F., 2015. Impacts of soil moisture on de novo monoterpene emissions from European beech, Holm oak, Scots pine, and Norway spruce, *Biogeosciences*, 12, 177-191, doi:10.5194/bg-12-177-2015.

Genard-Zielinski, A.-C., Boissard, C., Fernandez, C., Kalogridis, C., Lathière, J., Gros, V., Bonnaire, N., and Ormeño, E., 2014. Variability of BVOC emissions from a Mediterranean mixed forest in southern France with a focus on *Quercus pubescens*, *Atmos. Chem. Phys. Discuss.*, 14, 17225-17261, doi:10.5194/acpd-14-17225-2014.

## 9.0 Recommendations for Future Work

Comparison with available in-situ observations shows that all NLDAS-2 LSMs capture relative changes in the overall spatial and temporal variations of soil moisture such as the extent and evolution of drought potentially important for BVOC emission modeling. Depending on the specific location and season, Noah-MP, Mosaic, or Noah may have the best agreement with observations in the near-surface layers while the models predict substantially drier soil moisture at deeper soil layers compared to observations. However, absolute model biases may be large, with the magnitude partially dependent on LSM, soil depth, and location. In particular, absolute soil moisture values are consistently predicted as too wet by VIC for the near-surface layers and hence cannot capture extreme wet/dry events. In contrast, Noah-MP exhibits overly weak temporal variation at deeper layers in eastern Texas and so fails to reproduce conditions during the wet year of 2007 and drought events in 2011.

Utilization of the Noah, Noah-MP, and VIC soil moisture databases within MEGAN to predict isoprene emissions during drought showed regionally-averaged isoprene reductions within 15% of the basecase (i.e., impact of soil moisture not considered). In contrast, the simulations that employed the Mosaic database often predicted large emissions reductions during drought. Analysis of the Mosaic results show that emissions reductions were sometimes predicted even during non-drought periods especially in regions dominated by clay soils. The substantial differences in Mosaic isoprene predictions from the other models are due, in part, to the relatively high wilting point database employed by Mosaic.

The results of the MEGAN simulations indicate high sensitivity to the input soil moisture databases (absolute water contents as well as wilting points). Although there is large uncertainty in the evaluation of the NLDAS-2 LSMs due to sparse observational data within eastern Texas, we currently recommend the use of Noah based on the results and caveats from our work. Though beyond the scope of the current study, efforts to investigate differences in model structure and physics between the LSMs (even for a limited number of representative grid cells) would likely prove beneficial to understanding differences in the relevant LSM-specific soil properties (e.g., wilting points) as well as soil moisture predictions.

Other suggestions for future work include:

Analysis of additional soil moisture observations in eastern Texas as they become available (e.g., in-situ SCAN, CRN, COSMOS, and TxSON measurements; SMAP satellite observations) including comparisons to NLDAS-2 and/or other LSMs.

MEGAN simulations to quantify the impact of soil moisture within each modeled soil layer on predicted BVOC emissions. Isoprene predictions (as well as differences in absolute soil moisture contents predicted between LSMs) could be further investigated by the predominant NLDAS-2 grid cell (or locally observed) soil/vegetation characteristics such as PFT, soil texture and/or wilting point.

Comparison of LSM-specific wilting points to available observed (i.e., STATSGO/SSURGO) values. MEGAN simulations might be performed to investigate the sensitivity of using layer-specific rather than layer-averaged values.

Comparison of temporal and spatial trends in MEGAN predictions of BVOCs (especially during drought periods) to the results from other environmental regional datasets (particularly satellite-based vegetation-dependent observations such as fluorescence, LAI, NDVI, etc.)

Extensions of the MEGAN soil moisture algorithm to include additional BVOCs to isoprene such as monoterpenes; consideration of species-specific responses of BVOC emissions to both short- and long-term soil water deficits.

## 10.0 Audits of Data Quality

In support of our project, in-situ monitoring data collected at SCAN and CRN locations within the South Central U.S. were utilized. Daily and hourly measurements were retrieved directly from the NRCS and SCAN websites (<http://www.wcc.nrcs.usda.gov/scan>; <http://www.ncdc.noaa.gov/crn/qcdatasets.html>). Time series of observed soil moisture during years 2006-2013 at individual monitoring locations representative of eastern Texas and non-Texas areas were visualized for reasonableness, including an investigation of trends in spatial, seasonal, and inter-annual variability across the South Central U.S. (ref. Sections 3-5) and a direct comparison with observed precipitation at selected eastern Texas locations (e.g., ref. Figure 4). Throughout the 12km grid domain, annual rainfall in portions of the eastern region ranges from ~40 inches compared to less than 20 inches in the west; the overall spatial variability of observed soil moisture was consistent with spatial patterns of vegetation and annual precipitation (e.g., generally decreasing soil moisture moving east to west).

Because in-situ monitoring measurements are sparse and cannot be used to represent regional soil moisture conditions throughout the South Central U.S., we also investigated estimates of soil moisture provided by the NLDAS-2 LSMs Noah, Noah-MP, Mosaic, and VIC (ref. Sections 4-6). Monthly and hourly NLDAS-2 soil moisture outputs were retrieved from the Goddard Earth Systems Data and Information Services Center (<http://disc.sci.gsfc.nasa.gov/hydrology/data-holdings>). The 1/8th degree NLDAS-2 data were horizontally interpolated to the 12km grid domain (ref. Figure 1) and vertically interpolated to the standard in-situ measurement depths. Spatial maps of 12km seasonally averaged NLDAS-2 soil moisture were consistent with expected spatial variability related to eastern Texas soil types (e.g., ref. Figure 3), NLDAS-2 soil properties (e.g., ref. Figure 33a), and the large-scale spatial patterns of annual precipitation and vegetation across the 12km grid domain (e.g., ref. Section 6). The NLDAS-2 soil moisture predictions were compared in detail to the available soil moisture observations collected by the SCAN and CRN networks. As discussed in Section 4 of this report, results of the NLDAS-2 evaluations are in general agreement with the results found in other studies that used a similar methodology (e.g., Xia et al., 2012, 2014; Cai et al., 2014ab).

A primary outcome of this project was an assessment of the range of sensitivities in isoprene emissions estimates from MEGAN to alternative representations of soil moisture during March through October for years 2006, 2007, and 2011. The MEGAN applications developed and used in our analyses have been thoroughly assessed in support of additional LAI and isoprene analyses to the current study (e.g., Huang, 2014, 2015). In support of our project, a member of the research team who did not conduct the input data processing and model simulations with MEGAN reviewed at least 10% of the input data and model output for quality assurance purposes. Spatial maps of maximum hourly values of PAR, temperature, LAI, and soil moisture were visually reviewed for the June-August 2011 period, which represents >10% of the combined

MEGAN simulation periods. The review demonstrated that the range of values (i.e., minimum-to-maximum) and spatial patterns of these environmental inputs were reasonable; i.e., LAI values were 0.0-7.2 m<sup>2</sup>/m<sup>2</sup> and reflected the spatial pattern of eastern Texas vegetation densities during the summer growing season inferred from TCEQ land cover, average root zone soil moisture reflected the relative biases between LSMs documented in Section 5 and had spatial patterns consistent with NLDAS-2 soil properties in eastern Texas. Substantial variations in day-to-day environmental parameters were sometimes directly traced to variations in dominant weather patterns or geographic features. For example, a widespread (and rare for summer 2011) southward-moving rain event occurred during June 21-23, 2011 over eastern Texas; the pattern of spatial changes (relative to previous days) of decreased PAR and temperature and increased soil moisture were generally consistent with the temporal evolution of daily spatial changes in total precipitation. Overall, the review of MEGAN inputs and outputs on the 4km grid domain for June-August 2011 identified no issues of concern.

## References

Cai, X., Z.-L. Yang, C. H. David, G.-Y. Niu, and M. Rodell, 2014a. Hydrological evaluation of the Noah-MP land surface model for the Mississippi River Basin, *J. Geophys. Res. Atmos.*, 119, 23–38, doi:10.1002/2013JD020792.

Cai, X., Z.-L. Yang, Y. Xia, M. Huang, H. Wei, L. R. Leung, and M. B. Ek, 2014b. Assessment of simulated water balance from Noah, Noah-MP, CLM, and VIC over CONUS using the NLDAS test bed, *J. Geophys. Res. Atmos.*, 119, 13,751–13,770, doi:10.1002/2014JD022113.

Huang, L., McGaughey, G., McDonald-Buller, E., Kimura, Y., & Allen, D. T., 2015. Quantifying regional, seasonal and interannual contributions of environmental factors on isoprene and monoterpene emissions estimates over eastern Texas. *Atmospheric Environment*, 106, 120-128. 10.1016/j.atmosenv.2015.01.072

Huang, L., McDonald-Buller, E. C., McGaughey, G., Kimura, Y., & Allen, D. T., 2014. Annual variability in leaf area index and isoprene and monoterpene emissions during drought years in Texas. *Atmospheric Environment*, 92, 240-249.

Xia, Y., J. Sheffield, M. B. Ek, J. Dong, N. Chaney, H. Wei, J. Meng, and E. F. Wood, 2014. Evaluation of multi-model simulated soil moisture in NLDAS-2, *J. Hydrol.*, 512, 107–125, doi:10.1016/j.jhydrol.2014.02.027.

Xia, Y., K. Mitchell, M. Ek, J. Sheffield, B. Cosgrove, E. Wood, L. Luo, C. Alonge, H. Wei, J. Meng, B. Livneh, D. Lettenmaier, V. Koren, Q. Duan, K. Mo, Y. Fan, and D. Mocko, 2012. Continental-scale water and energy flux analysis and validation for the North American Land Data Assimilation System project phase 2 (NLDAS-2): 1. Intercomparison and

application of model products, *J. Geophys. Res.*, 117, D03109,  
doi:10.1029/2011JD016048.